VANM159.001AUS PATENT

IN THE UNITED STATES PATENT AND TRADEMARK OFFICE

Applicant	:	Remacle et al.
Appl. No.	:	09/574,626
Filed	:	May 19, 2000
For	:	METHOD FOR THE IDENTIFICATION AND/OR THE QUANTIFICATION OF A TARGET COMPOUND OBTAINED FROM A BIOLOGICAL SAMPLE UPON CHIPS
Examiner	:	Zhou, S.
Group Art Unit	:	1631

DECLARATION UNDER 37 C.F.R §1.132

Mail Stop Amendment
Commissioner for Patents
P.O. Box 1450
Alexandria, VA 22313-1450

Dear Sir:

1. This Declaration is being submitted to demonstrate that a person skilled in the art of biochips and microarrays would not be motivated to combine Lockhart et al. (USP 6,344,316) with Hacker et al. (Immunogold-silver staining – autometallography: recent developments and protocols, In "Analytical Morphology: Theory, Applications & Protocols", Eds. Jiang Gu, Eaton Publishing, Chapter 2, pages 41-54, 1997) and that the presently claimed invention provides unexpected advantages.

2. I am an inventor on the above-identified patent application and I am familiar with the specification and prosecution history.

3. I have extensive experience in the field of biochemistry and cell biology for many years and published more than 300 hundreds scientific articles in international Journals. My

Curriculum Vitae has been previously submitted with the Declaration filed on November 5, 2002.

4. Although both silver staining technology and microarray technology coexisted for many years, those skilled in the art had never been motivated to combine these technologies prior to the present invention. The main reason is that Gold labeling followed by silver precipitation was considered as a purely qualitative and very touchy method that could not be use for micro-detection in a reproducible and homogeneous assay as required in the microarray field. Gold and/or silver staining had been used in the context of blotting as long as 20 years ago. Microarray technology was developed more than 15 years ago. However, rather than using catalytically generated metallic precipitates as in the present invention, prior to the present invention those working in the microarray field used fluorescence to detect target molecules bound to the microarray. Thus, despite their coexistence for many years, prior to the present invention, those skilled in the microarray field were not motivated to utilize metallic precipitates generated by catalytic reduction for detecting target molecules bound to microarrays.

5. The use of metallic precipitates generated by catalytic reduction provides important advantages over alternative techniques. As stated in the Declaration submitted June 15, 2004, the present invention permits rapid and sensitive detection of target molecules bound to a microarray.

6. The advantages of metallic precipitates generated by catalytic reduction for detecting target molecules bound to microarrays have been recognized by others who utilized such technology after the priority date of the present application.

For example, in the article entitled "Scanometric Array Detection with Nanoparticle Probes" *Science*, 289:1757-1760 (published on September 8, 2000, provided herewith as **Exhibit A**) the authors (Taton et al.) state:

> "*Although silver enhancement has been used to visualize protein-, antibody-, and DNA-conjugated gold particles in histochemical electron microscope studies <...>, it has not been used in quantitative DNA hybridization assays or combinatorial chip-based detection formats. We found that our scanometric detection method not only enabled very low surface coverages of nanoparticles probes to be visualized by a simple flatbed scanner or by the naked eye (Fig. 1, C and F) but also permitted the quantification of target hybridization on the basis of*

the imaged greyscale of the darkened area (Fig 1H). "(page 1758, last sentence in the left column bridging middle column)

The authors also state:

> *"In addition, when coupled with a signal amplification method based on nanoparticle-promoted reduction of silver (I), the sensitivity of this scanometric array detection system exceeds that of the analogous fluorophore system by two orders of magnitude."* (page 1757, Abstract)

Finally, the authors also state:

> *"We expect that scanometric DNA array detection will be useful in applications such as single-nucleotide polymorphism analysis, where single-mismatch resolution, sensitivity, cost, and ease of use are important factors. Moreover, the sensitivity of this system, which has yet to be totally optimized, points toward a potential method for detecting oligonucleotide targets without the need for target amplification schemes such as the polymerase chain reaction."* (page 1759, last paragraph, bridging page 1760)

7. Other references published after the priority date of the present application also recognized the advantages of using metallic precipitates generated by catalytic reduction to detect target molecules bound to microarrays and further demonstrate the importance of such technology to the microarray field. See, for example, the following attached articles (**Exhibits B-E**:

Ji M. et al. 2004 "Colorimetric silver detection of methylation using DNA microarray coupled with linker-PCR." *Clin Chim Acta* 342(1-2):145-53, see page 146, left column, second paragraph;

Wang Y.F. et al. 2004 "Analytical performance of and real sample analysis with an HBV gene visual detection chip." *J Virol Methods* 121(1):79-84, see page 80, left col., first full paragraph, and page 81, right col., first full paragraph;

Liang R.Q. et al. 2005 "An oligonucleotide microarray for microRNA expression analysis based on labeling RNA with quantum dot and nanogold probe." *Nucleic Acids Res* 33(2):e17, see page 2, right column, and page 6, right col. bridging left col. on page 7; and

Wan Z. et al. 2005 "Development of array-based technology for detection of HAV using gold-DNA probes." *J Biochem Mol Biol* 38(4):399-406, see page 399, right col.

In fact, many of the references specified above make specific reference to the publication by Dr. I. Alexandre, the main inventor of the subject application, entitled "Colorimetric Silver

Detection of DNA Microarrays", *Anal. Biochem.* 295:1-8 (2001), which is also attached for the Examiner's information as **Exhibit F**.

8. Thus, the use of metallic precipitates generated by catalytic reduction to detect target molecules bound to microarrays provides significant advantages over alternative methods, such as those utilizing fluorescence.

9. In addition to the unexpected advantages of using metallic precipitates generated by catalytic reduction to detect target molecules bound to microarrays, Lockhart et al. and Hacker et al. provide no motivation to create the claimed invention. In particular, there is no disclosure describing metallic precipitates generated by catalytic reduction in Lockhart et al. While Lockhart et al. does mention the use of a colorimetric label (e.g. colloidal gold), the gold particles discussed are about 40-80 nm diameter size range size and scatter green light with high efficiency (page 24 line 49). Gold particles of 40-80 nm are highly suitable for detection by RLS (resonance light scattering) but are not compatible with catalytic reduction of metal such as silver which requires smaller particle size of equal or lower than 20 nm (see Bao et al. 2002 *Anal. Chem.* 74:1792-1793). The reason is that gold particles can only react if they are about the same size as the biological molecules which are bound to the particles, meaning a few nm. If too large, the reaction of catalytic reduction becomes slow and even does not take place at all.

10. Hacker et al. describe the use of antibodies having gold particles fixed thereto along with silver intensification in the context of localizing a molecule in a cell or tissue, a context which is significantly different than the microarrays utilized in the present invention. Hacker et al. teach away from the use of metallic precipitates generated by metallic reduction in the context of microarrays. For example, Hacker et al. teach that some immunogold reagents available on the market do not produce high labeling density and generate an unacceptable background labeling. When high-quality products are used, one still needs to check and optimize every step of the procedure (page 49, first paragraph). In addition, Hacker et al. teach that methods using gold particles and silver intensification are undesirable or labor intensive in quantitative analyses (see page 49).

Each of the foregoing drawbacks described Hacker et al. would discourage those in the microarray field from utilizing metallic precipitates generated by catalytic reduction in the

context of microarrays. For example, in the microarray field it is important to be able to detect small amounts of target molecules and to obtain reproducible results to allow comparison between target molecules bound to different locations on the same array or to different arrays. Hacker's teaching that some immunogold reagents available on the market do not produce high labeling density or generate unacceptable background labeling suggest that catalytically generated metallic precipitates would be incompatible with the demands of microarray technology.

In addition, it is important that microarray technology be amenable to automation. Hacker's teaching that even when high-quality products are used, one still needs to check and optimize every step of the procedure and that methods using gold particles and silver intensification are undesirable or labor intensive also suggests catalytically generated precipitates would be incompatible with the demands of microarray technology.

11. In conclusion, the claimed invention possesses unexpected advantages and is not suggested by the combination of the cited references.

12. I declare that all statements made herein of my own knowledge are true and that all statements made on information and belief are believed to be true; and further that these statements were made with the knowledge that willful, false statements and the like so made are punishable by fine or imprisonment, or both, under Section 1001 of Title 18 of the United States Code and that such willful false statements may jeopardize the validity of the application or patent issuing therefrom.

Dated: 15 December 2006

By: _____
Prof. José REMACLE

3113779
111406

25. T. D. Palmer, E. A. Maskakis, A. R. Willoite, F. Safcor F. H. Gage, *J. Neurosci.* **19**, 8487 (2000).
26. W. Li, C. A. Cogswell, J. J. LoTurco, *J. Neurosci.* **18**, 8853 (1998).
27. F. Doetsch, I. Caille, D. A. Lim, J. M. Garcia-Verdugo, A. Alvarez-Buylla, *Cell* **97**, 703 (1999).
28. I. L. Weissman, *Cell* **100**, 157 (2000).
29. H. Geiger, S. Sick, C. Bonifer, A. M. Müller, *Cell* **93**, 1055 (1998).
30. Details of the culture conditions and immunostaining methods are available as supplementary material to *Science* Online subscribers www.sciencemag.org/feature/data/1051654.shl.
31. We thank A. Mudge and members of the Raff laboratory for advice and comments on the manuscript. T.K. was supported by a Japan Society for the Promotion of Science Postdoctoral Fellowship for Research Abroad. M.R. is supported by a Programme Grant from the Medical Research Council, UK.

26 April 2000; accepted 20 July 2000

Scanometric DNA Array Detection with Nanoparticle Probes

T. Andrew Taton,[1,2] Chad A. Mirkin,[1,2]* Robert L. Letsinger[1]*

A method for analyzing combinatorial DNA arrays using oligonucleotide-modified gold nanoparticle probes and a conventional flatbed scanner is described here. Labeling oligonucleotide targets with nanoparticle rather than fluorophore probes substantially alters the melting profiles of the targets from an array substrate. This difference permits the discrimination of an oligonucleotide sequence from targets with single nucleotide mismatches with a selectivity that is over three times that observed for fluorophore-labeled targets. In addition, when coupled with a signal amplification method based on nanoparticle-promoted reduction of silver(I), the sensitivity of this scanometric array detection system exceeds that of the analogous fluorophore system by two orders of magnitude.

Sequence-selective DNA detection has become increasingly important as scientists unravel the genetic basis of disease and use this new information to improve medical diagnosis and treatment. Commonly used heterogeneous DNA sequence detection systems, such as Southern blots and combinatorial DNA chips, rely on the specific hybridization of surface-bound, single-strand capture oligonucleotides to complementary targets. Both the specificity and sensitivity of these assays are dependent on the dissociation properties of capture strands hybridized to perfect and to mismatched complements. Recently, we developed a nanoparticle-based detection scheme that uses two gold particle probes with covalently bound oligonucleotides that are complementary to a target of interest (*1*–*3*). When encountering target strands, these particle probes are polymerized and form network structures composed of thousands of particles. In addition, the polymerization process is accompanied by a red-to-blue color change, providing a means of detection. These network structures exhibit exceptionally sharp melting profiles; the full width at half-maximum (FWHM) for the first derivatives of these melting transitions is as low as 2°C. Sharp melting transitions allow one to differentiate a perfectly complementary target strand from a strand with a single base mismatch, regardless of position on a 24-nucleotide sequence. The sharp melting in this nanoparticle network system as compared with normal DNA duplex melting as monitored by ultraviolet (UV)–visible absorption at 260 nm derives, in part, from: (i) a cooperative effect due to the multiple duplex interconnects between particles in the network structure, and (ii) the monitoring of a nanoparticle optical signature that is sensitive to interparticle distance and particle aggregate size rather than a DNA base signature. Here we report that the use of single-nanoparticle probes in recognizing DNA segments immobilized on a chip affords substantially sharper and higher temperature melting profiles than those obtained with analogous, conventional fluorophore-based systems. This observation, combined with (i) the development of a quantitative signal amplification method based on nanoparticle-promoted reduction of silver(I) and (ii) the use of a conventional flatbed scanner as a reader, have allowed us to develop a new "scanometric" chip-based detection system for DNA that has single mismatch selectivity and a sensitivity that, at present, is 100 times greater than that of conventional, analogous fluorescence-based assays as monitored by confocal fluorescence microscopy.

Gold nanoparticles modified with oligonucleotides (*3*) were used to indicate the presence of a particular DNA sequence hybridized on a transparent substrate in a three-component sandwich assay format (Scheme 1). In a typical experiment, target-active substrates were fabricated by attaching 3′-thiol–modified capture oligonucleotides to the surface of float glass microscope slides (Fisher Scientific, Pittsburgh, Pennsylvania) according to procedures from the

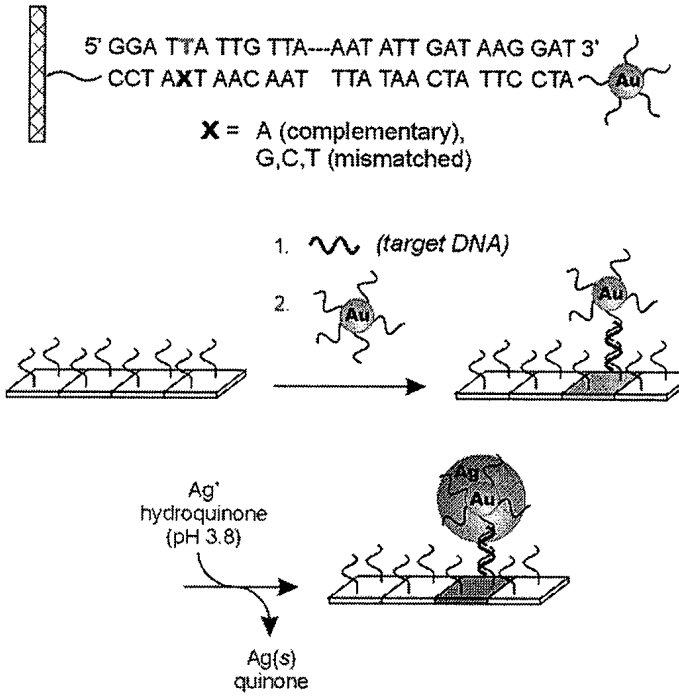

Scheme 1.

[1]Department of Chemistry, [2]Center for Nanofabrication and Molecular Self-Assembly, Northwestern University, Evanston, IL 60208, USA.

*To whom correspondence should be addressed. E-mail: camirkin@chem.northwestern.edu (C.A.M.); r-letsinger@chem.northwestern.edu (R.L.L.)

literature (*4*). In one set of experiments, the entire slide surface was modified with 12-base oligonucleotides of a given sequence; in another set, oligonucleotide arrays were generated by spotting various oligonucleotides with a commercial microarrayer. Nanoparticle probes and synthetic 27-base oligonucleotide targets (based on the anthrax lethal factor sequence) were then cohybridized to these substrates in buffer solution (Scheme 1). For tests at high target concentrations (≥1 nM), the high density of surface-hybridized nanoparticles made the surface appear light pink (Fig. 1, A and B). At lower target concentrations (≤100 pM), the attached nanoparticles could not be visualized with the naked eye (Fig. 1E), although they could be imaged by field-emission scanning electron microscopy (*5*). To facilitate visualization of nanoparticle labels hybridized to the array surface, we used a signal amplification method in which silver ions are reduced by hydroquinone to silver metal at the surfaces of the gold nanoparticles. This process increased the scanned intensity by a factor as large as 10^5. Although silver enhancement has been used to visualize protein-, antibody-, and DNA-conjugated gold nanoparticles in histochemical electron microscopy studies (*6*, *7*), it has not been used in quantitative DNA hybridization assays or combinatorial chip-based detection formats. We found that our scanometric detection method not only enabled very low surface coverages of nanoparticle probes to be visualized by a simple flatbed scanner or by the naked eye (Fig. 1, C and F) but also permitted the quantification of target hybridization on the basis of the imaged grayscale of the darkened area (Fig. 1H). In the absence of target or in the presence of noncomplementary target, no darkening of the surface was observed (Fig. 1G), demonstrating that neither nonspecific binding of nanoparticles to the surface nor nonspecific silver formation on bare glass occurs. Low nonspecific binding (in fact, undetectable with this technique) is an unusual feature of these heavily functionalized, oligonucleotide-nanoparticle conjugates (bearing approximately 220 oligonucleotides per 13-nm–diameter particle) (*8*), which enables ultrasensitive detection of DNA sequences.

We have found that oligonucleotide-functionalized nanoparticles exhibit unique hybridization properties that can lead to improved selectivity in assays on oligonucleotide arrays (or "gene chips") (*9*). The relative ratios of targets hybridized to different elements of an oligonucleotide array determine the effectiveness of the array in discriminating between different target sequences. In principle, the greater the difference in binding affinity at a given temperature between a complex containing a perfect target and one with a mismatched base, the higher this ratio and the better the discrimination. As a test of the relative selectivities of fluorophore and nanoparticle probes, we carried out experiments in which melting curves were obtained for surface-bound complexes comprising matched or mismatched capture oligonucleotides, a target oligonucleotide, and probes bearing either fluorophore or nanoparticle reporting groups (Scheme 1) (*10*). Although the fluorescein-labeled complexes dehybridized over a very broad temperature range (first derivative FWHM = 18°C), as expected for a complex containing a relatively small number of base pairs, the surface-bound complexes containing identical oligonucleotides but nanoparticle reporter groups melted over a very narrow temperature range (first derivative FWHM = 3°C). The sharp melting curves of the nanoparticle probe translate into high recognition selectivity, because a temperature can be selected so that a high proportion of labeled probe remains hybridized to perfectly matched capture strands while most of the probe is dehybridized from mismatched capture strands. (For the specific example in Fig. 2, 81% of the target was retained for the matched capture strand and only 19% for the mismatched capture strand at the stringency temperature shown.) The midpoint temperatures in the melting curves (T_m values) for the complexes with the nanoparticle probes also were significantly higher than the corresponding values for the fluorophore probes. This feature should increase the sensitivity achievable in the assay, because an increase in the melting temperature of the surface complex lowers the critical concentration below which the complex spontaneously melts at room temperature.

To evaluate the effectiveness of nanoparticles as scanometric indicators for oligonucleotide arrays, a synthetic target was hybridized to different capture strands immobilized onto glass chips and was then assayed separately with fluorophore and nanoparticle probes. The test arrays, the oligonucleotide target, and the Cy3 label strand (indodicarbocyanine 3; Cy3 is a trademark of Biological Detection Systems, now part of Amersham Pharmacia Biotech, Uppsala, Sweden) were made according to published protocols (*4*, *11*). Arrays contained four elements corresponding to each of the four possible nucleotides at position 5 of the target. The arrays were designed to evaluate discrimination between an A:T complement (X = A) and a G:T "wobble" pairing (X = G), a particularly difficult task for conventional fluorophore-based assays (*12*, *13*). The synthetic target and either fluorophore or nanoparticle probes were hybridized successively to arrays in hybridization buffer, and each step was followed with a stringency buffer wash (*14*). After the second wash, the arrays treated with nanoparticle probes were immersed in the silver am-

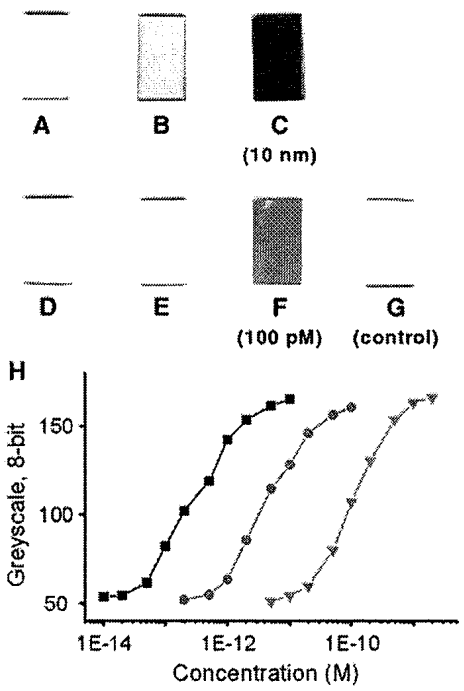

Fig. 1. Images of 7 mm by 13 mm, oligonucleotide-functionalized, float glass slides, obtained with a flatbed scanner. (**A**) Slide before hybridization of target and nanoparticle probe. (**B**) A slide identical to (A) after hybridization with oligonucleotide target (10 nM) and then nanoparticle probes (5 nM in particles). The pink color derives from the Au nanoparticle probes. (**C**) A slide identical to (B) after exposure to silver amplification solution for 5 min. (**D**) Slide before hybridization of target and nanoparticle probe. (**E**) A slide identical to (D) after hybridization with target (100 pM) and then nanoparticle probe (5 nM). The extinction of the submonolayer of nanoparticles is too low to be observed visually or with a flatbed scanner. (**F**) A slide identical to (E) after exposure to silver amplification solution for 5 min. Slide (F) is lighter than slide (C), indicating a lower concentration of target. (**G**) A control slide exposed to 5 nM nanoparticle probe and then exposed to silver amplification solution for 5 min. No darkening of the slide is observed. (**H**) Graph of 8-bit gray scale values as a function of target concentration. The gray scale values were taken from flatbed scanner images of oligonucleotide-functionalized glass surfaces that had been exposed to varying concentrations of oligonucleotide target, labeled with 5 nM oligonucleotide probe and immersed in silver amplification solution. For any given amplification time, the grayscale range is limited by surface saturation at high grayscale values and the sensitivity of the scanner at low values. Therefore, the dynamic range of this system can be adjusted by means of hybridization and amplification conditions (that is, lower target concentrations require longer amplification periods). Squares: 18-base capture-target overlap (*5*), 8× PBS hybridization buffer [1.2 M NaCl and 10 mM NaH_2PO_4/Na_2HPO_4 buffer (pH 7)], 15 min amplification time. Circles: 12-base capture-target overlap, 8× PBS hybridization buffer, 10 min amplification time. Triangles: 12-base capture-target overlap, 2× PBS hybridization buffer [0.3 M NaCl, 10 mM NaH_2PO_4/Na_2HPO_4 buffer (pH 7)], 5 min amplification time. The lowest target concentration that can be effectively distinguished from the background baseline is 50 fM.

plification solution for 5 min. Silver amplification darkened the array elements so that the 200-μm–diameter elements could be easily imaged with a flatbed scanner or even the naked eye.

Arrays challenged with the target and nanoparticle labels and amplified with the silver solution exhibited more selective hybridization to complementary array elements and higher signal intensity than did arrays challenged with target and fluorophore labels (Fig. 3). For both nanoparticle- and fluorophore-based arrays, a low-temperature wash did not dissociate the target from mismatched array elements and produced hybridization signal at all four elements. As the stringency temperature was increased, target dissociated from the different elements in the order of the predicted stability of the Watson-Crick base pairs (*15*): C:T and T:T mismatches first, followed by the G:T wobble pair, and finally by the A:T complement. It is clear that, as predicted by the dissociation curves (Fig. 2), these transitions occur much more sharply for the nanoparticle-labeled arrays than for the Cy3-labeled arrays (Fig. 3) (*16*). This sharpening has two important consequences with respect to the hybridization signal obtained at the optimum stringency temperature (shown by the dark boxes in Fig. 3). First, the relative signal intensity at the complementary (A) element versus the wobble (G) element is much greater for the nanoparticle-labeled array (Fig. 3, left) than for the fluorophore-labeled array (Fig. 3, right). This demonstrates the higher sequence selectivity of the array detection system based on nanoparticle probes. Although the fluorophore-based system shows 2.6:1 selectivity for the perfect complement at 35°C (the optimum stringency temperature), the nanoparticle-based system shows over 10:1 selectivity at 50°C (the optimum stringency temperature). Second, the absolute signal intensity at the complementary (A) element is greater for the nanoparticle array at the temperature of optimum stringency. As optimum stringency is approached with fluorophore probes, most of the hybridized target and label are dissociated from the array, leaving little signal to image. Note the decrease in signal as the temperature is increased from 15° to 35°C (Fig. 3, right). With nanoparticle probes, on the other hand, over 80% of the nanoparticle label is retained at the complementary element at stringency (Fig. 3, left, 50°C). Hybridization signal could be resolved at the X = A elements at target concentrations as low as 50 fM (*5*); this represents a 100-fold increase in sensitivity over that of Cy3-labeled arrays imaged by confocal fluorescence microscopy, for which target concentrations of 5 pM or greater were required. The higher melting temperatures observed for nanoparticle-target complexes immobilized on surfaces undoubtedly contributed to the sensitivity of the array. The greater stability of the probe/target/surface-oligonucleotide complex in the case of the nanoparticle system as compared with the fluorophore system presumably results in less target and probe lost during washing steps.

We expect that scanometric DNA array detection will be useful in applications such

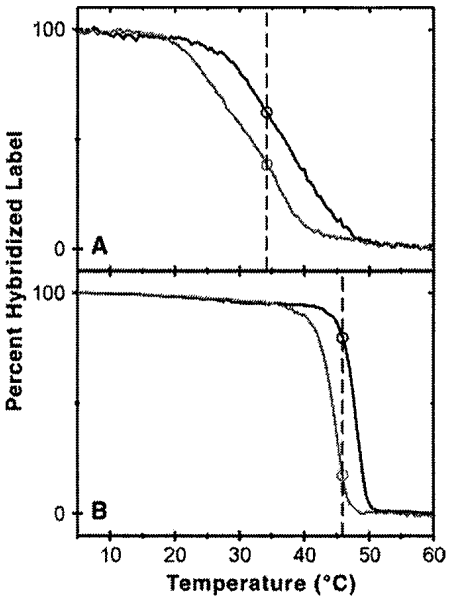

Fig. 2. (**A**) Dissociation of fluorescein-labeled target from the surfaces of oligonucleotide-functionalized glass beads, monitored by quantifying the fluorescence of the dissociated label at wavelength (λ) = 520 nm in the 2× PBS buffer solution (above the beads) as a function of temperature. The black curve describes the dissociation of target and probe from a perfectly complementary capture strand (Scheme 1, X = A; T_m = 37°C, first derivative FWHM = 18°C), and the red curve describes the analogous process for a capture strand with a single mismatch (Scheme 1, X = G; T_m = 32°C, first derivative FWHM = 19°C). The breadth of these curves is typical for dissociation of fluorophore-labeled targets from surface capture strands (*17*). The intercepts at the vertical dotted line in the graph can be used to estimate the expected relative fluorescence intensities at complementary and mismatched oligonucleotide array elements at a given temperature, and thus provide an estimate of the expected selectivity of sequence identification for fluorophore-based gene chips. In this case, halfway between the T_m's for the two curves (chosen arbitrarily), the expected ratio of fluorescence intensities is 62/38% = 1.6:1. (**B**) Dissociation of nanoparticle-labeled targets from the surfaces of oligonucleotide-functionalized glass beads, monitored by quantifying the absorbance of the dissociated label at λ = 520 nm (in the solution above the beads) as a function of temperature. The black curve describes the dissociation of target and nanoparticle probe from a perfectly complementary capture strand (Scheme 1, X = A; T_m = 48°C, first derivative FWHM = 3°C), and the red curve describes the analogous process for a capture strand with a single mismatch (Scheme 1, X = G; T_m = 45°C, first derivative FWHM = 3°C). The intercepts at the vertical dotted line allow one to estimate the expected ratio of nanoparticle label at complementary and mismatched array elements (at a temperature halfway between the T_m's for the two curves) and thus are an estimate of the expected selectivity of sequence identification for nanoparticle-based gene chips. At this temperature, this ratio is 81/19% = 4.3:1.

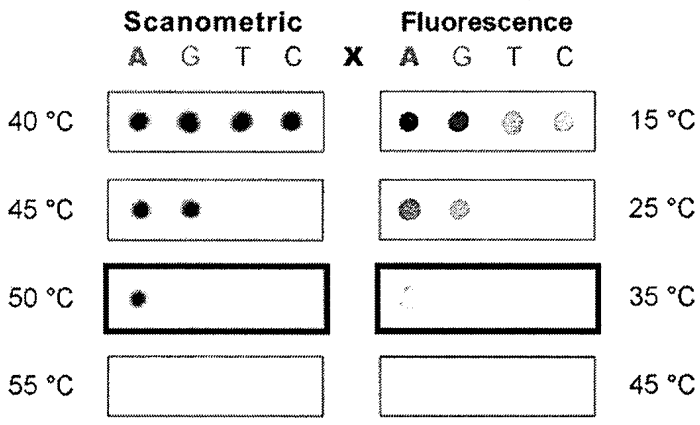

Fig. 3. (**Left**) Nanoparticle-labeled arrays developed at different stringency temperatures. Model oligonucleotide arrays (with the capture sequences shown in Scheme 1) were treated with oligonucleotide target and nanoparticle probes, followed by a 2-min buffer wash at the temperatures shown and subsequent silver amplification (*13*). Images were obtained with an Epson Expression 636 (600 dots per inch) flatbed scanner (Epson America, Long Beach, California). The darkened border indicates the array that showed optimum selectivity for the perfectly complementary target; at this temperature, the ratio of background-subtracted, 8-bit gray scale values for elements A:G:T:C, obtained from histogram averages in Adobe Photoshop (Adobe Systems, San Jose, California), is 96:9:7:6. (**Right**) Fluorophore-labeled arrays washed at different stringency temperatures. Model oligonucleotide arrays identical to those shown at left were treated with oligonucleotide target and Cy3-labeled oligonucleotide probes, followed by a 2-min buffer wash at the temperatures shown. Images were obtained with a ScanArray Confocal Microarray Scanner (GSI Lumonics, Billerica, Massachusetts). The darkened border indicates the array that showed the highest selectivity for the perfectly complementary target, as calculated by the QuantArray Analysis software package (GSI Lumonics); at this temperature, the intensity ratio (in percent, with the intensity of the X = A element at 15°C set to 100%) for elements A:G:T:C is 18:7:1:1.

as single-nucleotide polymorphism analysis, where single-mismatch resolution, sensitivity, cost, and ease of use are important factors. Moreover, the sensitivity of this system, which has yet to be totally optimized, points toward a potential method for detecting oligonucleotide targets without the need for target amplification schemes such as the polymerase chain reaction.

References and Notes

1. C. A. Mirkin, R. L. Letsinger, R. C. Mucic, J. J. Storhoff, *Nature* **382**, 607 (1996).
2. R. Elghanian, J. J. Storhoff, R. C. Mucic, R. L. Letsinger, C. A. Mirkin, *Science* **277**, 1078 (1997).
3. J. J. Storhoff, R. Elghanian, R. C. Mucic, C. A. Mirkin, R. L. Letsinger, *J. Am. Chem. Soc.* **120**, 1959 (1998).
4. L. A. Chrisey, G. U. Lee, C. E. O'Ferrall, *Nucleic Acids Res.* **24**, 3031 (1996).
5. Supplementary material is available at *Science* Online at www.sciencemag.org/feature/data/1051941.shl.
6. G. W. Hacker, in *Colloidal Gold: Principles, Methods, and Applications*, M. A. Hayat, Ed. (Academic Press, San Diego, CA, 1989), vol. 1, chap. 10.
7. I. Zehbe *et al.*, *Am. J. Pathol.* **150**, 1553 (1997).
8. R. C. Mucic, thesis, Northwestern University, Evanston, IL (1999).
9. For a review on oligonucleotide arrays, see S. P. A. Fodor, *Science* **277**, 393 (1997).
10. For the experiments reported in Fig. 2, dissociation measurements were made from the surface of glass beads 250 to 300 μm in diameter (Polysciences, Warrington, PA) rather than planar substrates to increase the UV-visible and fluorescence signal intensity.
11. 5′-Cy3–labeled oligonucleotide probes were synthesized on an Expedite automated synthesizer (Millipore, Bedford, MA) using Cy3 phosphoramidite (Glen Research, Sterling, VA) as the label source. Arrays of spots 175 μm in diameter separated by 375 μm were patterned with a GMS 417 Microarrayer (Genetic Microsystems, Woburn, MA).
12. R. K. Saiki and H. A. Erlich, in *Mutation Detection*, R. G. H. Cotton, E. Edkins, S. Forrest, Eds. (Oxford Univ. Press, Oxford, 1998), chap. 7.
13. S. Ikuta, K. Takagi, R. B. Wallace, K. Itakura, *Nucleic Acids Res.* **15**, 797 (1987).
14. First, 20 μl of a 1 nM solution of synthetic target in 2× phosphate-buffered saline (PBS) [0.3 M NaCl and 10 mM NaH_2PO_4/Na_2HPO_4 buffer (pH 7)] was hybridized to the array for 4 hours at 10°C in a CoverWell PC20 hybridization chamber (Grace Bio-Labs, Bend, OR) and was then washed at 10°C with clean PBS buffer. Next, 20 μl of a 100 pM solution of either oligonucleotide-functionalized gold nanoparticles or 5′-Cy3–labeled probe in 2× PBS was hybridized to the array for 4 hours at 10°C in a fresh hybridization chamber. The array was then washed at the stringency temperature (shown in Fig. 3) with clean 2× PBS buffer for 2 min. Arrays labeled with nanoparticle probes were washed twice at room temperature with 2× PBN [0.3 M $NaNO_3$ and 10 mM NaH_2PO_4/Na_2HPO_4 buffer (pH 7)], then submerged in Silver Enhancer Solution (Sigma) for 5 min at room temperature and washed with water.
15. H. T. Allawi and J. SantaLucia Jr., *Biochemistry* **36**, 10581 (1988).
16. The temperature ranges for the melting curves in Fig. 2 do not correspond exactly with the stringency temperatures associated with the oligonucleotide array experiments reported in Fig. 3. This is probably because the two sets of experiments are not identical with respect to the substrate.
17. J. E. Forman, I. D. Walton, D. Stern, R. P. Rava, M. O. Trulson, in *Molecular Modeling of Nucleic Acids*, N. B. Leontis and J. SantaLucia Jr., Eds. [American Chemical Society (ACS) Symposium Series 682, ACS, Washington, DC, 1998), pp. 206–228.

18. C.A.M. and R.L.L. acknowledge the Army Research Office (DAAG55-97-1-0133) and the National Institute of General Medical Sciences (GM 57356) for support of this work.

5 May 2000; accepted 19 July 2000

REPORTS

Printing Proteins as Microarrays for High-Throughput Function Determination

Gavin MacBeath[1]* and Stuart L. Schreiber[2]

Systematic efforts are currently under way to construct defined sets of cloned genes for high-throughput expression and purification of recombinant proteins. To facilitate subsequent studies of protein function, we have developed miniaturized assays that accommodate extremely low sample volumes and enable the rapid, simultaneous processing of thousands of proteins. A high-precision robot designed to manufacture complementary DNA microarrays was used to spot proteins onto chemically derivatized glass slides at extremely high spatial densities. The proteins attached covalently to the slide surface yet retained their ability to interact specifically with other proteins, or with small molecules, in solution. Three applications for protein microarrays were demonstrated: screening for protein-protein interactions, identifying the substrates of protein kinases, and identifying the protein targets of small molecules.

Historically, genome-wide screens for protein function have been carried out with random cDNA libraries. Most frequently, the libraries are prepared in phage vectors and the expressed proteins immobilized on a membrane by a plaque lift procedure. This method has been effective for a variety of applications (*1*–*4*), but it has several limitations. Most clones in the library do not encode proteins in the correct reading frame, and most proteins are not full-length. Bacterial expression of eukaryotic genes frequently fails to yield correctly folded proteins, and products derived from abundant transcripts are overrepresented. Moreover, because plaque lifts are not amenable to miniaturization on the micrometer scale, it is hard to imagine screening all the proteins of an organism hundreds or thousands of times by this approach.

With the advent of high-throughput molecular biology, it is now possible to prepare large, normalized collections of cloned genes. UniGene sets in the form of polymerase chain reaction products have been used extensively over the past decade to construct DNA microarrays for the study of transcriptional regulation (*5*). Recently, spatially segregated clones in expression vectors were used to study protein function in vivo using the yeast two-hybrid system (*6*) and in vitro using biochemical assays (*7*). We have built on these efforts by developing microarray-based methods to study protein function.

To accomplish these goals, it is necessary to immobilize proteins on a solid support in a way that preserves their folded conformations. One group has described methods of arraying functionally active proteins, using microfabricated polyacrylamide gel pads to capture their samples and microelectrophoresis to accelerate diffusion (*8*). In contrast, we have immobilized proteins by covalently attaching them to the smooth, flat surface of glass microscope slides. One of our primary objectives in pursuing this approach was to make the technology easily accessible and compatible with standard instrumentation. We use a variety of chemically derivatized slides that can be printed and imaged by commercially available arrayers and scanners. For most applications, we use slides that have been treated with an aldehyde-containing silane reagent (*9*). The aldehydes react readily with primary amines on the proteins to form a Schiff's base linkage. Because typical proteins display many lysines on their surfaces as well as the generally more reactive α-amine at their NH_2-termini, they can attach to the slide in a variety of orientations, permitting different sides of the protein to interact with other proteins or small molecules in solution.

To fabricate protein microarrays, we use a high-precision contact-printing robot (*10*) to deliver nanoliter volumes of protein samples to the slides, yielding spots about 150 to 200 μm in diameter (1600 spots per square centimeter). The proteins are printed in phosphate-buffered saline with 40% glycerol included to prevent evaporation of the nanodroplets. It is important that the proteins remain hydrated throughout this and subsequent steps to prevent denaturation. After a 3-hour incubation, the slides are immersed in a buffer containing bovine serum albumin (BSA). This step not only quenches the unreacted aldehydes on the slide, but also forms a molecular layer of BSA that reduces nonspecific binding of other proteins in subsequent steps.

Although appropriate for most applications, aldehyde slides cannot be used when peptides

[1]Center for Genomics Research, Harvard University, 16 Divinity Avenue, Cambridge, MA 02138, USA. [2]Howard Hughes Medical Institute (HHMI), Department of Chemistry and Chemical Biology, Harvard University, 12 Oxford Street, Cambridge, MA 02138, USA.

*To whom correspondence should be addressed. E-mail: gavin_macbeath@harvard.edu

ELSEVIER

Clinica Chimica Acta 342 (2004) 145–153

www.elsevier.com/locate/clinchim

Colorimetric silver detection of methylation using DNA microarray coupled with linker-PCR

Meiju Ji, Peng Hou, Song Li, Nongyue He, Zuhong Lu*

Chien-Shiung Wu Laboratory, Department of Biological Science and Medical Engineering, Southeast University, Nanjing 210096, China

Received 14 October 2003; received in revised form 15 December 2003; accepted 15 December 2003

Abstract

Background: Aberrant DNA methylation of CpG site is among the earliest and most frequent alterations in cancer. Detection of promoter hypermethylation of cancer-related genes may be useful for cancer diagnosis or the detection of recurrence. Recently, several DNA microarray methods have been developed to detect the methylation status of the multiple genes. However, the microarrays are currently detected in fluorescence using a sophisticated laser-based scanner. These methods are limited by their lower sensitivity. *Methods*: We present a sensitive colorimetric silver method coupled with linker-PCR to detect methylation status of four genes, including *p16*, *E-cadherin*, *VHL*, and *hMLH1*. The signal generated with this method results from the precipitation of silver onto nanogold particles bound to streptavidin used to detect biotinylated DNA. *Results*: We show that *p16*, *E-cadherin*, *VHL*, and *hMLH1* were all methylated in the positive control. However, no methylation was found in these genes for the negative control. *P16* gene was only methylated in the sample, whereas others were not methylated. Furthermore, as little as 0.1 fmol of target DNA amplicons could be detected on the arrays. The results were further validated by methylation-specific PCR (MSP) and bisulfite DNA sequencing. *Conclusions*: The colorimetric silver detection of DNA microarray could be used as an inexpensive, useful, and sensitive tool to detect methylation status of the multiple genes in the future.

Keywords: Methylation; Colorimetric silver detection; DNA microarray; Linker-PCR

1. Introduction

The methylation of DNA is an epigenetic modification that can play an important role in the control of gene expression in mammalian cells. The epigenetic event has been observed in GC-rich regions, called CpG islands, frequently located in the promoter and the first exon regions of genes. CpG island hypermethylation is closely associated with transcriptional inactivation of the classic tumor suppressor genes, which is a common feature in human carcinomas [1].

At present, a variety of methods are used to evaluate the methylation status of genes: Southern blot [2], bisulfite genomic DNA sequencing [3], restriction enzyme-PCR [4], methylation-specific PCR (MSP) [5], methylation-sensitive single nucleotide primer extension (MS-SnuPE) [6], electrochemistry [7], etc. However, each method is restricted to the evaluation of DNA methylation on a gene-by-gene basis. Such an

* Corresponding author. Tel.: +86-25-83792245; fax: +86-25-83792245.

E-mail address: zhlu@seu.edu.cn (Z. Lu).

0009-8981/$ - see front matter © 2004 Elsevier B.V. All rights reserved.
doi:10.1016/j.cccn.2003.12.017

approach has given researchers a limited picture of complex epigenetic alterations in cancer.

Recently, DNA microarray methods have been developed to detect methylation status of the multiple genes [8–12]. The technology uses a lot of short oligonucleotides arrayed on glass slide for detecting methylation status of target DNA. In these approaches, oligonucleotides known as probes are arrayed on solid supports, and the labeled and interrogated complex DNA mixtures are known as targets [13]. They have offered useful and high-throughput tools in studying the phenomenon of DNA methylation. However, the present methods, which usually apply fluorescence detection by a sophisticated laser-based scanner, are still laborious, time-consuming, less sensitive and not rigid enough for clinical applications.

Alexandre et al. [14] presented a new colorimetric detection method that is intended to make use of microarray as a powerful procedure and a low-cost tool in research and clinical settings. The signal generated with this method results from the precipitation of silver nanogold particles bound to streptavidin used for detecting biotinylated DNA. Colorimetric detection using silver precipitation has been to be well adapted for detection and analysis of hybridization on microarray. Its sensitivity is comparable to detection in fluorescence using a confocal scanner. This high sensitivity is the result of an amplification step that brings small nanoparticles to grow up 1 million times in volume. Compared with conventional fluorescence detection, silver colorimetric detection could be a cheap, versatile, and sensitive alternative.

The aims of the present work are to describe the sensitive colorimetric silver method coupled with linker-PCR to detect methylation status of four genes, including *p16*, *E-cadherin*, *VHL*, and *hMLH1*.

2. Materials and methods

2.1. Preparation of the biotinylated targets

2.1.1. MseI restriction

Whole blood cells of healthy human and gastric tumor tissue were obtained from ZhongDa Hospital (Nanjing, China). Genomic DNA was extracted from whole blood cells and gastric tumor tissue by standard methods using proteinase K digestion and phenol/chloroform extraction. The DNA derived from the blood cells of healthy human was divided into two parts. One aliquot was treated by methylase *Sss*I (SM) as positive control with the conditions recommended by the supplier (New England Biolabs, Beverly, MA). The other was not treated by methylase *Sss*I (SM) as negative control. The positive control generated in this way had 100% methylated cytosine in the test CpG sites, whereas the negative control had all unmethylated cytosine residues in the test CpG sites.

Approximately 2–3 μg genomic DNA was restricted to completion with 50 U of *Mse*I following the conditions recommended by the supplier (New England Biolabs). This enzyme restricts bulk DNA into small fragments. As its recognition site (TTAA) rarely occurs in GC-rich regions, most CpG islands remain intact after the restriction. The digests were purified with QIAquick column (Qiagen).

2.1.2. Ligation to linkers

The cleaved ends of DNA were ligated to unphosphorylated linkers. The linker sequences were H-24, 5′-AGG CAA CTG TGC TAT CCG AGG GAT, and H-12, 5′-TAA TCC CTC GGA [15]. The use of universal linkers allows to subsequently amplify all methylated fragments in ligated DNA samples. The ligation step began with the annealing of H-12 to H-24 (each 100 μmol/l) by mixing equal amounts of each oligonucleotide in a microcentrifuge tube and allowing the mixture to cool from 55 °C to room temperature over 1 h. The annealed linker-primers (10 μl/sample) were then added to the purified DNA, together with 1.5 μl 10 × Fast Link Buffer, 1.5 μl 10 mmol/l ATP, 1 μl Fast Link Ligase (Epicentre), and water to 15 μl. The ligation reaction was carried out at room temperature for 30 min. The mixture was then held 70 °C for 5 min to stop the reaction. The ligated products were purified with QIAquick column (Qiagen).

2.1.3. Methylation-sensitive restriction

The ligated products were digested with the methylation-sensitive endonuclease *Bst*UI following the conditions recommended by the supplier (New England Biolabs). The digest was used for PCR without further purification.

Genomic fragments containing methylated sites are protected from the digestion and can be amplified by linker-PCR. Many of these linker-ligated *Mse*I frag-

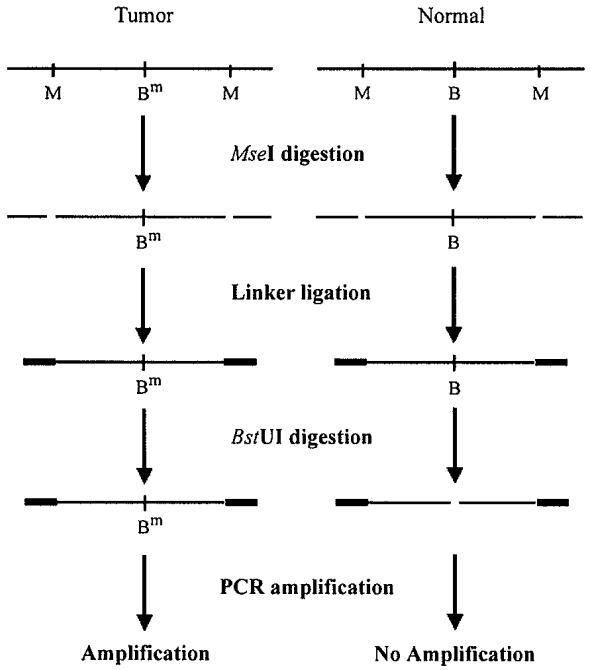

Fig. 1. A schematic outline of the procedure for the preparation of the DNA targets. M, B and B^m represent *Mse*I, unmethylated and methylated *Bst*UI recognition sites, respectively. Genomic DNA comes from whole blood cells of healthy human (Normal) and gastric tumor tissue (Tumor).

ments are expected to be present in the tumor sample due to aberrant methylation in the test site, whereas the same unmethylated fragments are digested and not present in the normal amplicon after PCR. The preparation process of targets can be illustrated in Fig. 1.

2.1.4. Linker-PCR

PCR reactions were performed for 20 cycles. At this level of amplification, especially if most unmethylated repetitive sequences are restricted away by the *Bst*UI digestion, the proportions of PCR products for most templates are expected to be in the linear range. PCR reactions were performed in a 100-μl volume, containing 0.4 μmol/l biotinylated H-24 primer; 4 U *Taq* DNA polymerase; 5% DMSO; 200 μmol/l dATP, dGTP, and dTTP; 150 μmol/l dCTP; 50 μmol/l biotin-11-dCTP (Roche) in a buffer provided by the supplier. The tubes were incubated for 3 min at 72 °C to fill in 5′-protruding ends of the ligated DNA and subjected to 20 cycles of amplification consisting of 1 min at 95 °C and 3 min at 72 °C in a PTC-225 thermocycler (MJ Research, Watertown, MA). The final extension was lengthened to 10 min.

2.2. Amplification of $p16^{Inka}$ gene

The 336 bp fragment of $p16^{Inka}$ gene was used as the target to determine the sensitivity of detection using colorimetric silver method. The positions of primer and capture probe are shown in Fig. 2. Forward primer, 5′-biotin-AAAGAGGAGGGGCTGGCTGGTCACCA-3′ and backward primer, 5′-TACCTGATTCCAATTCCCCTGCAAACT-3′. The PCR-reaction was performed in buffer containing 10 mmol/l Tris–HCl (pH 9.0), 50 mmol/l KCl, 0.1% Triton X-100, 5% DMSO, 1.75 mmol/l $MgCl_2$, 200 μmol/l dATP, dGTP, and dTTP, 150 μmol/l dCTP, 50 μmol/l biotin-11-dCTP (Roche) in a buffer provided by the supplier and 1 μl genomic DNA of gastric tumor tissue. The amplification was carried out for 35 cycles with denaturation at 95 °C for 1 min, annealing at 62 °C for 1 min and extension at 72 °C for 30 s.

2.3. Preparation of DNA microarray

The probes used in this study were synthesized and purified by Shenyou (Shanghai, China) and are summarized in Table 1. These probes are specially

GAAG**AAAGAGGAGGGGCTGGCTGGTCACCA**GAGGGTGGGGCGGACCG
CGTGCGCTCGGCGGCTGCGGAGAGGGGGAGAGCAGGCAGCGGGCGGCGG
GGAGCAGCATGGAGCCGGCGGCGGGGAGCAGCATGGAGCCTTCGGCTGA
CTGGCTGGCCACGGCCGCGGCCCGGGGTCGGGTAGAGGAGGTGCGGGCG
CTGCTGGAGGCGGGGGCGCTGCCCAACGCACCGAATAGTTACGGTCGGAG
GCCGATCCAGGTGGGTAGAGGGTCTGCAGCGGGAGCAGGGGATGGCGGGC
GACTCTGGAGGACGAAGTTTGC**AGGGGAATTGGAATCAGGTA**GCGC

Fig. 2. Underlining and bold indicate the capture probe sequences and primers of *p16*, respectively. Nucleotide sequences of the 5′ untranslated region and the first exon of the *p16* gene (Genbank, accession no. U12818.1 GI: 533724).

Table 1
Capture probe sequences

Capture probes	Sequence (5′→3′)
p16	5′-NH_2-$(T)_{10}$-GGGCGGACCGCGTGCGCTC-3′
E-cadherin	5′-NH_2-$(T)_{10}$-TCACCGCGTCTATGCGAGGCCG-3′
VHL	5′-NH_2-$(T)_{10}$-TTCTGCGCACGCGCACAGCCT-3′
hMLH1	5′-NH_2-$(T)_{10}$-GCGTTCGCGGGTAGCTACGATGA-3′

Underlining indicates the canonical restriction endonuclease *Bst*UI recognition sequence.

designed to fabricate a DNA microarray for determining the methylation status of four genes, including *p16*, *E-cadherin*, *VHL*, and *hMLH1*. They were suspended in sodium carbonate buffer (0.1 mol/l, pH 9.0) to a final concentration of 80 μmol/l. The various aminated oligonucleotides (capture probes) were spotted on the superaldehyde-coated glass slides (DAKO) using a PixSys5500 microarrayer (Cartesian Technology). The distance between two spots (center to center) was 600 μm. After spotting, the glass slides were incubated in a humid chamber at room temperature overnight, and then at 37 °C for 2 h. The slides were washed thoroughly in 0.1% SDS. After further treatment with a $NaBH_4$ solution for 15 min, the slides were ready for hybridization.

2.4. Hybridization of the biotinylated targets to DNA microarray

The biotinylated linker-PCR products were suspended in Unihybridization solution (1:3 dilution v/v; Telechem). Then, the mixture was denatured at 95 °C for 5 min, cooled to room temperature, and applied to the DNA microarray slides. The microarray hybridization was conducted in a moist hybridization chamber under a cover slip at 42 °C for 2 h. After hybridization, the slide was rinsed and washed at room temperature with 2 × SSC-0.1% SDS and 0.1 × SSC-0.1% SDS for a total of 15 min, respectively, and then dried by centrifugation at 600 rpm for 5 min.

2.5. Colorimetric silver detection of hybridized DNA microarray

The hybridized slides were incubated for 45 min with streptavidin–gold conjugate 10 × (Sigma, St. Louis, MO). The slides were then washed five times (1 min per wash) with a 10 mmol/l maleate buffer containing 15 mmol/l NaCl and 0.1% Tween, pH 7.5 and incubated at room temperature for 10 min in the Silver Blue solution. This Silver Blue solution is the combination of 1:1 (v/v) of two solutions: silver salt ($AgNO_3$) and hydroquinone. The slides were rinsed in the water, air-dried 5 h at 37 °C, and read with a fluorescence microscope equipped with a digital camera (Nikon, Japan).

2.6. Methylation-specific PCR (MSP) for methylation detection of $p16^{Inka}$ gene

Bisulfite processing of DNA was performed in principle as described by Frommer et al. [3] and modified by Clark et al. [16]. Briefly, 1 μg of genomic DNA was digested by *Eco*RI and denatured in 0.35 mol/l NaOH at 37 °C for 20 min. The bisulfite reaction was carried out in 3.2 mol/l sodium bisulfite and 0.5 mmol/l hydroquinone (Sigma) at 55 °C for 16–24 h. DNA was recovered by a desalting column (DNA Clean-Up System, Promega, Madison, WI) and desulphonated in 0.2 mol/l NaOH at 37 °C for 15 min, neutralized by ammonium acetate, precipitated with alcohol, dried and then dissolved in 30 μl of

Table 2
PCR primers used for methylation-specific PCR (MSP)

Primer set	Sense primer, 5′→3′	Antisense primer, 5′→3′	Size (bp)	Temperature (°C)	Genomic position
p16-M	TTATTAGAGGGTGGGGCGGATCGC	CCACCTAAATCGACCTCCGACCG	234	65	+167
p16-U	TTATTAGAGGGTGGGGTGGATTGT	CCACCTAAATCAACCTCCAACCA	234	60	+167

Sequence differences between methylation/modified and unmethylated/modified are underlined.
Primers were placed near the transcriptional start site. Genomic position is the location of the 5′ nucleotide of the sense primer in relation to the major transcriptional start site (Genbank, accession no. X94154).

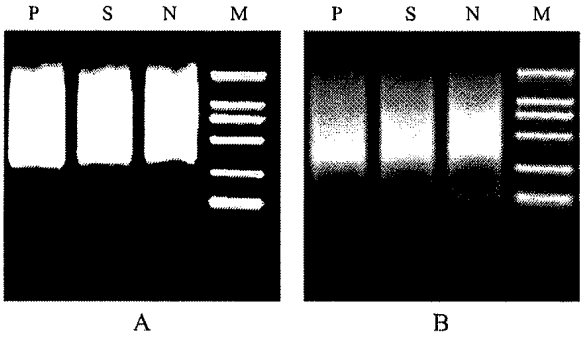

Fig. 3. The results of a test PCR. P, N, and S represent positive control, negative control, and sample, respectively. Maker (M): from top down, the bands are 2000, 1000, 750, 500, 250, and 100 bp, respectively. (A) Successful ligation reaction; (B) failure ligation reaction.

deionized water. After bisulfite processing, all unmethylated cytosine residues converted to uracil, whereas the methylated ones remained unchanged.

The 5′-CpG island regions of the $p16^{Ink4a}$ gene were amplified with primers for methylated and unmethylated DNA, respectively. The primer pairs were described in Table 2. The PCR-reaction was performed in buffer containing 10 mmol/l Tris–HCl (pH 9.0), 50 mmol/l KCl, 0.1% Triton X-100, 5% DMSO, 1.75 mmol/l $MgCl_2$, 0.2 mmol/l of each dNTP and 1 μl bisulfite-treated DNA. The amplification was carried out for 35 cycles (30 s at 95 °C, 30 s at the annealing temperature listed in Table 2, and 30 s at 72 °C), followed by a final 4-min extension at 72 °C. The PCR products were gel purified and sequenced using an automated sequence analyzer (ABI377A, Applied Biosystems, USA).

3. Results and discussion

3.1. Linker-PCR

To determine the efficiency of ligation, a test PCR was conducted. The PCR condition was the same as linker-PCR. Ten microliters of PCR products was analyzed on 1% agarose gel. A diffuse smear between 0.2 and 2.0 kb indicated a successful *Mse*I and linker ligation. However, a smear pattern different from that described above would indicate suboptimal digestion or ligation, indicating new DNA samples' need to be prepared (Fig. 3). Once the optimal smear pattern was achieved, the remaining ligated products were purified for methylation-sensitive restriction. Genomic fragments containing methylated sites are protected from the methylation-sensitive enzyme digestion and can be amplified by linker-PCR. Many of these linker-ligated *Mse*I fragments are expected to be present in the tumor sample due to aberrant methylation in the test site whereas the same unmethylated fragments are digested and not present in the normal amplicon after PCR.

3.2. Colorimetric silver detection of DNA microarray

The principle of the colorimetric method for detecting hybridized DNA on microarray is illustrated in

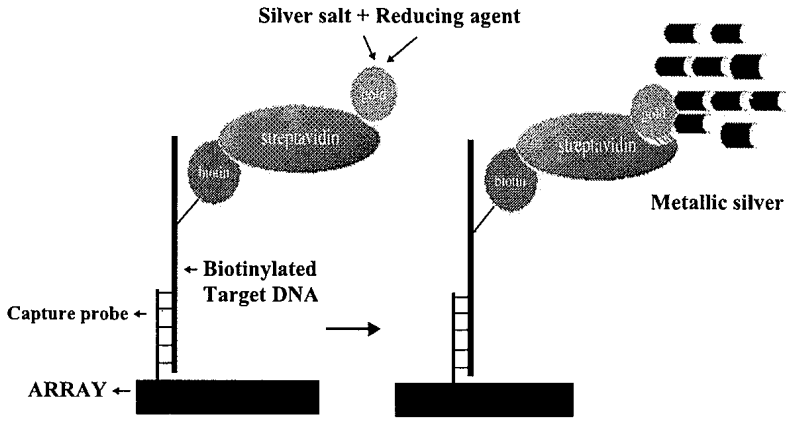

Fig. 4. Schematic representation of the colorimetric silver-staining detection of hybridized biotinylated targets on a microarray. The detection system is based on the use of streptavidin–nanogold particles and silver precipitation.

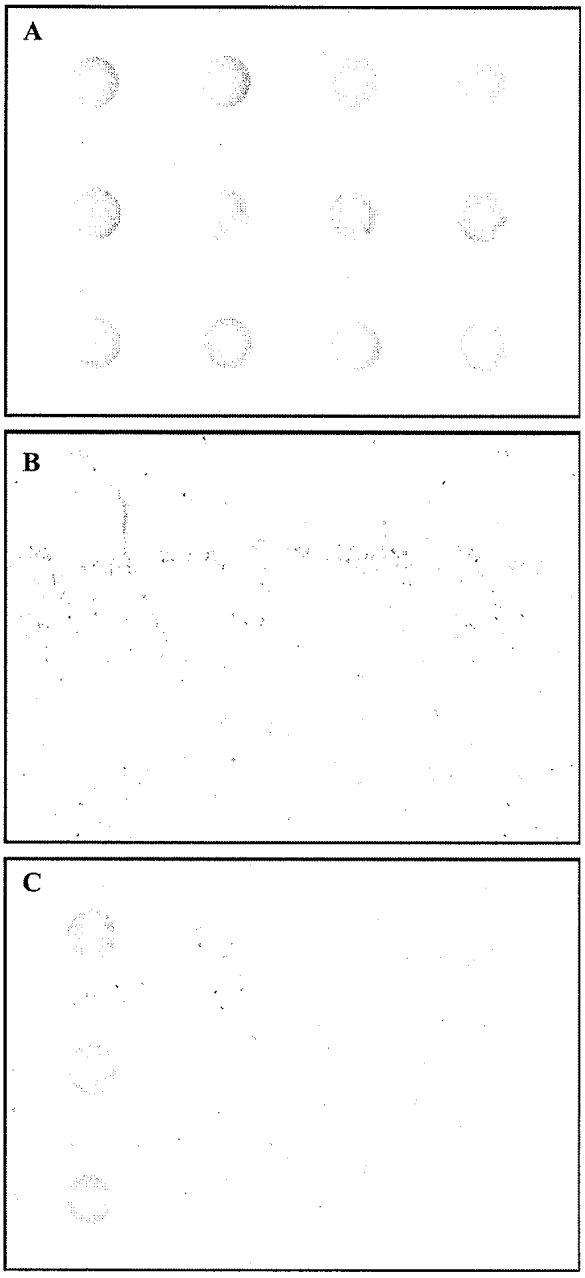

Fig. 5. Colorimetric silver detection of methylation for *p16*, *E-cadherin*, *VHL*, and *hMLH1* on the microarray. (A) The positive control (P); (B) the negative control (N); (C) sample (S). From left to right, the spots represent *p16*, *E-cadherin*, *VHL*, and *hMLH1*, respectively. Each oligonucleotides probe was spotted three times in a line.

Fig. 4. First, the target DNA is labeled with biotin by the incorporation of biotin-dCTP and biotinylated primer during amplification. After target hybridization on the microarray, streptavidin–nanogold particles are added for binding to biotin. Silver labeling relies on the catalytic activity of gold resulting in the reduction of silver ions into metallic silver and a deposition on gold particles. The silver shell around gold particles, in turn, autocatalyzes further silver depositions. At the end of the reaction, silver deposit onto gold particles leads to an increase of particle size going from 10 to about 1000 nm. This enhancement allows a direct visual detection of the microarray-labeled spots and a straightforward analysis using a colorimetric detector.

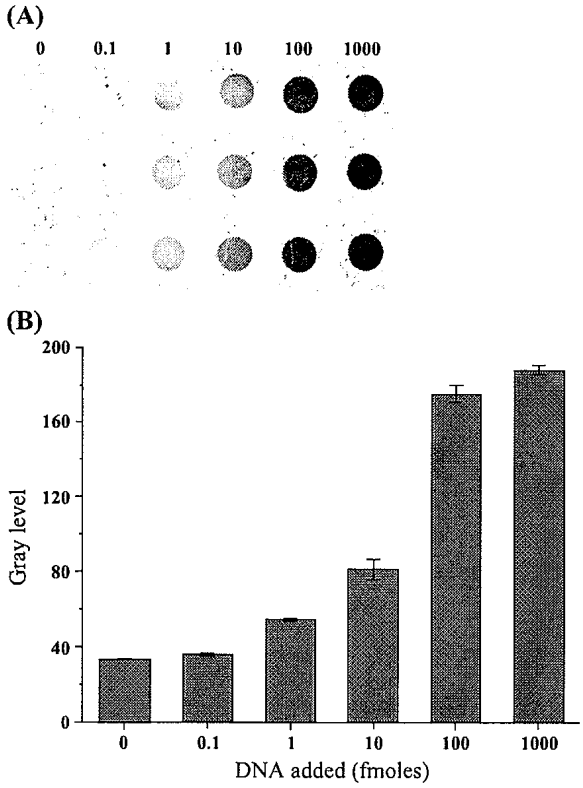

Fig. 6. Visualization of hybridizations of different concentrations of multibiotinylated $p16^{Ink4a}$ target DNA on the microarrays using silver blue detection method. The following DNA concentrations were hybridized: 0, 0.1, 1, 10, 100, and 1000 fmol in Fig. 5A. Quantification of raw data is presented in Fig. 5B. Results are expressed as the mean of gray level of the pixels inside a spot minus the background calculated as the mean of gray level of pixels around the spot. Results are the means of six replicates.

The microarray results indicated that *p16*, *E-cadherin*, *VHL*, and *hMLH1* were all methylated in the positive control (Fig. 5A). However, no methylation was found in these genes for the negative control (Fig. 5B). Fig. 5C displayed that *p16* gene was the only one methylated and the others were not methylated in the tumor sample. The positive control had 100% methylated cytosine in the test CpG sites, whereas the negative control had all unmethylated cytosine residues in the test CpG sites. Therefore, the fragments containing methylated sites are protected from the methylation-sensitive enzyme digestion and can be amplified by linker-PCR in the positive control and

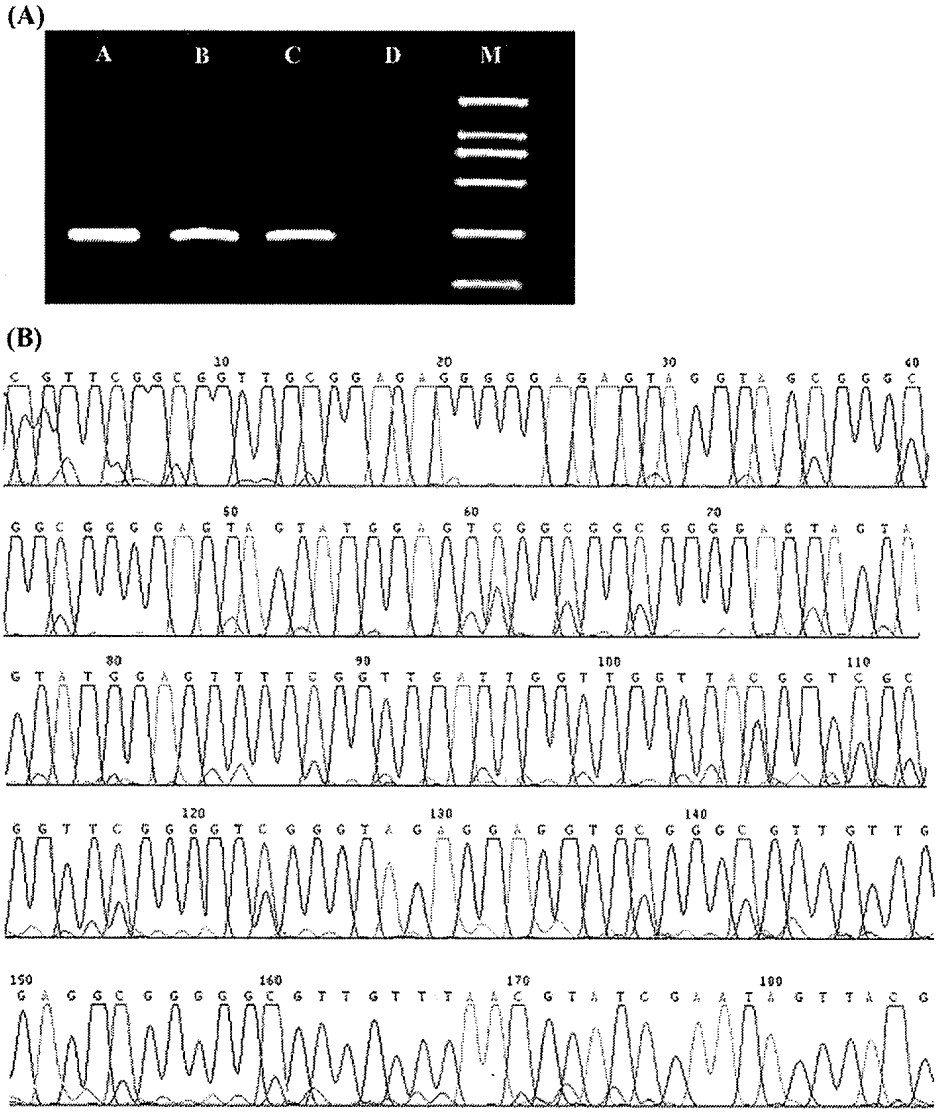

Fig. 7. Methylation-specific PCR (MSP) of *p16* gene (A). After bisulfite treating, amplification of DNA from gastric tumor tissue (A) and whole blood cells of healthy human (B) using unmethylated primer; amplification of DNA from gastric tumor tissue (C) and whole blood cells of healthy human (D) using methylated primer. Maker (M): from top down, the bands are 2000, 1000, 750, 500, 250, and 100 bp, respectively. Sequencing result of the PCR product with an ABI377A (B). The graph shows a part of the sequence. All cytosines in the CpG dinucleotides remain C, the sign of methylation.

sample, whereas the same unmethylated fragments are digested and not present in the negative control after PCR.

We then evaluated the sensitivity of target DNA detection after hybridization on microarray using colorimetric silver method (Fig. 6). Different concentrations of biotinylated p16 target DNA ranging from 0.1 to 1000 fmol in hybridization solution were incubated on separate arrays. Fig. 6 showed that as few as 0.1 fmol of target DNA amplicons could be detected on the arrays, whereas 1 fmol target DNA amplicons could be visualized by bare eyes. The detection signal increased steadily from 0.1 to 100 fmol of target DNA and then reached a plateau.

3.3. Methylation specific PCR (MSP) for methylation detection of p16 gene

Methylation-specific PCR (MSP), which can rapidly assess the methylation status of any group of CpG sites within a CpG island, independent of the use of methylation-sensitive restriction enzymes. This assay entails initial modification of DNA by sodium bisulfite, converting all unmethylated, but not methylated, and cytosines to uracil, and subsequent amplification with primers specific for methylated versus unmethylated DNA [5]. Primer pairs were designed to discriminate between methylated and unmethylated alleles following bisulfite treatment. To accomplish this, primer sequences were chosen for regions containing frequent cytosines, and CpG pairs near the 3′ end of the primers (to provide maximal discrimination in the PCR between methylated and unmethylated DNA) [5]. After bisulfite treatment, the amplification products were both detected with unmethylated primers (*p16*-U) in the genomic DNA from whole blood cells of healthy human and gastric tumor tissue. However, the amplification product was only obtained with methylated primers (*p16*-M) in the genomic DNA from the gastric tumor tissue (Fig. 7A). The results indicated that methylation was only detected in the gastric tumor tissue for $p16^{Ink4a}$ gene, which further confirmed the conclusion of the above analysis. The results of MSP were validated by bisulfite DNA sequencing. Fig. 7B displayed that the tested CpG sites were all methylated in the gastric tumor sample.

4. Conclusion

Colorimetric detection using silver precipitation has been here shown to be well adapted for detection and analysis of methylation on microarray. Its sensitivity is comparable to hybridization detection in fluorescence using a confocal scanner [14]. The high sensitivity is the result of an amplification step that brings small nanoparticles to grow up 1 million times in volume. The detection limit is 0.1 fmol of biotinylated target DNA hybridization on the array. With a controlled background, this technology allows a very good detection sensitivity of hybridized DNA onto glass microarrays that is equivalent to fluorescence. Because the combination of this gold label and silver enhancement is electron dense, a simple device such as the colorimetric array workstation can read deposits.

Another advantage of the methods is that silver deposit is stable and the microarray can be stored for a very long period of time. The colorimetric detection method is also well suited for supports other than glass, such as plastic supports, for instance, acrylic layer or polycarbonate. However, the fluorescent detection is not applicable on plastic arrays because of the strong autofluorescence of these polymers.

In summary, our experiments successfully demonstrated that the colorimetric silver detection of DNA microarray could be used as a cheap, useful, and sensitive tool to detect methylation status of the multiple genes in the future.

Acknowledgements

The National Key Fundamental Research Foundation, the National Natural Science Foundation of China, and the National High-Tech Research Programme supported this work.

References

[1] Baylin SB, Herman JG, Graff JR, Vertino PM, Issa JP. Alteration in DNA methylation, a fundamental aspect of neoplasia. Adv Cancer Res 1998;72:141–96.
[2] Bickle TA, Kruger DH. Biology of DNA restriction. Microbiol Rev 1993;57:434–50.
[3] Frommer M, McDonald LE, Millar DS, Collis CM, Watt F,

Grigg GW, et al. A genomic sequencing protocol that yields a positive display of 5-methylcytosine residues in individual DNA strands. Proc Natl Acad Sci U S A 1992;89: 1827–31.

[4] Kane MF, Loda M, Gaida GM, Lipman J, Misbra R, Goldman H, et al. Methylation of the *hMLH1* promoter correlates with lack of expression of *hMLH1* in sporadic colon tumors and mismatch repair-defective human cell lines. Cancer Res 1997;57:808–11.

[5] Herman JG, Graff JR, Myöhänen S, Nelkin BD, Baylin SB. Methylation-specific PCR: a novel PCR assay for methylation status of CpG islands. Proc Natl Acad Sci U S A 1996;93: 9821–6.

[6] Kuppuswamy MN, Hoffmann JW, Kasper CK, Spitzer SG, Groce SL, Bajaj SP. Single nucleotide primer extension to detect genetic diseases: experimental application to hemophilia B (factor IX) and cystic fibrosis genes. Proc Natl Acad Sci U S A 1991;88:1143–7.

[7] Hou P, Ji MJ, Ge CW, Shen JY, Li S, He NY, et al. Detection of methylation of human $p16^{Ink4a}$ gene 5′-CpG islands by electrochemical method coupled with linker-PCR. Nucleic Acids Res 2003;31:e92.

[8] Gitan RS, Shi H, Chen CM, Yan PS, Huang TH. Methylation-specific oligonucleotide microarray: a new potential for high-throughput methylation analysis. Genome Res 2002;12: 158–64.

[9] Adorján P, Distler J, Lipscher E, Model F, Müller J, Pelet C, et al. Tumour class prediction and discovery by microarray-based DNA methylation analysis. Nucleic Acids Res 2002; 30:e21.

[10] Hatada I, Kato A, Morita S, Obata Y, Nagaoka K, Sakurada A, et al. A microarray-based method for detecting methylated loci. J Hum Genet 2002;47:448–51.

[11] Balog RP, de Souza YE, Tang HM, DeMasellis GM, Gao B, Avila A, et al. Parallel assessment of CpG methylation by two-color hybridization with oligonucleotide arrays. Anal Biochem 2002;15:301–10.

[12] Hou P, Ji MJ, Liu ZC, Shen JY, Cheng L, He NY, et al. A microarray to analyze methylation patterns of $p16^{Ink4a}$ gene 5′-CpG islands. Clin Biochem 2003;36:197–202.

[13] Hacia JG. Resequencing and mutational analysis using oligonucleotide microarray. Nat Genet 1999;21:42–7.

[14] Alexandre I, Hamels S, Dufour S, Collet J, Zammatteo N, De Longueville F, et al. Colorimetric silver detection of DNA microarrays. Anal Biochem 2001;295:1–8.

[15] Yan PS, Efferth T, Chen HL, Lin J, Rodel F, Fuzesi L, et al. Use of CpG island microarrays to identify colorectal tumors with a high degree of concurrent methylation. Methods 2002; 27:162–9.

[16] Clark SJ, Harrison J, Paulb CL, Frommer M. High sensitivity mapping of methylated cytosines. Nucleic Acids Res 1994;22: 2290–997.

Available online at www.sciencedirect.com
SCIENCE DIRECT®
ELSEVIER
Journal of Virological Methods 121 (2004) 79–84
Journal of Virological Methods
www.elsevier.com/locate/jviromet

Analytical performance of and real sample analysis with an HBV gene visual detection chip

Ye-Fu Wang*, Jun-Tao Shen, Hui-Hui Liu

College of Life Sciences, Wuhan University, Wuhan 430072, PR China

Received 21 October 2003; received in revised form 19 May 2004; accepted 7 June 2004

Abstract

A novel hepatitis B virus (HBV) gene detection chip has been developed. The HBV-specific probes immobilized on glass slides were hybridized with polymerase chain reaction (PCR) products of different serum samples. The hybridization signal can be easily visualized upon a sandwich assay with nanoparticle amplification. The analytical performance (e.g., specificity, sensitivity, and accuracy) of this method has been evaluated. The chip-based detection method possesses a greater sensitivity and a better reproducibility than some of the conventional immunological or molecular biological methods (e.g., enzyme-linked immunosorbent assay, ELISA) and is simple, cost-effective, and highly selective.

Keywords: DNA sensing; HBV; Gold nanoparticles; Silver staining; Gene chip

1. Introduction

The human B hepatitis, which is a variant of Hepadnaviridae and can induce chronic or acute hepatitis, is one of the most widespread infectious diseases. Nowadays, about 200–300 million people are still suffering from this detrimental or fatal disease (Liu et al., 1999) around the world. In China alone, about 60% of the people have been infected with hepatits B (Liu et al., 1999). It is thus imperative to develop a simple, rapid, and effective methods to detect hepatitis B virus (HBV). Presently, enzyme-linked immunosorbent assays (ELISA) is the main method to clinically diagnose HBV (Moriya et al., 2002), However, information obtained from this method is indirect and the method itself has a low sensitivity. On the other hand, the endogenous DNA amplification and dot blot methods can detect only 0.1 pg HBV DNA, which corresponds to 3×10^4 virosomes (Liu et al., 1999). The sensitivity of clinical diagnosis has been enormously improved by the PCR method, which can sense 10^{-5} pg HBV DNA (Desmet et al., 1994). In addition to the above methods, methods based on the use of radioactive isotopes (Jilbert, 2000; Barlet et al., 1994), fluorescence dye markers (Park et al., 2000; Stefanini et al., 1983), or chemiluminescence labels (Barlet et al., 1994; Bronstein et al., 1989; Young et al., 2002; Cheng et al., 1999; Qi, 1998) have also been developed for the detection of viral hepatitis. However, the radioactive isotope is difficult to handle and hazardous; the fluorescence markers are prone to bleaching; and the chemiluminescence labels may yield irreproducible results in some cases (Moriya et al., 2002). Therefore, an alternative method characterized by simplicity, speed, and sensitivity is desired for the diagnosis of HBV in a typical clinical laboratory.

Metal nanoparticles, owing largely to their unique optical and mechanical properties, have found a wide range of applications in bio-sensing and chemo-sensing technologies (Reichert et al., 2000). Colloidal gold labeling in conjunction with silver enhancement was first used in histo-chemical microscopy for the visualization of DNA and protein samples and also cell surfaces (Zehbe et al., 1997; Birrell et al., 1986; Scopsi et al., 1986; Schneider et al., 2002; Herter et al., 1993). In the past few years, scanometric (Taton et al.,

* Corresponding author. Tel.: +86 27 87217627; fax: +86 27 87878354.
E-mail address: wangyf25@sohu.com (Y.-F. Wang).

0166-0934/$ – see front matter © 2004 Elsevier B.V. All rights reserved.
doi:10.1016/j.jviromet.2004.06.004

2000; Storhoff et al., 1998), colorimetric (Bronstein et al., 1989; Alexandra et al., 2001; Ballard and Boxall, 1997), and electrochemical methods (Wang et al., 2001; Wang et al., 2002), among others, have been devised for the detection of DNA hybridization or protein–protein interactions with the aid of silver deposition and signal enhancement. The resulting signal enhancement makes visual detection possible, simplifying the analytical procedure and obviating the need for special instrumentation.

Despite the tremendous potential of this approach, only few studies have focused on the detection of real samples of viral origins. Taton et al. (2000) and Storhoff et al. (1998) were the first to use oligonucleotide-capped gold nanoparticles to analyze oligonucleotide samples on DNA microarray slides. We have shown recently, that such an approach could be conveniently extended to the simultaneous visual detection of HBV and hepatitis C virus (Wang et al., 2003). In a separate study, it was also demonstrated that sequence-specific gene analysis through the microarray chips by a silver-enhanced DNA hybridization could be conducted with a scanning electrochemical microscope, and the sensitivity of these measurement were comparable to that of fluorescence measurements (Wang et al., 2002). However, the use of gold nanoparticle labeling and silver enhancement on a biochip platform for the detection of hepatitis viral genes, produced from real samples, has not been reported. A systematic evaluation of the performance of such a chip for the visual detection of real samples is described in this paper.

About 99 different HBV whole genome sequences (GenBank) and many HBV sub-types, such as adw, adr, ayw, etc. (defined in serology) or type A–F (termed in molecular biology), have been identified. Thus, to diagnose the sub-types of HBV, or analysis by a DNA microarray spotted with probes specific to individual sub-types appears to be an attractive approach. In events where only HBV detection is necessary, analysis can be performed by detecting the ubiquitous pre-S gene among all of the HBV sub-types. To demonstrate the feasibility of chip-based analysis for facile and sensitive HBV detection, oligonucleotide capture probes whose sequences were complementary to a short segment of the pre-S gene were spotted onto chemically modified glass slides. A sandwich format assay which involving subsequent attachment of gold nanoparticles functionalized with another probe (detection probe) specific to a different segment of the pre-S gene were followed. The hybridization signal can be significantly enhanced (visualized) by silver precipitation at the spots where the sandwich-like DNA duplexes have formed. By analyzing a large number of serum samples from different sources of the HBV gene, the method was validated by comparing the analytical "figures of merit" (specificity, sensitivity, and reliability) to those of traditional immunology methods, such as the enzyme-linked immunosorbent assay and fluorescence quantitative PCR. The visual detection of HBV saves the need of sophisticated instruments. The chips are easy to fabricate and simple to use, affording a possible alternative for an accurate detection route for clinical diagnosis.

2. Experimental

2.1. Serum samples

One hundred seventy eight HBV-positive serum samples were provided by Xiehe Hospital (Wuhan, China). Another set, also containing 178 samples, was collected from blood donors at Yunmeng Blood Station (Hubei Province, China). Some HBV-positive serum samples were also obtained from Zhongnan Hospital and the Hubei Import & Export Disease Inspection Bureau.

2.2. Instrument and reagent

The chip substrate was a glass slide (Fanchuan™, China). All reagents were treated with 0.1% DEPC (diethyl pyrocarbonate, Sigma). The containers were baked at 180 °C for 8 h. Disposable Eppendorf tubes (EP tubes), test tubes, and tips were sterilized. The centrifugation (Zentrifugen D-78532 Tuttlingen, Germany) was used for the sample separation. PCR regents were purchased from Promega Co. Primers were synthesized by Beijing Saibaisheng Genetech Co. Ltd. Sequences of the two primers for HBV gene amplification were 5′-GGACTTCTCTC AATTTTCTAGGG-3′ and 5′-CAAATGGCACTAGTAAACTGAGC-3′ respectively. The probes have the following sequences, 5′-GGACTTCTC-TCAATTTTCTAGGG-3′ (capture probe on the chip) and 5′-GCTCAGTTTACTAGTGCCATTTGTTTTTTTTT T-SH-3′ (probe linked to the gold nanoparticles via the thiol tether group). For PCR of the *Escherichia coli* sample, the Sequences of the two primers were: 5′-ATGAAGGATTATGTA ATGGAA-3′ and 5′-ACAGCCGTTGATCTGGCTATG-3′, respectively. All these primers and probes were obtained from Shanghai ShengGong Bioengineering Co. Ltd. The citric buffer was prepared by dissolving 2.55 g citric acid and 2.35 g sodium citrate in 100 mL of distilled water. There were four solutions for the silver staining process. Solution A contained 1% glutin (60 mL), solution B was a citric acid buffer (pH 3.5, 10 mL), solution C had 1.7 g hydroquinone dissolved in water, and solution D was a silver nitrate solution comprising 50 mg silver nitrate and 2 mL of distilled water. Prior to use, solutions A–C were thoroughly mixed and the resultant mixture was added into solution D.

2.3. Preparation of gold nanoparticles

Gold nanoparticles were prepared as described Liu et al. (1999). Briefly, 100 mL of 0.01% $HAuCl_4$ was heated until boiling. 5 mL of 1% sodium citrate solution was then added into the $HAuCl_4$ solution. After boiling for 15 min, a red color was developed. Upon cooling to room temperature, the final volume of the mixture was adjusted to 100 mL with deionized water and subsequently filtered through a 0.45 μm nylon membrane.

2.4. Extraction of the HBV DNA

Twenty microlitre serum sample and 30 μL lytic solution (0.5% NP-40, 0.5% Tween-20) were added into an EP tube. Upon standing for 10 min, the mixture was centrifuged at 12500 rpm for 10 min at 4 °C. Finally, 20 μL of the supernatant, which contained HBV DNA, was transferred into another EP tube.

2.5. PCR experiment

The supernatant obtained above was mixed with the primers, dNTPs, and Taq DNA polymerase (2 U). After an initial heating at 95 °C for 5 min, 25 PCR cycles, which consisted of denaturation at 94 °C for 45 s, annealing at 58 °C for 45 s, and extension at 72 °C for 45 s, were performed. The final mixture was allowed to stand at 72 °C for 5 min. The PCR products were checked using agarose gel electrophoresis with ethidium bromide (0.5 g/mL) staining.

2.6. Detection with the HBV Gene chip

The fabrication of the HBV gene detection chip was described in a previous paper (Wang et al., 2003). The procedure includes modification of the glass slides with 1,4-phenylene diisothiocyanate (PDITC), followed by the attachment of an amino-modified HBV Pre-S DNA probe with a sequence of 5′-H_2N-(CH_2)6-0-$(P0_3)$-(T)io-GGACTTCTCTCAATTTTCTAGGG-3′. In order to evaluate the relationship between the probe concentration and the final chip performance, 3.29×10^{-5} M probe stock solution was diluted down with 10-fold increments between 10 and 10^8-fold (a total of eight concentrations). The chip was incubated in each solution and allowed to hybridize with the PCR products of the HBV pre-S gene. Twenty microlitre solution containing gold nanoparticles capped with the detection probe that is complementary to a different segment of the pre-S gene was then cast onto the chip. Finally, the development of the spots for visual detection was accomplished by silver staining.

3. Results and discussion

Concentrations of both the capture probe (on the glass slide) and the detection probe (capping the gold nanoparticles) were first optimized for the method. Spots covered with capture probe from different concentrations were exposed to a sample containing the PCR products of the HBV pre-S gene. After the gold nanoparticle adsorption and silver staining steps, the effect of capture probe concentration on the HBV gene detection (Fig. 1) was visualized. It can be seen that a 1000-fold dilution of the stock probe solution (final concentration = 3.28×10^{-8} M) yielded the highest staining intensity. This trend is conceivable. At low probe concentrations, the surface coverage of the capture probe is too scarce

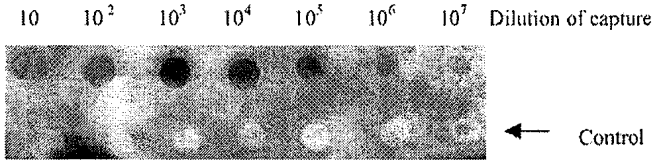

Fig. 1. An image of an HBV gene chip covered with spots formed with capture probe solution diluted from a 3.28×10^{-5} M stock solution (dilution factors shown above the image). Top row: spots that have undergone the sandwich assay with the HBV gene sample and the detection probes and subsequently developed by the silver precipitation (staining); Bottom row: spots that were treated without hybridization with an HBV gene sample.

to cause an extensive duplex formation on the chip. However, at high probe concentrations, the density of the immobilized capture probes could be so large that the duplex formation would be spatially hindered by the adjacent probes on the surface. Meanwhile, with a gray scanner, the gray degree of each spot was also measured (Table 1). Thus quantitatively confirming the above opinion.

The relationship between the concentration of the detection probe capping the gold nanoparticles and the signal intensity was also examined. The solution of gold nanoparticle-labeled with the detection probe (original concentration = 3.29×10^{-5} M) was diluted 10, 50, 100, 1000, and 10000 times with deionized H_2O. The intensity of the silver stains was found to decrease with lower concentration of the detection probe-capped gold nanoparticles (data not shown). The results indicated that dilution between 100 and 1000 times could still produce easily discemable spots on the glass slide.

3.1. Specificity

Fifty HBV-positive serum samples and 50 HBV-negative serum samples were both analyzed with agarose gel electrophoresis and the gene detection chips. As shown in Fig. 2a that a prospect 430 bp band of HBV Pre-S gene appeared. The band is associated with all HBV-positive samples and one HBV-negative sample after the PCR amplification. Moreover, after the PCR products were purified, results indicated that the PCR products indeed contained a fragment of the HBV pre-S gene, in accordance with the GenBank's HBV.abO33553's S261-692bp. When the PCR products were analyzed by the "sandwich assay", visual detection was achieved with the silver particle precipitation occurring only at spots where the HBV pre-S gene had formed duplexes with the surface-confined probes (top row in Fig. 2b). To further demonstrate that the method is sequence-specific, two control experiments were conducted and the results are shown in Fig. 2b. In the first control (middle row), the capture probes were replaced with probes whose sequence is selective towards the hepatitis G viral gene. As can be seen, essentially no spots were developed, suggesting that the spots displayed in the top row are attributable to the hybridization of the HBV pre-S gene with the capture probe. In the second control (bottom row), an entirely different gene detection system, wherein the PCR products

Table 1
Grayness scanning of developed gene chip in Fig. 1

Parameters	1	2	3	4	5	6	7
Row A							
Brightness	137.04	136.17	91.20	110.35	120.14	155.4	184.08
Ratio (B/D)	12.73	23.10	38.39	30.74	28.18	22.4	14.12
Standard deviation	134	128	77	102	119	153	192
Pels	400	400	400	400	400	400	400
Row B							
Brightness	163.74	184.33	188.51	178.07	199.6	193.22	187.29
Ratio (B/D)	15.34	15.49	16.07	14.56	14	14.03	14.01
Standard deviation	160	192	192	178	204	192	192
Pels	400	400	400	400	400	400	400

of *tna* gene fragment from *E. coli* were hybridized with probes of different sequences, was adopted. Sequences of the capture and detection probes were 5′-H_2N-(CH_2)6-CTTTAAACATCTCCCTG AACCGTTCCGCATTCG-3′ and 5′-CGTTCTCTAACTATTTCTTTGATACCACGCA GG-SH-3′. The appearance of the spots in Fig. 2b indicates that the "sandwich" assay followed by silver staining, is not just restricted to the sequences of HBV genes. Sensitivity: It is worth mentioning that the method is highly sensitive. Spots in the top row of Fig. 2b correspond to the detection of 10^3 copies/mL of the HBV pre-S gene. This is in contrast to the detection level achievable by agarose gel electrophoresis. Shown in Fig. 3 is an agarose gel electrophoresis diagram of 9 lanes. Lanes 1–4 and 6–9 correspond to the serial dilutions of positive serum samples (containing 10^8–10^9 copies/mL),

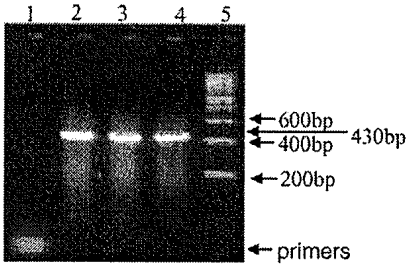

(a)

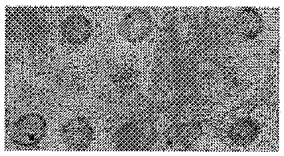

(b)

Fig. 2. (a) An agarose gel electrophoresis diagram of the HBV-positive PCR products. Lane 1: marker; lanes 2–4: PCR products of the HBV-positive samples (432 bp); and lane 5: an HBV-negative serum sample, (b) An image of an HBV gene detection chip upon reaction with the PCR products generated from the serum sample. Top row: HBV-positive (ca. 10^3 copies/mL) hybridization signals on the spots of HBV-specific capture probes; middle row: negative control, the HBV gene sample cast no spots upon the immobilized probes whose sequence (5′H_2N-(CH_2)6-GTGGTGGATGGGTGATGACA-3′) is selective towards the hepatitis G viral gene; and bottom row: positive control, spots castted by sandwich format hybridization of PCR product of TNA gene fragment from *E. coli*, and its correspondance capture probe (on the chip) and detection probe (capping the gold nanoparticles).

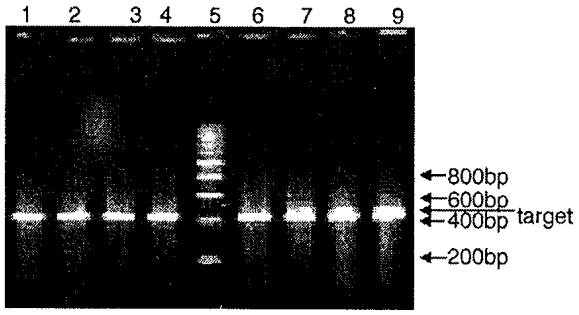

Fig. 3. An agarose gel electrophoresis diagram of the PCR products of HBV-positive sera. Lanes 1–4, 6–9 represent the HBV-positive samples diluted at intervals of 2, 2^2–2^8, respectively, and spot 5 corresponds to a marker.

by 2-fold increment each, and lane 5 is a marker. On the basis of the diagram, the agarose gel electrophoresis method could only detect samples that had been diluted by 2^5–2^6 fold (i.e., 10^6–10^7 copies/mL). It is therefore evident that the gene detection chip is 2–3 orders more sensitive than the agarose gel electrophoresis method.

3.2. Method validation

To establish the viability of the method for real sample analysis, 50 HBV-positive and 50-negative serum samples, verified with fluorescence quantitative PCR, were tested with the HBV gene chip detection method. A standard deviation value of at least 15 between positive signal versus background was used to determine a detection result. Ten replicate measurements were carried out for each sample on different days. Ninety nine percent of the gene chip measurements of the HBV-positive samples are consistent with those from the fluorescence quantitative PCR results and all of the gene chips exposed to HBV-negative samples did not reveal any positive detection results. Thus, it is concluded that the method is highly accurate and reliable.

Table 2 shows the results of the analyses performed on 178 serum samples collected from blood donors and 178 serum samples from patients at a hospital, in comparison to both ELISA and fluorescence quantitative PCR methods. It is clear from Table 2 that results based on the HBV gene chip detection are completely consistent with the fluorescence quantita-

Table 2
Comparison of the gene chip, ELISA, and quantitative fluorescence PCR measurements

Samples	Number of samples	Chip		ELISA		Quantitative fluorescence PCR	
		Number of positive	Percent of positive	Number of positive	Percent of positive	Number of positive	Percent of positive
Blood donors	178	46	25.8	45	25.3	46	25.8
Patients	178	15	8.4	14	7.9	15	8.4

Note: A deviation of at least 15 between positive signal vs. background was used.

tive PCR measurements and highly comparable to the ELISA determination. Therefore, the fidelity of the HBV gene visual detection is high and the protocol should satisfy the stringent requirements for clinical testing.

4. Conclusion

A new method based on gene chip, has been developed for the detection of HBV gene in different serum samples. The sandwich hybridization consisted of an initial hybridization between the PCR amplified HBV gene and the capture probe on the chip and a follow-up hybridization of the HBV gene with a second probe-capped onto gold nanoparticles. The optimal concentrations for immobilizing the capture probe and for capping the gold nanoparticles were determined. Visual detection was accomplished via deposition of silver particles (staining) onto spots where sandwich hybridizations had taken place. The specificity, sensitivity, and reliability of this method had been assessed, and the detection limit for HBV was found to be as low as picomolar. Performance of the method was compared to that of conventional molecular biological or immunological techniques (e.g., ELISA, fluorescence quantitative PCR, and gel electrophoresis) and the consistency indicates that this method may afford a new avenue and sensitive detection of hepatitis viruses and/or their sub-types. The method is simple and cost-effective and does not require dedicated or specialized instrumentation.

Acknowledgements

This work was supported by the Hubei Provincial R&D Program, and Wuhan Bureau of Science & Technology. Many thanks are also acknowledged to Xiehe Hospital, Yunmeng blood station, and Hubei Import & Export Disease Inspection Bureau for supplying the serum samples used in this study.

References

Alexandra, I., Hamels, S., Dufour, S., Collet, J., Zammatteo, N., De Longueville, F., Gala, J.-L., Remacle, J., 2001. Colorimetric silver detection of DNA microarrays. Anal. Biochem. 295, 1–8.

Barlet, V., Cohard, M., Thelu, M.A., Chaix, M.J., Baccard, C., Zarski, J.P., Seigneurin, J.M., 1994. Quantitative detection of hepatitis B virus DNA in serum using chemiluminescence: comparison with radioactive solution hybridization assay. J. Virol. Methods 49, 141–152.

Ballard, A.L., Boxall, E.H., 1997. Colorimetric point mutation assay: for detection of precore mutants of hepatitis B. J. Virol. Methods 67, 143–152.

Birrell, G.B., Habliston, D.L., Hedberg, K.K., Griffith, O.H., 1986. Silver-enhanced colloidal gold as a cell surface marker for photoelectron microscopy. J. Histochem. Cytochem. 34, 339–345.

Bronstein, I., Voyta, J.C., Edwards, B., 1989. A comparison of chemiluminescent and colorimetric substrates in a hepatitis B virus DNA hybridization assay. Anal. Biochem. 180, 95–98.

Cheng, Y., Dubovoy, N., Hayes-Rogers, M.E., Stewart, J., Shah, D., 1999. Detection of IgM to hepatitis B core antigen in a reductant containing, chemiluminescence assay. J. Immunol. Methods 230, 29–35.

Desmet, V.J., Gerber, M., Hoofnagle, J.H., Manns, M., Scheuer, P.J., 1994. Classification of chronic hepatitis: diagnosis, grading and staging. Hepatology 19, 1513–1520.

Herter, P., Laube, G., Gronczewski, J., Minuth, W.W.P., 1993. Silver-enhanced colloidal-gold labelling of rabbit kidney collecting-duct cell surfaces imaged by scanning electron microscopy. J. Microstruct. 171, 107–115.

Jilbert, A.R., 2000. In situ hybridization protocols for detection of viral DNA using radioactive and nonradioactive DNA probes. Method Mol. Biol. 123, 177–193.

Liu, X.G., Qi, Z.B., Xiong, S.S., 1999. Laboratory Diagnostics of Viral Hepatitis,, second Ed. People Health Press, pp. 3–76.

Moriya, T., Kuramoto, I.K., Yoshizawa, H., Holland, P.V., 2002. Distribution of hepatitis B virus genotypes among American blood donors determined with a PreS2 epitope enzyme-linked immunosorbent assay kit. J. Clin. Microbiol. 40, 877–880.

Park, J.H., Cho, E.W., Lee, D.G., Park, J.M., Lee, Y.J., Choi, E.A., Kim, K.L., 2000. Receptor-mediated endocytosis of hepatitis B virus preSl protein in EBV-transformed B-cell line. J. Microbiol. Biotech. 10, 844–850.

Qi, Y.P., 1998. Genes and Principle of Gene Manipulation. Wuhan University Press, Wuhan (p. 5).

Reichert, J., Csaki, A., Kohler, J.M., Fritzsche, W., 2000. Chip-based optical detection of DNA hybridization by means of nanobead labeling. Anal. Chem. 72, 6025–6029.

Stefanini, G.F., Meliconi, R., Miglio, F., Mazzetti, M., Baraldini, M.A.F., Gasbarrini, G., 1983. Lymphocytotoxicity against autologous hepatocytes and membrane-bound IgG in viral and autoimmune chronic active hepatitis. Liver 3, 36–45.

Storhoff, J.J., Elghanian, R., Mucic, R.C., Mirkin, C.A., Letsinger, R.L., 1998. One-pot colorimetric differentiation of polynucieotides with single base imperfections using gold nanoparticle probes. J. Am. Chem. Soc. 120, 1959–1964.

Schneider, G., Anderson, E., Vogt, S., Knoehel, C., Weiss, D., Legros, M., Larabell, C., 2002. Computed tomography of cryogenic cells. Surf. Rev. Lett. 9, 177–183.

Scopsi, L., Larsson, L.I., Bastholm, L., Nielsen, M.H., 1986. Silver-enhanced colloidal gold probes as markers for scanning electron microscopy. Histochemistry 86, 35–41.

Taton, T.A., Mirkin, C.A., Letsinger, R.L., 2000. Scanometric DNA array detection with nanoparticle probes. Science 289, 1757–1760.

Wang, J., Polsky, R., Xu, D.K., 2001. Silver-enhanced colloidal gold electrochemical stripping detection of DNA hybridization. Langmuir 17, 5739–5757.

Wang, J., Song, F., Zhou, F., 2002. Silver-enhanced imaging of DNA hybridization at DNA microarrays with scanning electrochemical microscopy. Langmuir 18, 6653–6658.

Wang, Y.F., Pang, D.W., Zhang, Z.L., Zheng, H.Z., Cao, J.P., Shen, J.T., 2003. Visual gene diagnosis of HBV and HCV based on nanoparticle probe amplification and silver staining enhancement. J Med. Virol. 70 (2), 205–211.

Young, K.C., Chang, T.T., Hsiao, W.C., Cheng, P.N., Chen, S.H., Jen, C.M., 2002. A reverse-transcription competitive PCR assay based on chemiluminescence hybridization for detection and quantification of hepatitis C virus RNA. J. Virol. Methods 103, 27–39.

Zehbe, I., Hacker, G.W., Su, H., Hauser-Kronberger, C., Hainfeld, J.F., Tubbs, R., 1997. Sensitive in situ hybridization with catalyzed reporter deposition, streptavidin-nanogold, and silver acetate autometallography: detection of single-copy human papillomavirus. J. Pathol. 150, 1553–1561.

Nucleic Acids Research, 2005, Vol. 33, No. 2 **e17**
doi:10.1093/nar/gni019

An oligonucleotide microarray for microRNA expression analysis based on labeling RNA with quantum dot and nanogold probe

Ru-Qiang Liang, Wei Li[1], Yang Li[1], Cui-yan Tan, Jian-Xun Li[2], You-Xin Jin[1] and Kang-Cheng Ruan*

Key Laboratory of Proteomics and [1]State Key Laboratory of Molecular Biology, Institute of Biochemistry and Cell Biology, Shanghai Institutes for Biological Sciences, Chinese Academy of Sciences, Graduate School of the Chinese Academy of Sciences, 320 Yue-Yang Road, Shanghai 200031, China and [2]Department of Oral Biology, College of Dentistry, University of Illinois at Chicago, Chicago, IL 60612, USA

Received August 24, 2004; Revised December 3, 2004; Accepted January 10, 2005

ABSTRACT

MicroRNAs (miRNAs) play important regulatory roles in animals and plants by targeting mRNAs for cleavage or translational repression. They have diverse expression patterns and might regulate various developmental and physiological processes. Profiling miRNA expression is very helpful for studying biological functions of miRNAs. We report a novel miRNA profiling microarray, in which miRNAs were directly labeled at the 3′ terminus with biotin and hybridized with complementary oligo-DNA probes immobilized on glass slides, and subsequently detected by measuring fluorescence of quantum dots labeled with streptavidin bound to miRNAs through streptavidin–biotin interaction. The detection limit of this microarray for miRNA was ~0.4 fmol, and the detection dynamic range spanned about 2 orders of magnitude. We made a model microarray to profile 11 miRNAs from leaf and root of rice (*Oryza sativa* L. ssp. *indica*) seedlings. The analysis results of the miRNAs had a good reproducibility and were consistent with the northern blot result. To avoid using high-cost detection equipment, colorimetric detection, a method based on nanogold probe coupled with silver enhancement, was also successfully introduced into miRNA profiling microarray detection.

INTRODUCTION

MicroRNAs (miRNAs) are a highly evolutionarily conserved class of small noncoding RNAs that can play important regulatory roles in animals and plants by targeting mRNAs for cleavage or translational repression (1,2). They are ~22 nt transcripts cleaved from ~70 nt hairpin precursors in animals or ~100 nt in plants with signature 3′-hydroxyl and 5′-monophosphate termini of an RNase III cleavage event that leaves a 2 nt overhang. They have diverse expression patterns and might regulate various developmental and physiological processes. Misregulation of miRNA function might contribute to human disease (2). So, profiling miRNA expression is very important in studying the biological functions of miRNAs.

Large-scale studies on miRNA expression profiles were carried out in many model organisms by using northern blot analysis and miRNA cloning (3–8). Both of these methods are time consuming. DNA microarray technology has resulted in profiling expression of thousands of genes simultaneously. Applying similar technology would make miRNA profiling more efficient. To profile expression patterns of neuronal miRNAs, Krichevsky *et al.* designed an oligonucleotide array on charged nylon membranes and detected the miRNAs by labeling filtered low molecular weight RNA with radioactive isotopes (9). To avoid the need of large amounts of total RNA and using radioactive isotopes as in the above methods, Liu *et al.* developed an oligonucleotide microchip on glass slides to profile miRNA by detecting the 5′ biotin-labeled cDNAs of miRNAs introduced through a random primer (10,11). However, this labeling method may be ineffective because of the inability for 8 nt random primer to bind on such short templates as ~22 nt miRNAs. Recently, Miska *et al.* developed a microarray for miRNA expression analysis, in which miRNAs were ligated to 3′ and 5′ adaptor oligonucleotides followed by reverse transcription and amplified by PCR with Cy3-labeled primer to label the sense strand of PCR products (12). Yet, miRNA population may be distorted by hybridization with

*To whom correspondence should be addressed. Tel: +86 21 5492 1168; Fax: +86 21 5492 1011; Email: kcruan@sibs.ac.cn
Correspondence may also be addressed to You-Xin Jin. Tel: +86 21 5492 1222; Fax: +86 21 5492 1011; Email: yxjin@sunm.shcnc.ac.cn

cDNAs or sense strands of PCR product of miRNAs because of enzymatic reverse transcription and/or amplification (13). To direct-label RNA, Babak *et al.* used a platinum-based chemical labeling reagent for nucleic acids (Ulysis Alexa Fluor from Molecular Probes) (14). However, this reagent cannot label miRNAs lacking G residuals, and labeling of residuals in miRNA may interfere the following hybridization. The best target for miRNA profiling microarray hybridization should be fluorescently labeled miRNAs directly at either 3′ adjacent hydroxyl or 5′-monophosphate terminus. One method to direct-label RNA at 3′ terminus is by using T4 RNA ligase to couple the 3′ end of RNA to a fluorescent-modified ribodinucleotide (13,15). This method has been successfully used to investigate the role of small noncoding RNAs by directly labeling total RNA and hybridizing the target to whole-genome querying microarrays (16). Recently, Thomson *et al.* used this method in direct-labeling of miRNAs on a microarray platform for analysis of miRNA gene expression (17). However, this method needs labeled donor ribodinucleotide and RNA ligase that have a poor reputation for reliability and differential ligation efficiency toward the acceptor nucleotide on the miRNA.

We have developed a method for small RNA sequencing by direct fluorescence labeling in which 3′ adjacent hydroxyl of RNA were periodate-oxidized into a dialdehyde followed by conjugation with fluorescein-5-thiosemicarbazide through a condensation reaction, resulting in that trace amounts (<10 fmol) of RNA, which can be detected on sequencing PAGE by measuring fluorescence (18). Quantum dots (QDs) are a new type of fluorescence probe with important advantages over classical organic dyes (19,20). In particular, QDs have high extinction coefficient and high quantum yield, which should dramatically increase the sensitivity for microarray detection in theory. QDs have been successfully conjugated to DNA and used in many applications (21,22). Therefore, it was thought that the direct-labeling of miRNA with QDs could be well used in miRNA detection and applied in microarray. Here, we report a novel miRNA profiling microarray in which miRNA targets were biotinylated at 3′ terminus, hybridized with corresponding complementary oligo-DNA probes immobilized on glass slides, then detected by measuring fluorescence of QDs labeled on miRNA. Analysis of a model microarray indicated that the detection limit for miRNA was ~0.4 fmol and detection dynamic range spanned about 2 orders of magnitude, from 156 to 20 000 pM. In addition, miRNAs from leaf and root of rice (*Oryza sativa* L. ssp. *indica*) seedlings were profiled using a model microarray for 11 miRNAs in rice. On the other hand, a low-cost colorimetric detection method based on nanogold probe labeling coupled with silver enhancement demonstrated equal detection ability as fluorescent dyes in DNA and protein microarray (23–26). In this method, a flat scanner for DNA microarray or a commercial digital camera for protein chip were used as detector, resulting in great decrease in cost. Therefore, this method was also introduced into miRNA profiling microarray detection.

MATERIALS AND METHODS

Principle of the miRNA profiling microarray

The principle of miRNA profiling microarray includes two parts (Figure 1). First, miRNAs were oxidized with sodium periodate to convert 3′ terminal adjacent hydroxyl groups (2′ and 3′ position of ribose) into dialdehyde, which was then reacted with biotin-X-hydrazide through a condensation reaction resulting in biotinylated miRNA. Second, 5′ amine-modified oligonucleotide probes antisense to miRNAs were immobilized on amine-reactive glass slides. Then the biotinylated miRNAs were captured on the microarray by oligonucleotide probes in hybridization. Quantum dots were labeled on the captured miRNAs through the strong specific interaction of streptavidin and biotin. QDs have a high extinction coefficient and a high quantum yield, so trace amounts of miRNAs are easily detected with a laser confocal scanner. As an alternative, the colorimetric gold–silver detection

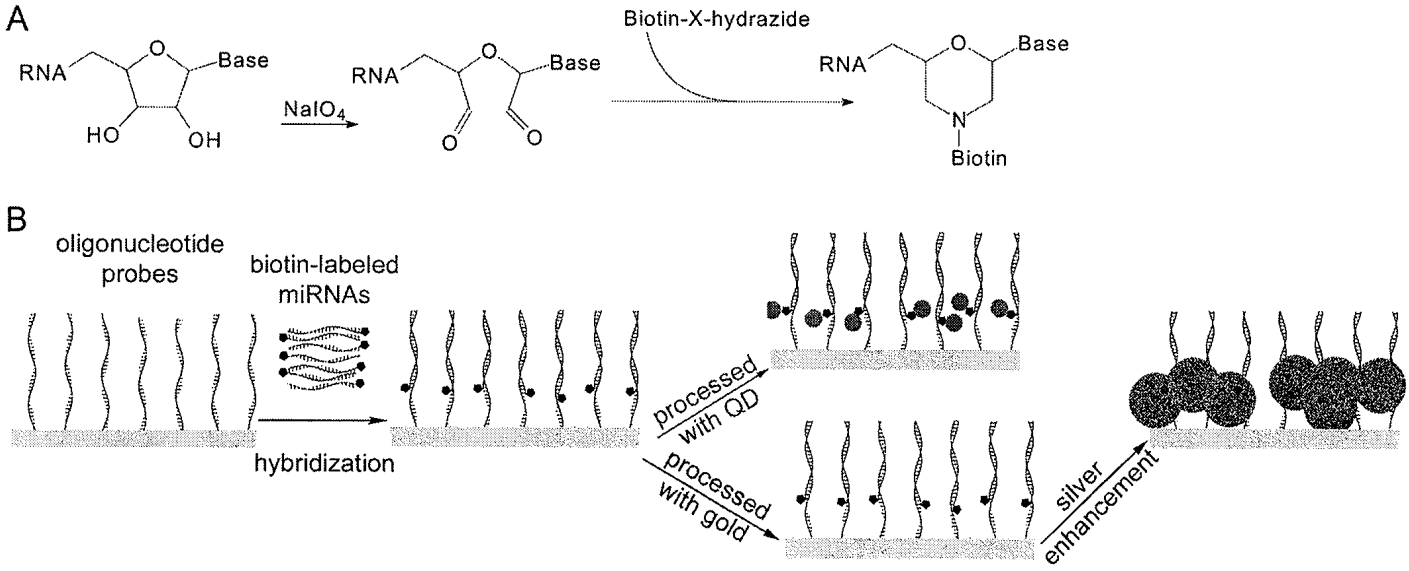

Figure 1. Schematic principles of the miRNA profiling microarray. (**A**) Principle of labeling miRNA at the 3′ terminus with biotin. (**B**) Principle of the miRNA profiling microarray detected with QD or colorimetric method.

method was used: captured miRNAs were labeled with streptavidin-conjugated gold followed by silver enhancement. During silver enhancement, the gold nanoparticles bound to miRNAs catalyzed the reduction of silver ions to metallic silver, which further autocatalyzed the reduction of silver ions to form metallic silver precipitation on gold, resulting in a signal enhancement (27). This process allowed straightforward detection of the microarray with an ordinary charge-coupled device (CCD) camera mounted on a microscope.

Microarray fabrication

Standard 1″ × 3″ microscope glass slides from Sigma were activated with glycidyloxipropyltrimethoxysilane (GOPTS) as previously described (26). The activated glass slides immobilize amine-containing molecules such as amino-modified oligonucleotide DNA. Eleven rice miRNAs were selected for the model miRNA profiling microarrays. Five of the 11 miRNAs were recently cloned in our lab (Li, Y., Li, W., Zhao, B.T. *et al.*, in preparation); the remaining six were from the miRNA Registry (28). The specific oligonucleotide DNA probes for these miRNAs were designed as shown in Table 1, along with a negative control RNA, all purchased from Beijing SBS Genetech Co. (China). Each DNA probe was complementary to a corresponding full length of mature miRNA and contained 10 deoxyadenosines in the 5′ terminus to minimize the spatial obstacle in hybridization and detection. The probes were dissolved in 50 mM phosphate buffer (pH 8.0, with 10 mM EDTA) at 50 μM concentration, then printed onto the GOPTS-activated slides with PixSys 5500 spotting robot (Cartesian Technology), in which ArrayIt SMP3 spotting pin from TeleChem was used; humidity was maintained at 80%. The diameter of spots was about 80 μm, and the distance between spots was set as 0.2 mm. The pattern of the model microarrays are shown in Figure 3A. Each microarray contained four subarray replicates (a, b, c and d), and each subarray contained 48 spots of the 12 probes in quadruplicate. The fabricated microarrays were processed with 1% BSA in phosphate-buffered saline (PBS) containing 10 mM EDTA to block intact amine-reactive groups on slides before hybridization. To examine the detection limit and dynamic range of the miRNA profiling microarrays, a synthesized 21 nt single-strand siRNA (5′-GATAATGGACCCCAATCAAAC-3′) was used as a model miRNA. Similarly, an amino-modified oligonucleotide DNA probe complementary to this siRNA with 10 deoxyadenosines in the 5′ terminus was synthesized and printed pentaplicately onto activated glass slides at 50 μM as mentioned above.

Table 1. Oligonucleotide probes in the model miRNA profiling microarray

miRNAs	Oligonucleotide probes
osa-miR156	amino-5′-$(A)_{10}$GTGCTCACTCTCTTCTGTCA-3′
osa-miR166	amino-5′-$(A)_{10}$GGGGAATGAAGCCTGGTCCGA-3′
osa-miR169	amino-5′-$(A)_{10}$TCGGCAAGTCATCCTTGGCTG-3′
osa-miR172	amino-5′-$(A)_{10}$TGCAGCATCATCAAGATTCT-3′
osa-miR393	amino-5′-$(A)_{10}$GATCAATGCGATCCCTTTGGA-3′
osa-miR396	amino-5′-$(A)_{10}$CAGTTCAAGAAAGCCTGTGGA-3′
III2-012[a]	amino-5′-$(A)_{10}$TCCCCTCTCCCACAACCCCG-3′
III2-013[a]	amino-5′-$(A)_{10}$GCCAGGGAAGAGGCAGTGCAG-3′
III2-016[a]	amino-5′-$(A)_{10}$GTTGCATCTGCCTCTGCAC-3′
III2-017[a]	amino-5′-$(A)_{10}$GTAGGTGCAGGTGCAAATGCA-3′
III2-020[a]	amino-5′-$(A)_{10}$CTACCATCTGAGCTACATCCCC-3′
Negaive Ctrl.	amino-5′-$(A)_{10}$GTGTGTGTGTGTGTGTGTGT-3′

[a]miRNAs recently cloned from rice by Li, Y., Li, W., Zhao, B.T., Yao, C.G., Qin, W.M, and Jin, Y.X. (in preparation) without official names assigned yet.

miRNA labeling

Total RNA was extracted from leaf and root of liquid nitrogen-frozen rice seedlings by using TRIZOL reagent (Invitrogen) according to the manufacturer's instructions. miRNAs were enriched from total RNA (termed enriched miRNA) according to a protocol from Drs Natalie Doetsch and Richard Jorgensen (29).

The enriched miRNAs were labeled with biotin-X-hydrazide (Sigma) according to a protocol described previously and modified slightly (18). Briefly, 18 μl of 0.5 μg/μl enriched miRNAs from 90 μg total RNA was diluted with 9 μl labeling buffer (0.25 M sodium acetate, pH 5.6) and 4 μl doubly distilled water (DEPC treated), then 5 μl of 5 mM sodium periodate was added. The oxidization of the 3′ terminus of RNA was carried out at 25°C in the dark for 90 min. Then, 2-fold excess of sodium sulphite over sodium periodate was added to the reaction mixture followed by 15 min incubation at 25°C. Finally, 37.5 nmol of biotin-X-hydrazide was added and incubated at 37°C for 3 h. The biotinylated miRNAs were precipitated with ethanol and stored in −80°C. The labeling of 21 nt siRNA was performed in the same way.

Microarray hybridization and detection

Each miRNA profiling microarray was hybridized with 1.5 μg biotinylated miRNAs in 10 μl formamide prehybridization/hybridization solution at 37°C overnight. The hybridized microarray was washed with 1× SSC/0.5% SDS at 37°C for 10 min. For detection with QD, the microarray was incubated with 10 μl of 2 nM Qdot 655 streptavidin conjugate (QD-streptavidin, from Quantum Dot Corp.) for 1 h at room temperature. After a thorough washing, the microarray was scanned on a PerkinElmer ScanArray 5000 Scanner with the laser 1 (633 nm) and filter 8, power at 100%, photomultiplier at 80%, and a scan resolution of 5 μm. For simplification, this QD-based detection method is termed the detection with QD in this report. For detection with the colorimetric gold–silver method, the microarray was incubated with 10 μl of 0.5 OD_{520} streptavidin-conjugated gold (gold-streptavidin, from Sigma). After a thorough washing, the microarray analysis was then performed with silver enhancer kit (Sigma) for 20 min, and detected with a commercial CCD camera (Olympus C-4000Z digital camera) mounted on a microscope. This method is termed the colorimetric method.

Northern blot

Total RNA from rice seedling leaves and roots were loaded on a 12.5% denaturing polyacrylamide gel. The resolved RNA was transferred to a Zeta-Probe GT blotting membrane (Bio-Rad) overnight. Oligodeoxynucleotides labeled at the 5′ end with [γ-^{32}P]ATP were used as probes. Prehybridization and hybridization were carried out using ExpressHyb Hybridization Solution (Clontech) according to the manufacturer's instruction. The sequences of probes were same as shown in Table 1, unless the 5′ amino and 10 deoxyadenosines were removed.

Data analysis

Images of miRNA microarray obtained with QD detection were quantified by QuantArray software (PerkinElmer). Meanwhile, grey-scale images of miRNA microarray obtained in the colorimetric method were processed with Photoshop 7.0 (Adobe System) to map the lightest and darkest pixels into black and white before quantifying with QuantArray software. Signal intensities of each spot in images obtained by both detection methods were calculated by subtracting local background from total intensities of the spot.

Radioactivity contained in northern blot bands was quantified with the NIH ImageJ software, and was expressed as a ratio of background subtracted signal in the band of hybridization to background subtracted signal in the band of stained 5S rRNA as loading control.

RESULTS

Detection limit and dynamic range of the miRNA microarrays in QD detection

Figure 2 shows a set of images for various concentrations of miRNA (21 nt siRNA) detected by QD. The signals become gradually weaker with the decrease in miRNA concentration. When the miRNA concentration was as low as 39 pM, the fluorescence signal could be detected, indicating that the lower detection limit of miRNA microarrays is at least 0.4 fmol. As shown in Figure 2B, the fluorescence intensity of the spots is linear to the model miRNA in logarithm from 156 to 20 000 pM, and the dynamic range is about 2 orders of magnitude, which implies that this method can be used to quantify miRNAs with broad concentration range. In Miska's method in which signal amplification with 10 rounds of PCR was employed, the lower detection limit of input miRNA was 0.1 fmol and the dynamic range was also 2 orders of magnitude (from 0.1 to 10 fmol) (12). While in quantitative northern blot, the lower detection limit of miRNA was 1 fmol and dynamic range was about 3 orders of magnitude, due to the high capacity of membrane in which the miRNA was immobilized (7).

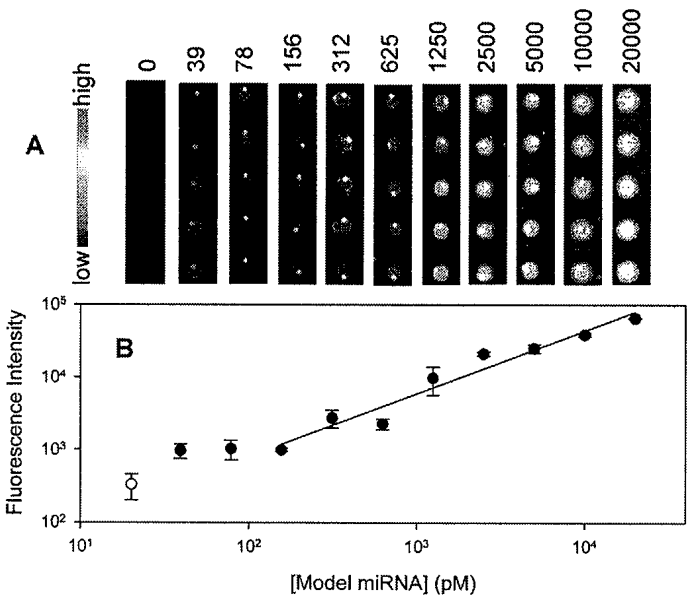

Figure 2. Detection limit and dynamic range of the model miRNA detection microarray. (**A**) Image sets of microarrays hybridize with various concentrations of miRNAs from 20 nM to 39 pM and the backgound. The 50 μM concentration of oligonucleotide probes printed on slides pentaplicately. The volume of model miRNA needed to hybridize with microarray was 10 μl. (**B**) Correlation between fluorescence intensity of spots and concentrations of model miRNA. The values were calculated from image in (A). Open circle represents the background.

Model miRNA profiling microarray for 11 rice miRNAs

When the microarray was applied to profile the 11 miRNAs in rice seedling leaves with QD detection, the image clearly showed different fluorescence intensities corresponding to these miRNAs, while the negative control was almost zero (see Figure 3B). This indicated that rice seedling leaves do contain these miRNAs. Figure 4 shows the reproducibility of the modeling microarrays for the 11 miRNA profiling. The Panels A and B were for the reproducibility among four subarrays in a microarray and four micrarrays (slides), respectively. The correlation coefficients obtained in Panel A were 0.98, 0.96 and 0.96, showing a high reproducibility between these subarray replicates. The correlation coefficients in Panel B were very similar, indicating high reproducibility

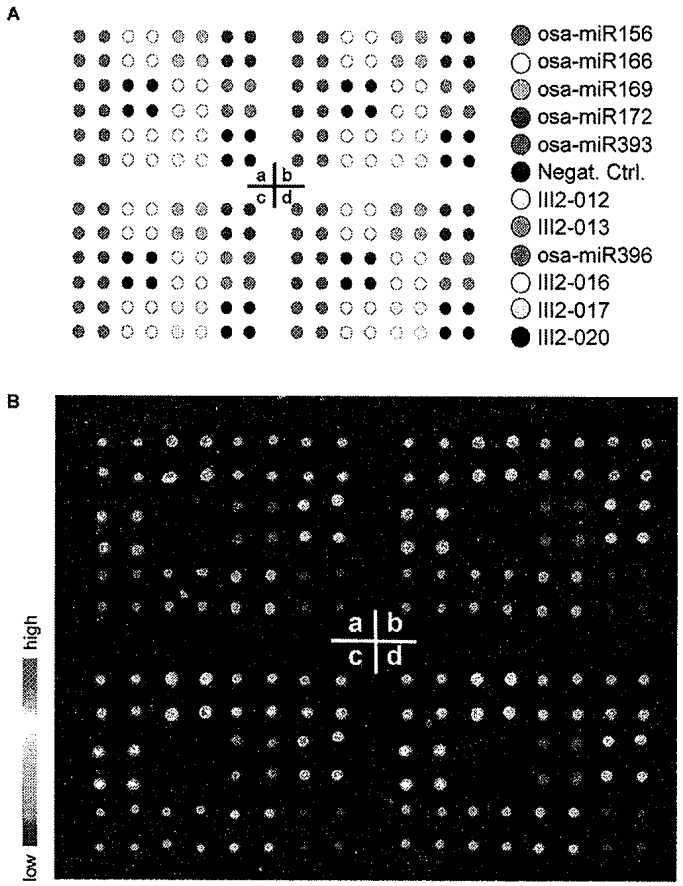

Figure 3. Model miRNA profiling microarray for 11 rice miRNAs. (**A**) Pattern of the model miRNA profiling microarray for 11 rice miRNAs. The microarray contains four replicate subarrays (a, b, c and d). Each subarray contains spots of probes for 11 miRNAs and 1 negative control in quadriplicate. (**B**) Image of the model miRNAs profiling microarray detected with QD. The microarray was hybridized with biotinylated miRNAs from rice seedling leaves.

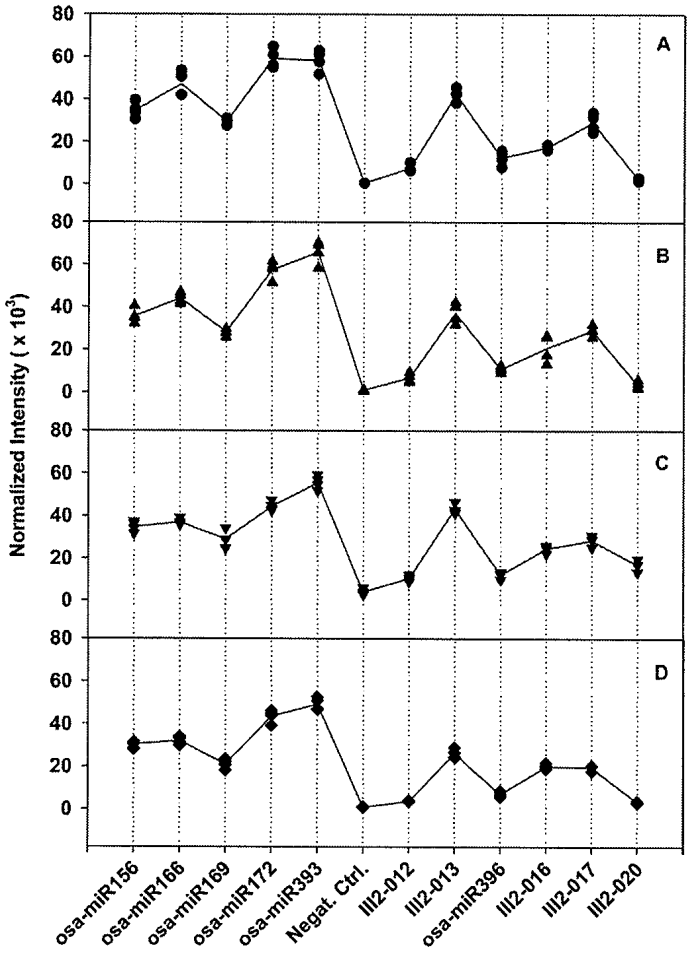

Figure 4. Reproducibility of miRNA profiling microarray detected with QD. (**A**) Mean normalized intensities of four subarray replicates in the microarray shown in Figure 3B. Straight-line plot represents the mean normalized intensities of four subarray replicates for each miRNA. The signal intensities of each four-spot replicates were normalized by using a per-subarray normalize to total method, which allowed comparison among subarrays in a chip. (**B**) Mean normalized intensities of four microarrays for 11 miRNA from seedling leaves. Straight-line plot represents the mean normalized intensities of the four microarrays for each miRNA. As in (A), a per-chip normalize to total method was used in comparison among chips. (**C**) As in (B), except that the miRNA was from seedling roots. (**D**) As in (A), except that 0.2 μg instead of 1.5 μg of enriched miRNA was used for hybridization.

between microarrays. Furthermore, when a two-cluster self-organization map was used, GeneCluster software (30) automatically clustered the eight samples shown in Figure 4B and C into two classes based on the expression profile of 11 miRNAs, one cluster contained the exact same four samples from leaf and the other four from root (Figure 5). These results indicate that our miRNA profiling microarray is reliable and sensitive. Although 1.5 μg of enriched miRNAs were mostly used for hybridization in this work giving a good result (see Figures 3B and 4A–C), 0.2 μg of enriched miRNAs was also tested and the normalized fluorescence intensities of the 11 miRNA in leaves are shown in Figure 4D. A correlation coefficient of 0.99 between the average intensity values of corresponding miRNAs in Figure 4B (1.5 μg miRNAs) and Figure 4D (0.2 μg miRNAs) was obtained, indicating that as low as 0.2 μg enriched miRNAs can be used. As known, at least 20 μg of total RNA was ordinarily used for each northern

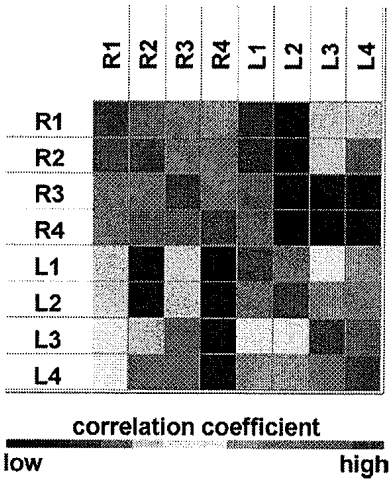

Figure 5. Cluster of samples from leaves and roots of rice seedling based on the expression profile of 11 miRNAs. Correlation coefficients between every two samples are presented. L1 to L4 and R1 to R4 represent four independent assays to profiling miRNAs from leaves and roots of rice seedlings respectively.

blot and the corresponding enriched miRNAs were about 2 μg. Consequently, about 10% of total RNA used in northern blots would be enough for one miRNA profile microarray experiment.

As the hybridization efficiency between different miRNA with its DNA probe is different, it is hard to estimate the molecular abundance of each miRNA according to the corresponding fluorescence intensities in microarray. However, for one miRNA, its fluorescence intensity do quantitatively relate to its amount as shown in Figure 2, therefore the miRNA microarray can be used to profile the same miRNA in different samples, for instance, to profile the 11 miRNAs in roots and leaves of the rice. The changes in fluorescence intensities of each miRNA should reflect the relative changes of each miRNA expression in these two samples. Figure 6 shows the fluorescence intensities of the 10 miRNAs in roots and leaves of rice seedling, indicating that the expression of the 10 miRNAs in root were higher than that in leaves. Among them, the III2-020 miRNA was almost undetectable in seedling leaves, but was strongly expressed in seedling roots, suggesting us to further explore it in future. These results were validated with northern blots. From Figure 6, it can be seen that most results from microarray and northern blots showed a similar pattern, indicating that the miRNA microarray described above could offer a high-throughput method that generally captures changes in miRNA expression. Only for osa-miR156, the relative levels of expression of osa-miR156 in root and leaf obtained from the microarray differed from that of the northern blot. As is the case for mRNAs, small differences may be seen between these methods, and northern blot analysis is superior to microarrays for quantitative analysis (31). This result reminds us to take care in using the results from microarrays.

Detection with colorimetric gold–silver method

Microarray hybridized with biotin-labeled miRNAs from rice seedling leaves was also detected by gold-streptavidin with silver enhancement. Figure 7A shows the image taken from

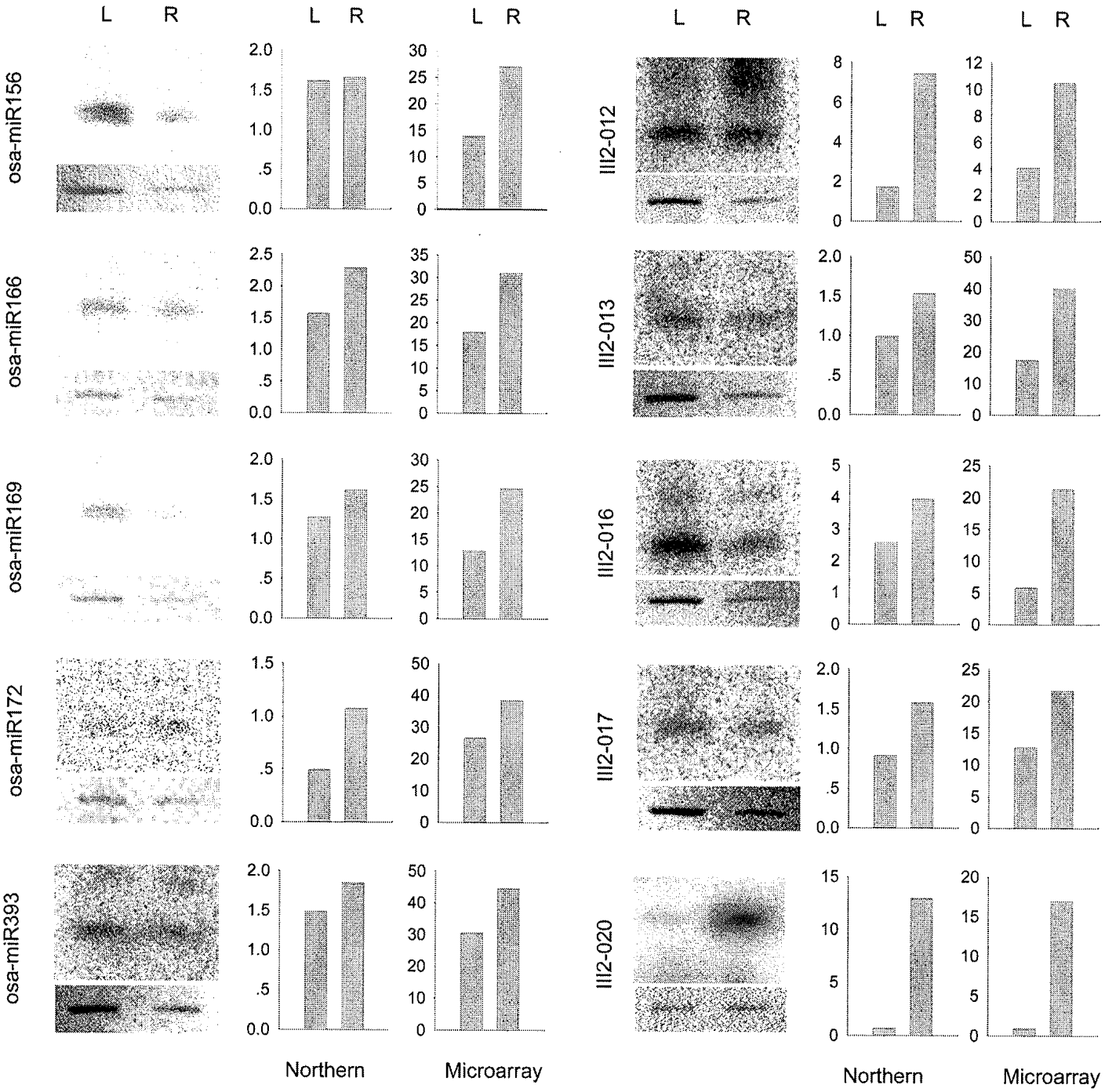

Figure 6. Comparison of microarray data with northern blots of miRNAs from leaves and roots of rice seedlings. Left panel for the five miRNAs selected from miRNA Registry and right panel for the five miRNAs cloned in our laboratory. The *y*-axis for the microarray data refers to the averaged mean fluorescence intensities, and *y*-axis for northern blots data to radioactivity. 5S rRNA immobilized on membrane was stained as control for comparison.

the colorimetric-detected microarray. Different miRNAs show different grey levels, while the negative control is indistinguishable from the background. Figure 7B shows the quantitative analysis of the colorimetric detection, in which the grey level profile is very similar to that seen in Figure 4A. This means that the colorimetric detection has a similar detection sensitivity as that of the QDs method. The correlation coefficient between the fluorescence detection and colorimetric detection was 0.93, a reasonable value for two different detection methods. Reproducibility between subarrays was also evaluated. The correlation coefficients between the subarray replicates were 0.97, 0.99 and 0.98, showing the high reproducibility between subarrays in the microarray. Alexander *et al.* (24) proved that when using the colorimetric method to detect multibiotinylated target DNA with DNA microarray, the lower detection limit was 0.1 fmol and dynamic range was from 0.1 to 10 fmol. These results indicate that colorimetric gold–silver detection

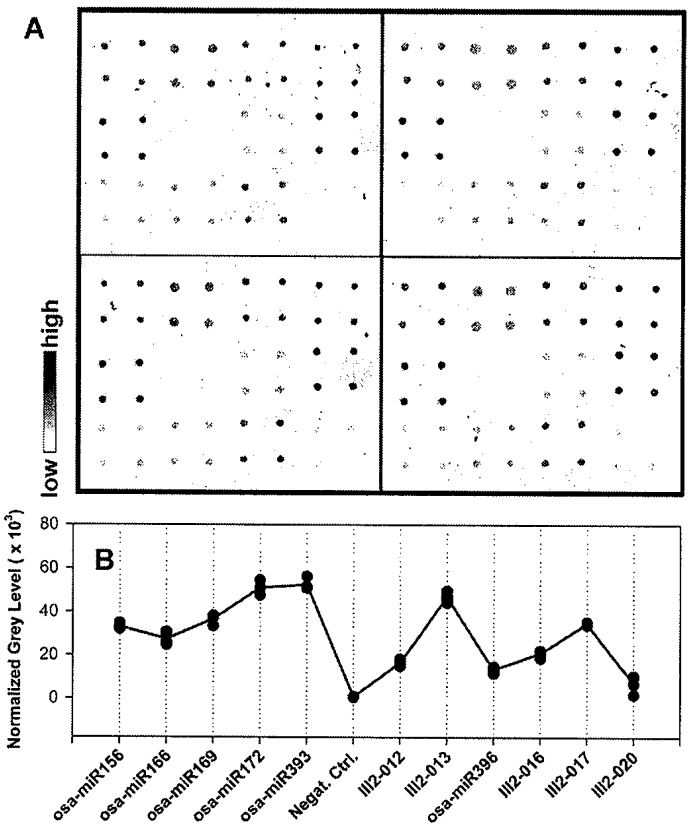

Figure 7. Detection of microarray for 11 rice miRNAs from seedling leaves with colorimetric gold–silver method. (**A**) Image of the model miRNAs profiling microarray detected with colorimetric method. (**B**) Quantitative analysis of the microarray image in panel (A). Filled circles represent the mean normalized intensities of the four spots for each miRNA in the four subarrays shown in (A). Straight-line plot represents the mean normalized intensities of the four subarray replicates for each miRNA.

can be used in miRNA profiling microarray detection in a low-cost and efficient manner.

DISCUSSION

Although northern blot can effectively profile the expression of a miRNA in many different conditions simultaneously, it is inefficient in profiling the expression of hundreds of miRNAs. The reason is that in northern blots, the miRNA mixture is immobilized on the membrane and hybridized with one certain probe. Such a characteristic also makes it inconvenient to evaluate molecular amounts of various miRNAs. To the contrary, in miRNA profiling microarray, a number of known probes are immobilized in addressable spots and hybridized with corresponding miRNAs in the sample, thereby providing a parallel and high throughput method of detecting thousands of miRNAs simultaneously. The linear dependence of fluorescence intensities on miRNA concentration in 2 orders of magnitude described above indicates that the microarrays can be used effectively to describe the miRNA expression profile. The results that the expression of the 11 miRNA in root were mostly higher than that in leaves, which is in agreement with the results obtained from northern blot experiment provided a solid evidence to prove that this microarray can be used to profile miRNA. Of course, this microarray cannot be used to compare the relative expression of different miRNAs at the moment as mentioned above, but there is no doubt that the microarray can be used to compare the expression of the same miRNAs in different sample or in different physiological condition for a same sample. And we believe that the microarrays could reveal the molecular abundance of different miRNAs after correcting the binding efficiency of each miRNA with its DNA probe. Until recently, a total of 1345 miRNAs from 12 species have been deposited in the miRNA Registry (Release 5.0); 207 miRNAs have been identified in human and 125 in rice. A bioinformatic study has suggested that there exist 200–255 miRNAs in human (32). Our miRNA profiling microarray can be easily expanded to profile thousands of features of miRNAs. Also it should not be difficult to make a universal microarray for several species. This universal microarray could be used in trans-species miRNA expression profiling for each known miRNA under various conditions.

Sensitivity to detect target miRNA is a very important parameter for miRNA profiling microarrays. We found that only 0.4 fmol of miRNA was needed for QD detection with microarrays when a 633 nm laser was used as excitation light. In fact, we speculate that the detection sensitivity could easily be raised, using a 488 nm laser. The extinction coefficient of QD 655 at 488 nm is $2.9 \times 10^6\ cm^{-1}\ M^{-1}$, about 4-fold higher than that at 633 nm ($0.85 \times 10^6\ cm^{-1}\ M^{-1}$). So, for the same concentration of miRNA, the fluorescent signal excited at 488 nm would be about 4-fold higher than that excited at 633 nm. Even with the 633 nm excitation, we would expect that the detection limit would be lower than 0.4 fmol because the signal obtained at 633 nm excitation (Figure 2) would be 2-fold higher than the minimum readable level of the laser confocal scanner. Therefore, one can expect that the detection limit can reach as low as 0.05–0.1 fmol of miRNA when a 488 nm laser is used. Such a high sensitivity is essential to detect trace amounts of miRNAs. Molecular amounts of miRNAs have been estimated to be 1000–50 000 molecules per cell (7). For the lowest amount of miRNAs (i.e. 1000 miRNA molecules per cell), only 6×10^4 cells would be required to detect these miRNAs with a detection limit of 0.1 fmol, and only 2.5×10^5 cells with a detection limit of 0.4 fmol. This translates to only 5 mg of tissue or one well of a 24-well plate, which makes high throughput assay feasible.

Based on quantum dot or colorimetric method, miRNA is measured by detecting fluorescence or grey-level of labeled miRNA, in which miRNAs were captured by corresponding antisense oligonucleotide probes. This method has at least three advantages. First, fluorescence coming from directly labeled miRNA can accurately reveal relative miRNA amounts in a sample, whereas the miRNA population might be distorted with labeling cDNA of miRNA through reverse transcription and/or enzymatic amplification (13). Second, preparation of the sample and the procedure of microarray hybridization and detection are relatively simple. Third, the miRNA profiling microarrays can be used to evaluate amounts of both the miRNAs and their targets. For the latter, the miRNA targets should be reverse-transcribed into cDNA. These advantages of miRNA profiling microarray will make miRNome deciphering more efficient and will contribute much to the studies of miRNA target identification, miRNA

expression regulation and even pathological studies of diseases.

ACKNOWLEDGEMENTS

We thank Dr David Armbruster for his critical reading. This work was funded by National Key Basic Research and Development Program (No. 2002CB713802), National 863 Program (030431002), National Natural Science Foundation of China (No. 30430210), and a key basic research grant (No. 04DZ14006) from the Shanghai Council of Science and Technology. The Open Access publication charges for this article were waived by Oxford University Press.

REFERENCES

1. Bartel,D.P. (2004) MicroRNAs: genomics, biogenesis, mechanism, and function. *Cell*, **116**, 281–297.
2. He,L. and Hannon,G.J. (2004) MicroRNAs: small RNAs with a big role in gene regulation. *Nature Rev. Genet.*, **5**, 522–531.
3. Lagos-Quintana,M., Rauhut,R., Yalcin,A., Meyer,J., Lendeckel,W. and Tuschl,T. (2002) Identification of tissue-specific microRNAs from mouse. *Curr. Biol.*, **12**, 735–739.
4. Sempere,L.F., Sokol,N.S., Dubrovsky,E.B., Berger,E.M. and Ambros,V. (2003) Temporal regulation of microRNA expression in *Drosophila melanogaster* mediated by hormonal signals and broad-Complex gene activity. *Dev. Biol.*, **259**, 9–18.
5. Houbaviy,H.B., Murray,M.F. and Sharp,P.A. (2003) Embryonic stem cell-specific MicroRNAs. *Dev. Cell*, **5**, 351–358.
6. Aravin,A.A., Lagos-Quintana,M., Yalcin,A., Zavolan,M., Marks,D., Snyder,B., Gaasterland,T., Meyer,J. and Tuschl,T. (2003) The small RNA profile during *Drosophila melanogaster* development. *Dev. Cell*, **5**, 337–350.
7. Lim,L.P., Lau,N.C., Weinstein,E.G., Abdelhakim,A., Yekta,S., Rhoades,M.W., Burge,C.B. and Bartel,D.P. (2003) The microRNAs of *Caenorhabditis elegans*. *Genes Dev.*, **17**, 991–1008.
8. Sempere,L.F., Freemantle,S., Pitha-Rowe,I., Moss,E., Dmitrovsky,E. and Ambros,V. (2004) Expression profiling of mammalian microRNAs uncovers a subset of brain-expressed microRNAs with possible roles in murine and human neuronal differentiation. *Genome Biol.*, **5**, R13.
9. Krichevsky,A.M., King,K.S., Donahue,C.P., Khrapko,K. and Kosik,K.S. (2003) A microRNA array reveals extensive regulation of microRNAs during brain development. *RNA*, **9**, 1274–1281.
10. Liu,C.G., Calin,G.A., Meloon,B., Gamliel,N., Sevignani,C., Ferracin,M., Dumitru,C.D., Shimizu,M., Zupo,S., Dono,M. *et al.* (2004) An oligonucleotide microchip for genome-wide microRNA profiling in human and mouse tissues. *Proc. Natl Acad. Sci. USA*, **101**, 9740–9744.
11. Calin,G.A., Liu,C.G., Sevignani,C., Ferracin,M., Felli,N., Dumitru,C.D., Shimizu,M., Cimmino,A., Zupo,S., Dono,M. *et al.* (2004) MicroRNA profiling reveals distinct signatures in B cell chronic lymphocytic leukemias. *Proc. Natl Acad. Sci. USA*, **101**, 11755–11760.
12. Miska,E.A., Alvarez-Saavedra,E., Townsend,M., Yoshii,A., Sestan,N., Rakic,P., Constantine-Paton,M. and Horvitz,H.R. (2004) Microarray analysis of microRNA expression in the developing mammalian brain. *Genome Biol.*, **5**, R68.
13. Cole,K., Truong,V., Barone,D. and McGall,G. (2004) Direct labeling of RNA with multiple biotins allows sensitive expression profiling of acute leukemia class predictor genes. *Nucleic Acids Res.*, **32**, e86.
14. Babak,T., Zhang,W., Morris,Q., Blencowe,B.J. and Hughes,T.R. (2004) Probing microRNAs with microarrays: tissue specificity and functional inference. *RNA*, **10**, 1813–1819.
15. Igloi,G.L. (1996) Nonradioactive labeling of RNA. *Anal. Biochem.*, **233**, 124–129.
16. Kampa,D., Cheng,J., Kapranov,P., Yamanaka,M., Brubaker,S., Cawley,S., Drenkow,J., Piccolboni,A., Bekiranov,S., Helt,G. *et al.* (2004) Novel RNAs identified from an in-depth analysis of the transcriptome of human chromosomes 21 and 22. *Genome Res.*, **14**, 331–342.
17. Thomson,J.M., Parker,J., Perou,C.M. and Hammond,S.M. (2004) A custom microarray platform for analysis of microRNA gene expression. *Nature Methods*, **1**, 47–53.
18. Wu,T.P., Ruan,K.C. and Liu,W.Y. (1996) A fluorescence-labeling method for sequencing small RNA on polyacrylamide gel. *Nucleic Acids Res.*, **24**, 3472–3473.
19. Chan,W.C., Maxwell,D.J., Gao,X., Bailey,R.E., Han,M. and Nie,S. (2002) Luminescent quantum dots for multiplexed biological detection and imaging. *Curr. Opin. Biotechnol.*, **13**, 40–46.
20. Tan,C.Y., Liang,R.Q. and Ruan,K.C. (2002) Application of quantum dot to life science. *Acta Biochim. Biophys. Sin.*, **34**, 1–5.
21. Kim,J.H., Morikis,D. and Ozkan,M. (2004) Adaptation of inorganic quantum dots for stable molecular beacons. *Sens. Actuators B: Chem.*, **102**, 315–319.
22. Patolsky,F., Gill,R., Weizmann,Y., Mokari,T., Banin,U. and Willner,I. (2003) Lighting-up the dynamics of telomerization and DNA replication by CdSe–ZnS quantum dots. *J. Am. Chem. Soc.*, **125**, 13918–13919.
23. Taton,T.A., Mirkin,C.A. and Letsinger,R.L. (2000) Scanometric DNA array detection with nanoparticle probes. *Science*, **289**, 1757–1760.
24. Alexandre,I., Hamels,S., Dufour,S., Collet,J., Zammatteo,N., Longueville,F.D., Gala,J.-L. and Remacle,J. (2001) Colorimetric silver detection of DNA microarrays. *Anal. Biochem.*, **295**, 1–8.
25. Huber,M., Wei,T.F., Muller,U.R., Lefebvre,P.A., Marla,S.S. and Bao,Y.P. (2004) Gold nanoparticle probe-based gene expression analysis with unamplified total human RNA. *Nucleic Acids Res.*, **32**, e137.
26. Liang,R.Q., Tan,C.Y. and Ruan,K.C. (2004) Colorimetric detection of protein microarrays based on nanogold probe coupled with silver enhancement. *J. Immunol. Methods*, **285**, 157–163.
27. Holgate,C.S., Jackson,P., Cowen,P.N. and Bird,C.C. (1983) Immunogold–silver staining: new method of immunostaining with enhanced sensitivity. *J. Histochem. Cytochem.*, **31**, 938–944.
28. Griffiths-Jones,S. (2004) The microRNA Registry. *Nucleic Acids Res.*, **32**, D109–D111.
29. Park,W., Li,J., Song,R., Messing,J. and Chen,X. (2002) CARPEL FACTORY, a Dicer homolog, and HEN1, a novel protein, act in microRNA metabolism in *Arabidopsis thaliana*. *Curr. Biol.*, **12**, 1484–1495.
30. Taniguchi,M., Miura,K., Iwao,H. and Yamanaka,S. (2001) Quantitative assessment of DNA microarrays–comparison with Northern blot analyses. *Genomics*, **71**, 34–39.
31. Reich,M., Ohm,K., Angelo,M., Tamayo,P. and Mesirov,J.P. (2004) GeneCluster 2.0: an advanced toolset for bioarray analysis. *Bioinformatics*, **20**, 1797–1798.
32. Lim,L.P., Glasner,M.E., Yekta,S., Burge,C.B. and Bartel,D.P. (2003) Vertebrate microRNA genes. *Science*, **299**, 1540.

Journal of Biochemistry and Molecular Biology, Vol. 38, No. 4, July 2005, pp. 399-406

JOURNAL OF
Biochemistry and Molecular Biology

Development of Array-based Technology for Detection of HAV Using Gold-DNA Probes

Zhixiang Wan, Yefu Wang[‡,*], Shawn Shun-cheng Li[†,*], Lianlian Duan and Jianxin Zhai
Department of Biotechnology, College of Life Sciences, Wuhan University, Wuhan 430072, P. R. China
[†]Department of Biochemistry, University of Western Ontario, London, Ontario N6A 5C1, Canada

Received 11 December 2004, Accepted 2 March 2005

A sensitive method for detection of Hepatitis A virus (HAV) by utilizing gold-DNA probe on an array was developed. Amino- modified oligodeoxynucleotides at the 5' position were arrayed on an activated glass surface to function as capture probes. Sandwich hybridization occurred among capture probes, the HAV amplicon, and gold nanoparticle-supported oligonucleotide probes. After a silver enhancement step, signals were detected by a standard flatbed scanner or just by naked eyes. As little as 100 fM of HAV amplicon could be detected on the array. Therefore, the array technology is an alternative to be applied in detection of HAV due to its low-cost and high-sensitivity.

Keywords: Array, Gene detection, Gold-DNA probe, HAV, Sensitivity

Introduction

Hepatitis A virus (HAV), a major cause of acute hepatitis infections in humans in many countries, is a positive strand RNA virus belonging to the picornavirus family. HAV infection occurs primarily by the fecal-oral route, by person-to-person contact or through the ingestion of contaminated food or water. Thus, it is essential to develop special and efficacious methods for the detection of HAV in clinical or biological samples. Sequence-specific gene detection has been a topic of significant interest because of its application in areas ranging from the environmental monitoring to diagnostics. Several laboratories have attempted to develop methods based on the polymerase chain reaction (PCR) or nucleic acid hybridization for detecting the HAV gene (Therasal *et al.*, 1997; David HK *et al.*, 2002). But, these methods need improvement, especially in regard to the false positive incidence with PCR methods. There remains a need to develop a more sensitive and specific detection method for the HAV gene at low cost. Microarray-based biological techniques play an important role in gene detection. The development of these techniques is driven by the need for low cost, minimal sample consumption, high throughput and efficiency.

In recent years, the application of gold nanoparticles as oligonucleotide labels instead of fluorescence dyes in DNA detection assays was very common. Gold nanoparticles were also used for microgravimetric analysis of DNA in connection with dendritic signal amplification (Patolsky *et al.*, 2000). Electrochemical stripping detection of a hybridization event based on gold-DNA probes has also been reported (Hong *et al.*, 2002; Urban *et al.*, 2003). Specifically, Mirkin and co-workers exploited a series of DNA detection methods in which gold-DNA probes were utilized (Elghanian *et al.*, 1997; Taton *et al.*, 2000; Taton *et al.*, 2001; Park *et al.*, 2002). Their experiments revealed that gold- labelled probes were compatible with gene microarray or gene-chip and would be used as an alternative marker because of their high stability, high labelling density and superior sensitivity.

To improve the detection signal of gold nanoparticles on the array, a silver enhancement step was included (Alexandre *et al.*, 2001; Csaki *et al.*, 2003). The amplification of signal increased the sensitivity of gene detection and could be detected by flatbed scanner or the naked eyes (Taton *et al.*, 2000). With gold nanoparticle probes amplification coupled with silver enhancement, the sensitivity of microarrays increased markedly. Compared to Cy3-based fluorescence, silver amplified gold nanoparticle probes produce approximately 1000-fold increase in sensitivity (James *et al.*, 2004).

Mirkin and co-workers were first to propose gold nanoparticle modified DNA probe coupled with silver enhancement for DNA microarray probing. Analysis of the microarray with a simple flatbed scanner provided sufficient sensitivity to detect a 50fM concentration of a 30-mer single-stranded DNA target (Taton *et al.*, 2000). We previously reported simultaneous

*To whom correspondence should be addressed.
Tel: 86-27-68754627; Fax: 86-27-68754627
E-mail: wangyf86@yahoo.com.cn

diagnosis of HBV and HCV using gold nanoparticle probes and silver enhancement method (Wang *et al.*, 2003). Based on this work and with a few improvements, we established a HAV detection technology using gold-DNA probe on an array. Characterization and optimization of the sensitivity of this method were carried out. The 100 fM HAV amplicon was readily detectable after exposing to the silver enhancer solution for 8-12 min.

Materials and Methods

Reagents Silanizing coupling reagent - γ-aminopropyltriethoxysilane (APTES) from Organosilicon Engineering Research Center of MOE (Wuhan, China), 1,4-phenylene diisothiocyanate (PDITC, Aldrich), M-MLV reverse transcriptase (Biostar Com., Taipei Hsien, Taiwan), Taq DNA polymerase, uracil-DNA glycosylase (UDG, Gene Co. Ltd.), salmon sperm DNA, bovine serum albumin and dNTPs (Promega, Madison, USA) were used as received from the manufactures. Other chemicals and biological reagents were of analytical reagent (AR) grade. All solutions were treated with 0.1% diethyl pyrocarbonate (DEPC, Sigma, St. Louis, USA). The glassware was pre-cleaned by immersing in aqua regia (HCl : HNO_3 = 3 : 1) followed by rinsing with deionized water and then dried at 180°C for 8 h. All EP tubes and tips were sterilized under high pressure.

Silver enhancement solution was prepared as follows. Sixty milliliters of 1% (w/v) gelatin solution, 10 ml of citric acid buffer (pH 3.8) and 1.7 g of hydroquinone were dissolved in 30 ml, water, filtered and mixed prior to use. Lastly, 50 mg of $AgNO_3$ dissolved in 2 ml water was added to the mixed solution. The freshly-prepared solution was kept away from light. Citric acid buffer (pH 3.8) was obtained by dissolving 2.55 g citric acid ($C_6H_8O_7.H_2O$) and 2.35 g sodium citrate ($C_6H_5Na_3O_7.H_2O$) in 100 ml distilled water. 0.2% (w/v) PDITC solution was prepared by mixing anhydrous pyridine and *N,N*-dimethylformamide (DMF) in a ratio of 1 : 9, followed by addition of appropriate amount of PDITC to the mixture.

HAV samples Hepatitis serum samples and sewage samples were received from the Bureau of Import and Export Inspection and Quarantine of Hubei Province, Xiehe Hospital of Huazhong University of Science & Technology (HUST), Hubei Provincial Yunmeng Blood Station, and Wuhan University Zhongnan Hospital. Samples were stored at –80°C until use.

Sewage samples collected from the contaminated sewage network were ultracentrifuged at 229,000 *g* for 1 h at 4°C to sediment the virus particles together with any suspended material. Viruses retained in the sediment were eluted by mixing with 0.25 M glycine buffer (pH 9.5) on ice for 30 min. The suspended solids were then removed by centrifugation at 12,000 *g* for 15 min after the addition of sodium phosphate buffer (PBS). Viruses in the supernatant were pelleted by ultracentrifugation for 1 h at 4°C, resuspended in PBS.

Primers and probes Primers and probes were designed with the Primer Premier 5.00 program and synthesized by Shenggong Bioengineering Co. (Shanghai, China). Designed PCR primers and hybridization probes met the following demands: (1) primers and probes of HAV derived from the VP1 region which are highly conservative sequence elements (2323-2571) of HAV gene, (2) capture probes were modified with amino group at 5'-position in order that the probes can covalently attach to the activated glass. 3'-mercapto detection probes can associate with gold nanoparticles due to high affinity of mercapto group to gold surface, (3) ten T base inserted into probes increased the distance between the substrate and probes, which reduced the effect of steric hindrance on hybridization of the probes with complementary target DNA(Wang *et al.*, 2003). The primers for amplification of the HAV gene were named A1 and A2. Sequences of primers and probes used are listed in Table 1.

Extraction and amplification of HAV gene RNA extraction by proteinase K Method: One hundred microliters of serum or sewage suspension were treated with an equal volume of proteinase K (2 g/ml in 20 M Tris, pH 7.5, 10 mM EDTA, 0.1% SDS) at 45°C for 1 h. RNA was extracted with phenol-chloroform, precipitated with ethanol, and resuspended in 20 ml DEPC-treated water prior to reverse transcription. After centrifugation, the pellet was washed with 70% ethanol, air dried, and resuspended in 10 μl DEPC treated water. Reverse transcription reaction was carried out using 10 μl RNA, 25 pmol of the primer A2 and 200 U of reverse transcriptase in a final volume of 20 μl at 42°C for 1h, followed by incubation at 95°C for 5 min. Twenty microlitres of cDNA was used for PCR.

PCR amplification was carried out in a 100 μl reaction mixture containing 10 mM Tris-HCl (pH 8.3 at 25°C), 50 mM KCl, 1.5 mM $MgCl_2$, 200 μM dNTPs (note that: 2/5 of dTTP was replaced with dUTP), 25 pmol A1 primer and 2 units of *Taq* DNA polymerase. After denaturation for 4 min at 94°C, the DNA was amplified for 30 cycles at 94°C for 30 s, 40°C for 30 s, and 72°C for 45 s (and an additional 5 min at 72°C in the last cycle). The HAV amplicon fragment size was determined by electrophoresis on a 1.5% agarose gel containing 0.5 mg/ml EB.

Table 1. Sequences of the synthetic primers and probes

	Sequence
Primer A1 of HAV	5'-GATGGATGTTTCAGGAGTG-3' (2323-2341)
Primer A2 of HAV	5'-TGAGGAGGATTAGAAGTCG-3' (2553-2571)
Capture probe of HAV	5'-H_2N-$(CH_2)_6$-O-(PO_3)-$(T)_{10}$-GAGCTATCAGCAACAATTGAAC-3' (2356-2377)
Detection probe of HAV	5'-TAAAGAGTACACATTTCCAATA-$(T)_{10}$-SH-3' (2521-2542)
Capture probe of positive control	5'-H_2N-$(CH_2)_6$-O-(PO_3)-$(T)_{10}$-CTCCCTGAACCGTTCCGCATTCG-3' (557-579)
Detection probe of positive control	5'-CGTTCTCTAACTATTTCTTTGATA-$(T)_{10}$-SH-3' (927-950)
Capture probe of negative control	5'-H_2N-$(CH_2)_6$-O-(PO_3)-$(T)_{10}$-AAACTTCTTTAAGTTTTGCG-3'
Detection probes of negative control	5'-GCTCAGTTTACTAGTGCCATTTG-$(T)_{10}$-SH-3'

Preparation of gene array for the detection of HAV Procedures for pretreatment and functionalization of glass slide surfaces and immobilization of DNA probes were similar to the study (Christy *et al.,* 1996). Glass slides (Fan chuan, China) used for gene arrays were washed in hot concentrated HNO_3 for 10 min, rinsed with distilled water (5 times, 2 min each time), and then dried in an oven at 37°C. The pre-cleaned slides were soaked for 2 h in APTES solution prepared by mixing double-distilled water, acetone and APTES in a volume ratio of 15 : 280 : 6, washed 5 times with acetone (5 min each time), and then dried. The slides were subsequently kept in 0.2% PDITC solution at 37°C for 2 h and then washed 3 times with methanol (5 min each time), 2 times each with acetone and double-distilled water, and air dried.

The 5' amino-modified DNAs (HAV, positive and negative controls) for surface-immobilization were diluted in a 1 M NaCl, 10 mM sodium phosphate buffer to yield 3.37×10^{-7} M and 3.37×10^{-8} M working solution. One microlitre droplets of solution were applied to every designated binding spot and the arrays were incubated in a humidity chamber at 37°C for 2 h. Afterwards, the arrays were washed with distilled water (1 × 2 min), blocked with 1% bovine serum albumin (BSA) with shaking at 45°C for 30 min, rinsed with distilled water (3 × 3 min) and dried at 40-45°C. The gene arrays obtained were stored at 4-8°C.

Preparation and size determination of gold nanoparticles Gold nanoparticles were prepared according to the literature (Grabar *et al.,* 1995) by citrate reduction of $HAuCl_4$. The experimental conditions were as follows: 100 ml $HAuCl_4$ solution was brought to boil with stirring at 300 rpm. To the solution, 10 mL 38.8 mmol/L sodium citrate solution was added as quickly as possible. The mixture was kept boiling for 15 min, and left to cool at room temperature. The prepared gold nanoparticles were recovered to the original volume with distilled water and filtered through a 0.45 μm nylon filter. The size distribution of the resultant gold nanoparticles was measured by transmission electron microscopy (TEM HITACHI H-8100, Japan) and UV-Visible spectrum (UNICO™, Beijing, China). An average diameter of 14 ± 2 nm was obtained. The gold solution exhibited a sharp plasmon absorption band with maximum absorbance at wavelength 520 nm.

Preparation of thiol-modified DNA-gold probes Gold-DNA probes were synthesized by exposing 50 μl 3'-thiol modified oligodeoxynucleotides (32.5 μM) to 1 ml gold nanoparticle solution for 16 h at room temperature. The mixture was adjusted to pH 7.0 using 0.1 M NaCl, 10 mM sodium phosphate buffer, kept for 40 h at room temperature, and then centrifuged at 16,000 rpm for 30 min. The precipitates were washed with and re-dispersed in 1 ml of 0.3 M NaCl, 10 mM sodium phosphate buffer, pH 7.0. Different concentrations of gold-DNA probes were prepared by centrifugation and re-dispersion in appropriate volumes of 0.3 M NaCl, 10 mM sodium phosphate buffer. The concentration of gold nanoparticles was determined using absorbance values at 520 nm in conjunction with the molar absorption coefficient (Demers *et al.,* 2000). The gold-DNA probes were stored at 4°C.

Sandwich hybridization Each tube of PCR product was diluted 10 fold with hybridization buffer (0.3 M NaCl/10 mmol/L pH7.0 PBS). Meanwhile, 1000 fM *E. coli* gene was used as positive control. The DNAs were heated in a slightly boiling water bath for 5 min, rapidly cooled in an ice bath for 2 min and were loaded on to the prepared HAV array chip. Hybridization was carried out in a humidity chamber at 50°C for 2 h. The array was washed twice with 0.3 M PBS solution to remove non-hybridized and non-specific products. Subsequently, the array was treated with a 0.3 M PBS solution of nanoparticle probes. Hybridization was carried out in a moist chamber at 40°C for another 2 h .The HAV array was rinsed three times (3 min each time) with 0.3 M $NaNO_3$ in 10 mM phosphate buffer (pH 7) to remove chloride ions.

Silver enhancement and detection The arrays were immersed in a silver enhancer solution, as described above, at room temperature for 8-12 min. When appearance of positive control signal spots was evident, the chip was removed from the silver enhancer solution and rinsed immediately with water, and air-dried. The HAV array signal can be detected by the naked eye or with a flatbed scanner. In this method, arrays were imaged using a standard flatbed scanner (Founder, China) in reflective mode. Image and statistical analysis of the data were performed using software provided by the manufacturer.

Results and Discussion

The principle of the HAV detection array based on gold-DNA probe coupled with silver enhancement is illustrated in Fig. 1A. The main procedure taken for HAV array detection was as follows. (1) Amino-modified capture probes were covalently immobilized on to PDITC functionalized APTES-glass surface; (2) Sandwich hybridization among capture probes and HAV PCR products and gold-DNA probes; (3) Catalytic precipitation of silver onto the gold nanoparticle followed by flatbed scanner imaging or eye inspection. The pattern of HAV detection arrays was designed as shown in Fig. 1B. Glass substrates 2.5 × 3 cm were cut from super-flat slides. Each row was immobilized different capture probe. Row A represents positive control spots, row B represents HAV detection spots, and row C represents negative control spots. Columns 1, 2, 3, 4 represent the different detection spots of repetition and variability. The concentration of the probes of columns 1 and 2 is 3.37×10^{-7} M, the concentration of the probes of columns 3 and 4 is 3.37×10^{-8} M. The control system was composed of two parts: (1) negative control was reconstructed gene fragment which was not complementary with HAV, (2) Positive control was the 413 bp fragment of *E.coli* tnaA gene (547-959), which was not homologous with HAV and synthesized by Shenggong Bioengineering Co. (China).

Characteristics of gold labeled probe In a typical HAV detection array, stability of gold labeled probe is a crucial factor. To characterize the stability of gold probes, TEM was used to determine the size and the morphology of Au nanoparticles. The prepared DNA-gold nanoparticle solution exhibits substantially high stability (Storhoff *et al.,* 1998). Increased stability of DNA-modified nanoparticles is due to higher oligonucleotide surface coverage, which leads to

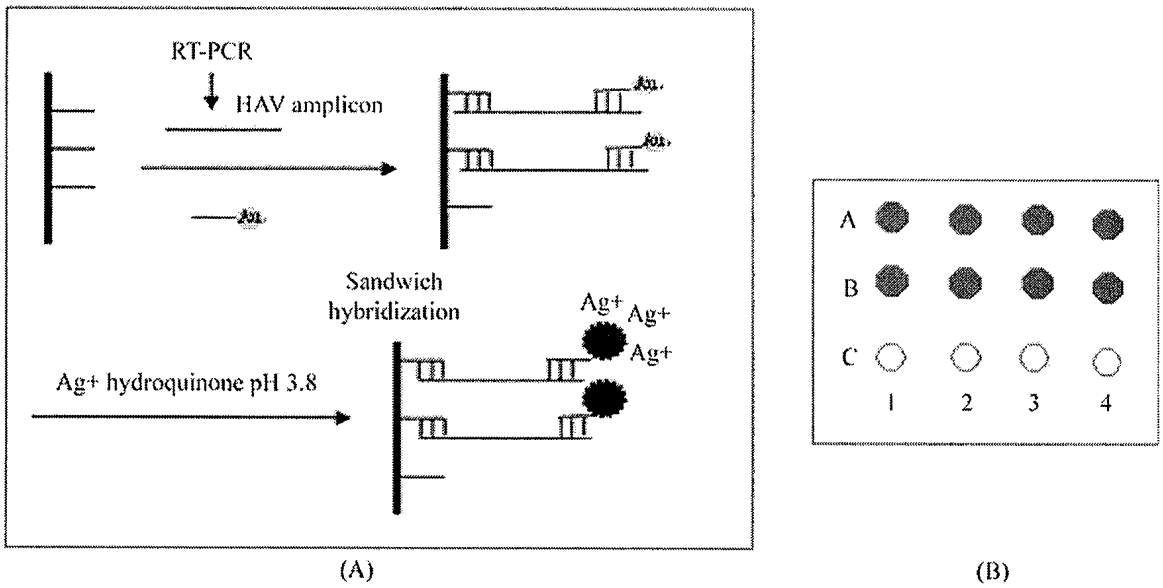

Fig. 1. The principle (A) and pattern (B) of the HAV array detection. In pattern (b): Positive controls were arranged in row A, detection spots of HAV were arranged in row B, and negative controls were arranged in row C. Columns 1, 2, 3, 4 represent the different detection spots of repetition and variability. The concentration of the probes of columns 1 and 2 is 3.37×10^{-7} M, the concentration of the probes of columns 3 and 4 is 3.37×10^{-8} M.

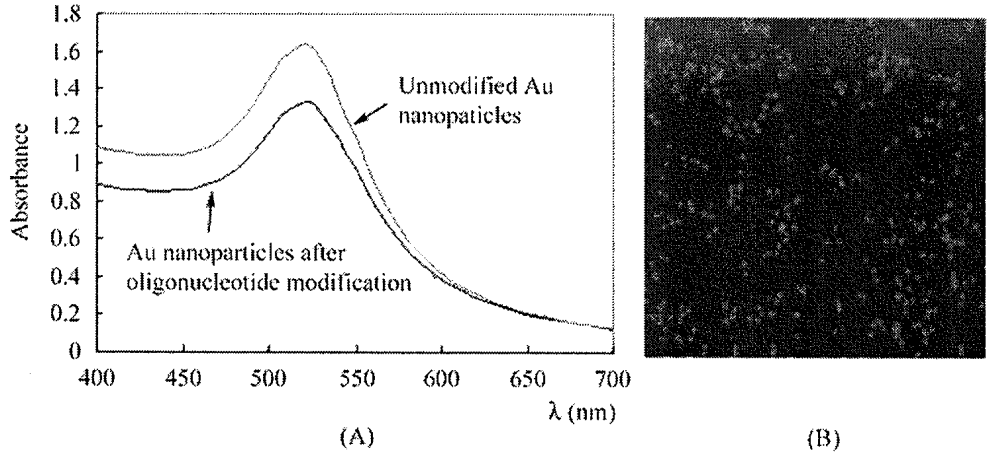

Fig. 2. Characteristics of the nanoparticles. (A) Comparison between UV-Vis spectum of Au colloids and gold-DNA probes. (B) TEM image DNA-gold nanoparticles (standing for 6 month at 4°C). Briefly, a drop (50 μl) of colloidal gold suspension was deposited on a nicked grid and allowed to evaporate at room temperature. The grid was then observed at a magnification of 22,000×.

greater steric and electrostatic protection (Demers *et al.*, 2000). The prepared DNA-gold nanoparticles (left standing for 6 months at 4°C) did not show detectable aggregation by TEM after heating for 2 hour at 60°C, as demonstrated in Fig. 2B. The prepared DNA-gold nanoparticle conjugates were much more stable than bare Au colloids when exposed to increased salt concentrations and elevated temperatures. In high salt buffers (0.3 M NaCl), bare Au colloids showed an immediate color change from red to black, which indicated that Au colloids occurred irreversible aggregation. The UV-Vis spectra scanned Au colloids in aqueous solution and DNA-gold nanoparticles at 0.3 M NaCl/10 mM PBS, respectively. After modification, the maximum absorbance had no obvious shift, as shown in Fig. 2a. An obvious decrease in absorbance at 520 nm of DNA-gold nanoparticle solution was observed, because approximately 25-30% of the nanoparticles in original solution were lost during centrifugation. The absorbance curve of the stored DNA-gold nanoparticles (left standing for 6 months at 4°C) had no apparent change, and was similar to that of the fresh DNA-gold nanoparticle.

Characterization and purification of HAV amplicon To determine the size and specificity of HAV amplified products before establishing the HAV array detection method, HAV amplicons were analyzed and purified. HAV amplicons were separated by agarose (1.5%) gel electrophoresis at electric field strength of 6 V/cm and detected by ultraviolet light. An expected band was observed (lane B) and determined to be

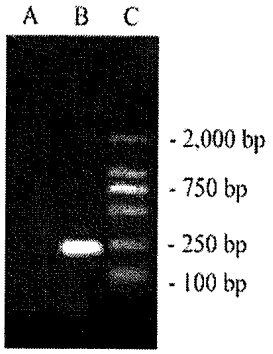

Fig. 3. Agarose gel electrophoresis of HAV amplicon. A: Negative control; B: HAV; C: Marker.

249 bp when compared to the PCR marker (Tube C) as shown in Fig. 3.

HAV PCR product was added in 100 μl aliquots to each tube containing 1,500 μl of 100% ice-cold isopropanol and the tubes were centrifuged at 14,000 rpm for 30 min to pellet the PCR product. The pellet was washed in 75% ethanol and re-pelleted by centrifugation at 14,000 rpm for 15 min. After centrifugation the pellet was re-suspended in 10 μl ddH.

Optimization of capture probe concentration on HAV detection arrays In order to explore the most suitable concentration of amino-modified DNA probes on the HAV arrays under BSA-blocked conditions, three kinds of capture probes (HAV, positive control, and negative control) were each diluted in 10 fold increments to produce a series of probe concentrations ranging from 3.37×10^{-5} M to 3.37×10^{-10} M. Various concentrations of capture probes were attached to the activated glass slide in a predefined pattern (Fig. 4A). The results showed that when the capture probe concentrations were higher than 3.37×10^{-6} M, the spot intensities of HAV and positive control were weak and not significantly different from those of the negative control.

The slope of the signal versus concentration plots is another indicator of the dynamic range for capture probe concentration

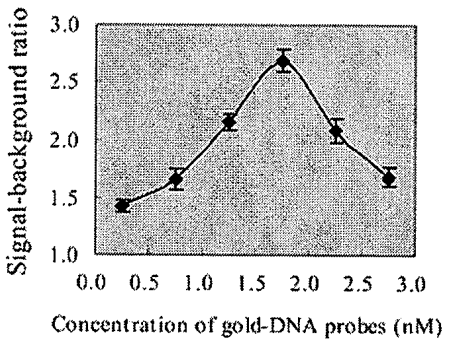

Fig. 5. Influence of concentration of gold nanoparticle probes on signal-to-background ratio. The Y-axis is the ratio of HAV spots intensity to the background intensity. Concentration of positive control or HAV amplicon was 1,000 fM. Results are the means of four array replicates.

(Fig. 4B). Signal intensity of positive control could obtain a best result at the concentration of 3.37×10^{-7} M. When the concentrations were below 3.37×10^{-8} M, the HAV spot intensities showed a weakening signal, which were the same as that of positive controls. Based on these observations, we concluded that the optimal spotting concentrations of amino-modified DNA probes were between 3.37×10^{-7} M and 3.37×10^{-8} M. Concentrations above or below this range were less likely to generate optimal results.

Influence of gold nanoparticle probe concentration on signal-to-background ratio After silver enhancement, the gold-labeled DNA chip yielded a high signal-to-background ratio (Reichert *et al.*, 2000). With concentrations of DNA-modified particles increasing, a few gold nanoparticles can be adsorbed to the chip surface due to unspecific binding, resulting in an increased background signal. Unspecific binding of DNA-modified nanoparticles to PDC-activated APTES glass surface has been investigated by scanning force microscopy (Möller *et al.*, 2000). Here, the influence of the concentration of DNA-modified nanoparticles on signal-to-

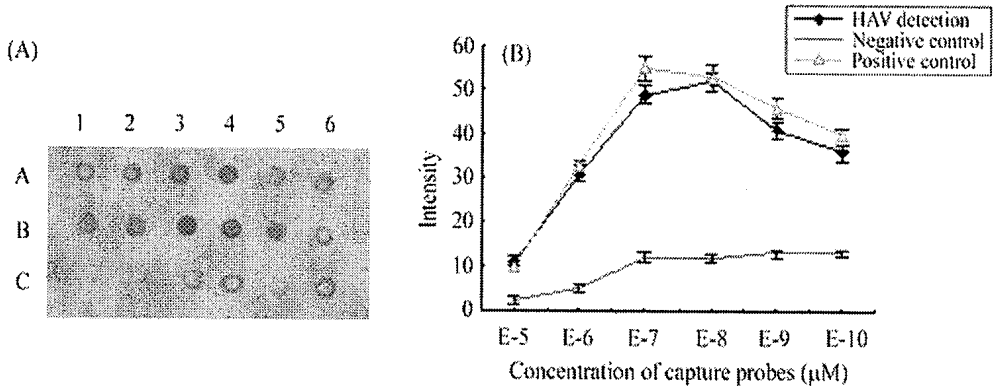

Fig. 4. Different concentrations of capture probes on the HAV detection arrays. A: positive control, B: HAV; C: negative control. The concentration of capture probes: 1 and E-5: 3.37×10^{-5} M, 2 and E-6: 3.37×10^{-6} M, 3 and E-7: 3.37×10^{-7} M, 4 and E-8: 3.37×10^{-8} M, 5 and E-9: 3.37×10^{-9} M, 6 and E-10: 3.37×10^{-10} M. Numbers reported in b represent the means of eight replicates of arrays. Concentration of positive control and HAV amplicon used was 1,000 fM.

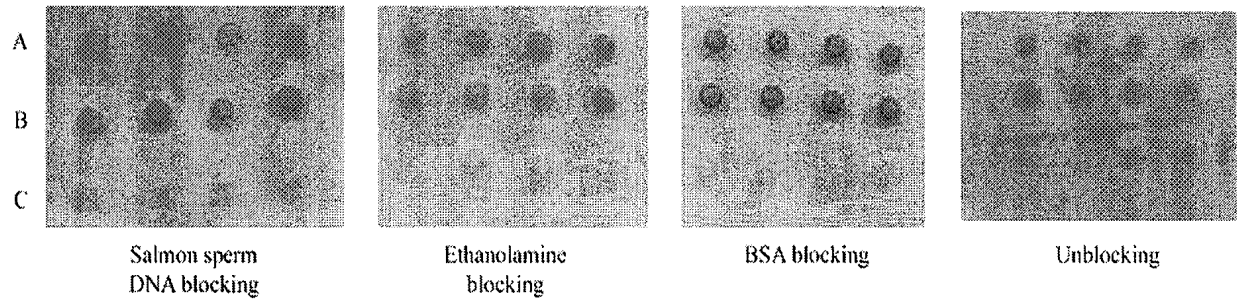

Fig. 6. Detection of HAV employing different blocking strategies on arrays. A: positive control, B: HAV, C: negative control. Concentration of positive control or HAV amplicon was 1,000 fM.

background ratio was investigated, as showed in Fig. 5.

In the present work, the concentration of nanoparticle probe solutions of varied from 0.25 nM to 2.75 nM. It was found that the signal intensities were proportional to the concentrations from 0.25 nM to 2.25 nM, and the background intensity also increased with the concentrations of gold-DNA probes increasing. When the concentration of HAV gold probes was 1.75 nM, a signal-to-background ratio of approximately 2.7 can be determined. However, when the concentrations of probes were higher than 1.75 nM, the arrays did not yield a higher signal-to-background ratio, because higher concentration of probes could cause much darker background. On the other hand, when the gold probe concentrations were lower than a certain quantity (e.g., 0.75 nM), the signal intensities of HAV and positive control were too weak to be clearly discriminated from the negative controls by standard flatbed scanners or the naked eye. Taking the factors into consideration, we estimated that the optimal concentration of nano-gold probes of HAV was 1.75 nM. The result of positive control in the test of the DNA-modified nanoparticles concentration was similar to that of HAV (data not shown).

Detection of HAV employing different blocking strategy on arrays Pre -hybridization blocking strategies are typically used to block the unreacted functional groups of the prepared chip that have low affinity for DNA. Here, blocking reactions are employed to prevent RT-PCR product and labeled probes from non-specific binding to the surface of the array during the hybridization reaction. Three of the common blocking methods to address non-specific adsorption on arrays involve blocking with 1% salmon sperm DNA, bovine serum albumin (BSA), or ethanolamine.

We explored the following condition for blocking: salmon sperm DNA solution: 1× Denhardt's solution, 0.1% SDS, and 100 μg of denatured salmon sperm DNA/ml; BSA solution: 1.0% BSA in 3 M NaCl/10 mmol/L PBS (pH 7.0); ethanolamine solution (Guo *et al.*, 2002): 50 mM ethanolamine, 0.1% SDS in H_2O, pH 9.0. All glass slides were blocked by one of the three blocking solutions by incubating at 42°C for 30 min, followed by washing five times in ddH_2O, then dried. The effect of each of these three blocking strategies to reduce post-hybridization background intensity was investigated, and the results are displayed in Fig. 6.

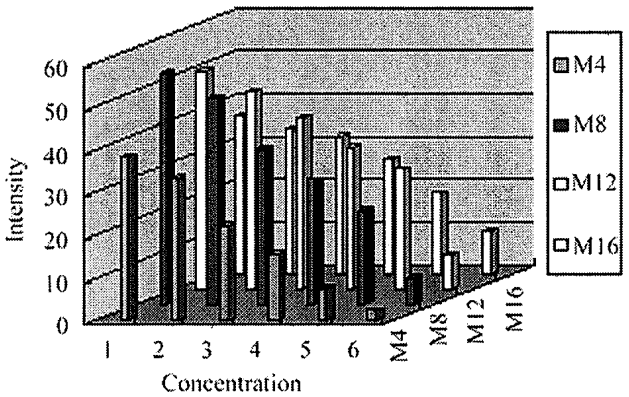

Fig. 7. Intensities of the HAV array were measured at different silver enhancement time and HAV amplicon concentrations. M4, M8, M12, and M16 represent 4, 8, 12, and 16 minutes, respectively. The following concentrations of HAV amplicon were applied: 1; 10,000 fM, 2: 5,000 fM, 3: 1,000 fM, 4: 500 fM, 5: 100 fM, 6: 50 fM. Results are the mean of eight replicates of array.

BSA is a globular protein that readily adsorbs to the surface of the prepared array (Hegde *et al.*, 2000). The blocking BSA solution result in lower background intensities compared with the blocking solution containing ethanolamine, or 1% salmon sperm DNA. Unblocked arrays yielded a lower signal vs. background ratio, and the corresponding signals of detection spots were weak and unclear.

In our previous work (Wang *et al.*, 2003), the blocking strategy of salmon sperm DNA solution was employed, but in this assay the array blocked by BSA displayed the cleaner background than that blocked by salmon sperm DNA solution. And BSA is more economical.

The sensitivity of HAV targets of detection In order to test the sensitivity of HAV detection arrays, different concentrations of HAV targets ranging from 10 to 5000 fM were incubated on separate arrays. After hybridization, silver enhancement was monitored at four different times. The results are shown in Fig. 7. With HAV amplicon concentration increasing, the signal intensified when the time of silver staining was arranged from 4-12 min, but fell at 16 min, due to a marked

increased in the background intensity. Silver enhancement is based on hydroquinone reduction of silver ions to silver metal at the surface of gold nanoparticles, resulting in a growth of the particles. Silver deposition increases with prolonged exposure to the silver enhancer solution, and the particles exhibit different growth rates, which can be imaged using emission scanning electron microscopy (FE-SEM) (Park *et al.*, 2002).

The results obtained showed that as little as 100 fM of HAV amplicon could be detected on the array after having been exposured to the silver enhancer solution for 12 min. When the concentration of HAV amplicon was 50 fM, intensity decreased apparently, and the spots couldn't be detected legibly. With concentrations of HAV amplicon increasing, less time (8 min) was required for the signal intensity to reach the maximum. Therefore, an exposure time of 8-12 min was optimal.

In conclusion, our results indicated that in this assay, the signal could be significantly strengthened and easily detected without expensive setup. Gold-labeled probe is a promising novel label for microarray and chip technology. Compared with the fluorescence label, it costs less and is more sensitive (Alexandre *et al.*, 2001). A variety of proof-of-principle experiments in the research laboratories point to a powerful technology for molecular diagnostics. In our laboratory, a biochip platform using gold nanoparticles labeling has been built for detection of hepatitis viral genes (Wang *et al.*, 2003; Wang *et al.*, 2004). Due to its high sensitivity and cost-effective, the array detection technology can be applied to clinical diagnosis of serum samples, but also to environmental monitoring of HAV contaminated food or water.

Acknowledgments This work was supported by the Hubei Provincial R&D Program, and Longren Enterprises Group (Wuhan). Many thanks are also acknowledged to Xiehe Hospital, Wuhan seventh Hospital, Hubei Renmin and Zhongnan Hospital and Hubei Import& Export Disease Inspection Bureau for supplying the HAV samples used in this study.

References

Alexandre, I., Hamels, S., Dufour, S., Collet, J., Zammatteo, N., De Longueville, F., Gala, J. L. and Remacle, J. (2001) Colorimetric silver detection of DNA microarrays. *Anal. Biochem.* **295**, 1-8.

Chrisey, L. A., Lee, G. U. and O'Ferrall, C. E. (1996) Covalent attachment of synthetic DNA to self-assembled monolayer films. *Nucleic Acids Res.* **24**, 3031-3039.

Csaki, A., Kaplanek, P., Möller, R. and Fritzsche, W. (2003) Single particle sensitivity in the optical detection of individual DNA-conjugated nanoparticle after metal enhancement. *Nanotechnology* **14**, 1262-1268.

David, H. K., Gloria, K. M. and Gary, P. R. (2002) Detection of both hepatitis A virus and norwalk-like virus in imported clams associated with food-borne illness. *Appl. Envir. Microbiol.* **68**, 3914-3918.

Demers, L. M., Mirkin, C. A., Mucic, R. C., Reynolds, R. A., Letsinger, R. L., Elghanian, R. and Viswanadham, G. A. (2000) Fluorescence-based method for determining the surface coverage and hybridization efficiency of thiol-capped oligonucleotides bound to gold thin films and nanoparticles. *Anal. Chem.* **72**, 5535-5541.

Elghanian, R., Storhoff, J. J., Mucic, R. C., Letsinger, R. L. and Mirkin, C. A. (1997) Selective colorimetric detection of polynucleotides based on the distance-dependent optical properties of gold nanoparticles. *Science* **277**, 1078-1081.

Grabar, K. C., Freeman, R. G., Hommer, M. B. and Natan, M. J. (1995) Preparation and characterization of Au colloid monolayers. *Anal. Chem.* **67**, 735-743.

Guo-Jun, Z., Robert, M., Andrea, C. and Wolfgang, F. (2002) Optical Detection of DNA constructs based on nanoparticles and silver enhancement. *AIP Conference Proceedings* **640**, 13-22.

Hegde, P., Qi, R., Abernathy, K., Gay, C., Dharap, S., Gaspard, R., Hughes, J. E., Snesrud, E., Lee, N and Quackenbush, J. (2000) A concise guide to cDNA microarray analysis. *Biotechniques* **29**, 548-550.

Hong, C., Yanqing, W., Pingang, H. and Yuzhi, F. (2002) Electrochemical detection of DNA hybridization based on silver-enhanced gold nanoparticle label. *Anal. Chim. Acta.* **469**, 165-172.

James, J. S., Sudhakar, S. M., Paul, B., Susan, H., H, M., Adam, L., V, G., Tim, P., Wes, B., William, C. and Uwe, R. M. (2004) Gold nanoparticle-based detection of genomic DNA targets on microarrays using a novel optical detection system. *Biosens. Bioelectron.* **19**, 875-883.

Patolsky, F., Ranjit, K. T., Lichtenstein, A. and Willner, I. (2000) Dendritic amplification of DNA analysis by oligonucleotide functionalized Au-nanoparticles. *Chem. Commun.* **12**, 1025-1026.

Möller, R., Csaki, A., Köhler, J. M. and Fritzsche, W. (2000) DNA probes on chip surfaces studied by scanning force microscopy using specific binding of colloidal gold. *Nucleic Acids Res.* **28**, 20-91.

Park, S. J., Taton, T. A. and Chad, A. M. (2002) Array-based electrical detection of DNA with nanoparticle probes. *Science* **295**, 1503-1506.

Reichert, J., Csaki, A., Möller, R., Köhler, J. M. and Fritzsche, W. (2000) Chip-based optical detection of DNA-hybridization by means of nanobead labelling. *Anal. Chem.* **72**, 6025-6029.

Storhoff, J. J., Elghanian, R., Mucic, R. C., Mirkin, C. A. and Letsinger, R. L. (1998) One-Pot colorimetric differentiation of polynucleotides with single base imperfections using gold nanoparticle probes, *J. Am. Chem. Soc.* **120**, 1959-1964.

Taton, T. A., Mirkin, C. A. and Letsinger, R. L. (2000) Scanometric DNA array detection with nanoparticle probes. *Science* **289**, 1757-1760.

Taton, T. A., Lu, G. and Mirkin, C. A. (2001) Two-color labeling of oligonucleotide arrays via size-selective scattering of nanoparticle probes. *J. Am. Chem. Soc.* **123**, 5164–5165.

Therasal, C., Omanav, H. and M. (1997) Detection of hepatitis A virus RNA in oyster meat. *Appl. Envir. Microbiol.* **63**, 2460-2463.

Urban, M., Möller, R. and Fritzsche, W. A. (2003) A paralleled

readout system for an electrical DNA-hybridization assay based on a microstructured electrode array. *Rev. Sci. Instrum.* **74**, 1077-1081.

Wang, Y. F., Pang, D. W., Zhang, Z. L., Zheng, H. Z., Cao, J. P. and Shen, J. T. (2003) Visual gene diagnosis of HBV and HCV based on nanoparticle probe amplification and silver staining enhancement. *J. Med. Virol.* **70**, 205-211.

Wang, Y. F., Shen, J. T. and Liu, H. H. (2004) Analytical performance of and real sample analysis with an HBV gene visual detection chip. *J. Virol. Methods.* **121**, 79-84.

Analytical Biochemistry 295, 1–8 (2001)
doi:10.1006/abio.2001.5176, available online at http://www.idealibrary.com on IDEAL®

Colorimetric Silver Detection of DNA Microarrays

I. Alexandre,*[,1] S. Hamels,* S. Dufour,* J. Collet,* N. Zammatteo,* F. De Longueville,* J.-L. Gala,† and J. Remacle†

Laboratoire de Biochimie Cellulaire, Facultés Universitaires Notre Dame de la Paix, 61 Rue de Bruxelles, 5000 Namur, Belgium; and †Advanced Array Technology, 61 Rue de Bruxelles, 5000 Namur, Belgium

Received December 12, 2000; published online June 27, 2001

Development of microarrays has revolutionized gene expression analysis and molecular diagnosis through miniaturization and the multiparametric features. Critical factors affecting detection efficiency of targets hybridization on microarray are the design of capture probes, the way they are attached to the support, and the sensitivity of the detection method. Microarrays are currently detected in fluorescence using a sophisticated confocal laser-based scanner. In this work, we present a new colorimetric detection method which is intented to make the use of microarray a powerful procedure and a low-cost tool in research and clinical settings. The signal generated with this method results from the precipitation of silver onto nanogold particles bound to streptavidin, the latter being used for detecting biotinylated DNA. This colorimetric method has been compared to the Cy-3 fluorescence method. The detection limit of both methods was equivalent and corresponds to 1 amol of biotinylated DNA attached on an array. Scanning and data analysis of the array were obtained with a colorimetric-based workstation. © 2001 Academic Press

Microarrays represent one of the main new breakthroughs in molecular analysis through miniaturization of the assay and the ability to permit the monitoring a large number of genes simultaneously (1, 2).

Despite other alternatives like the electronic support, the two main DNA array supports are the nylon filters and the glass slides.

High-density filter arrays are easily accessible to the scientific community due to their compatibility with commonly used hybridization methods and equipment. Their major drawback is the use of radioactive DNA labeling (3).

Glass slides are now becoming the standard support for microarrays mostly because they are compatible with fluorescence labeling. Target DNA sample is directly labeled either by incorporation of fluorophore-labeled nucleotides or by using fluororophore-labeled streptavidin which binds to biotinylated nucleotides (1, 4). Since several fluorochromes are available, simultaneous and distinct analyses of samples and controls can be performed. Two-color analysis allows competitive hybridization between a sample target DNA and a reference standard DNA on the same array (5). The analysis is performed by specific excitation of each fluorophore by the appropriate laser wavelength. This working protocol reduces experimental analytical variations of the analysis but introduces bias because efficiency of fluorescent emission is not equivalent for both fluorophores. Although such method perfectly suits the requirements for gene expression analysis, the cost of the equipment restricts its use to the research field and makes it unsuitable for the reading of microarray in a wide clinical and daily-based practice.

Accordingly, alternative methods for the reading of hybridization results on microarray have been proposed. Chemiluminescent detection has been proposed for filter arrays (6). Sensitivity seems to equivalent to fluorescence and radioactive detection but the spatial analysis is limited by the diffusion of light emitted on X-ray photographic film. Colorimetric detection appears to be another choice. Chen and colleagues (7) proposed a two-color labeling using peroxidase and alkaline phosphatase detection. The method is however limited by its lower sensitivity.

In this work, we reviewed many different colorimetric detection methods and found that the photographic-based silver precipitation gave unexpected sensitive detection of DNA on microarray compared to other precipitates.

[1] To whom correspondence should be addressed. Fax: 32-81-724135. E-mail: isabelle.alexandre@fundp.ac.be.

0003-2697/01 $35.00

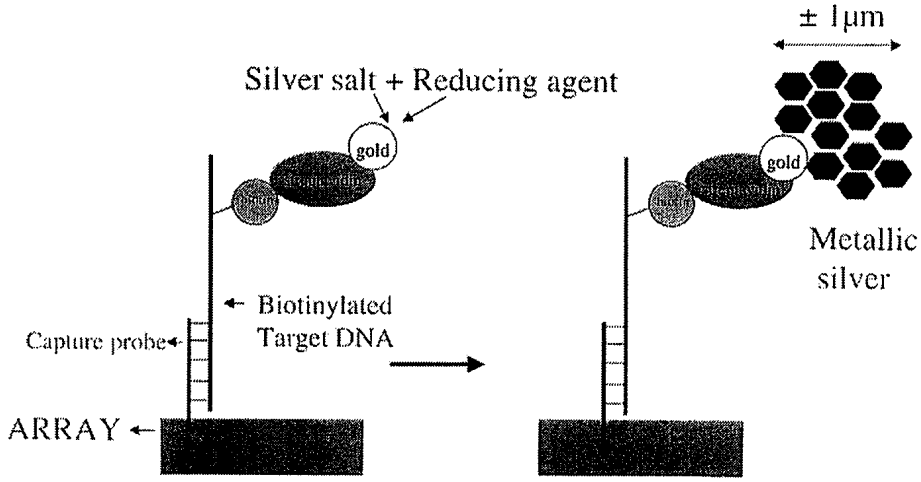

FIG. 1. Schematic representation of the colorimetric silver staining detection of hybridized target DNA on a microarray. The detection system is based on the use of streptavidin–nanogold particles and silver precipitation.

Immunogold staining has been used over the past 20 years in order to detect tissue antigens (8, 9). It is based on the use of gold nanoparticles coated with antibodies. The colloidal gold particles are electron dense and they allow high resolution for the localization of the antigen with the electron microscope.

To enhance the detection signal of gold particles, an additional silver staining enhancement can be used (10–12).

This method has several advantages. The metallic deposition is an autocatalytic process whose amplification power can exceed that for catalytic deposition of chromogenes by enzyme-labeled reagents. Second, silver deposit strongly reflects light in the visible spectrum, a feature allowing the use or development of light reflection-based readers.

Recently, a similar method of silver precipitation based on the use of DNA-gold particles has been described (13). The use of DNA probe bound to colloidal gold particles is followed by silver reduction as assessed here.

MATERIALS AND METHODS

Amplification of Cytomegalovirus DNA

Human cytomegalovirus DNA was used as target for the optimization of the detection. Target DNA and capture probes were synthesized by PCR within exon 4 of the major immediate early gene of human cytomegalovirus as described by Zammatteo *et al.* (14).

Two primers, MIE-4 and MIE-5, were used to amplify the target amplicon of cytomegalovirus (14). For PCR amplification, 1 ng of cytomegalovirus template was supplemented with PCR buffer (0.075 M Tris, pH 9, 50 mM KCl, 2 mM $MgCl_2$, 20 mM $(NH4)_2SO_4$) containing 50 μM dATP, dCTP, and dGTP; 25 μM dTTP; and biotin-11–dUTP (Roche, Indianapolis, IN), 0.1 μM each primer, and 2.5 units of DNA polymerase (Biotools, Madrid, Spain). Amplification was performed in a DNA PE 9600 thermocycler (Perkin–Elmer, Foster City, CA). An initial denaturation step (94°C for 3 min) was followed by 40 cycles (94°C for 30 s, 65°C for 30 s, and 72°C for 30 s) and a final extension step at 72°C for 7 min.

The capture probes of cytomegalovirus were amplified using the same protocol as above except that 5′ aminated primer MIE-4 was substituted to MIE-4 and that 50 μM dTTP was substituted to the mix dTTP and biotin–dUTP.

Amplification of femA Gene from Staphylococcus

The use of *femA* gene for specific identification of the *Staphylococci* based on consensus and species-specific sequences was proposed by Vannuffel *et al.* (15). Accordingly, *femA* gene from *S. epidermidis* has been used in this work. Amplification was based on the use of degenerated primers, consensus for the genus *Staphylococcus:* APcons3-1 (5′-TAAYAAARTCACCAACATAYTC-3′)–APcons3-2 (5′-TYMGNTCATTTATGGAAGATAC-3′) (where Y is C or T, R is A or G, M is A or C, and N is A, G, C or T) (Eurogentec, Seraing, Belgium) as described by Hamels *et al.* (16). The amplification of the *femA* genetic marker sequence was performed in a final volume of 50 μl containing 2.5 mM $MgCl_2$, 75 mM Tris–HCl, pH 9.0; 50 mM KCl; 20 mM $(NH_4)_2SO_4$; 0.5 μM each degenerated primer; 200 μM dATP, dCTP, and dGTP; 150 μM dTTP; 50 μM biotin-16–dUTP (Roche); 0.5 U of uracil–DNA–glycosylase (Roche); 1.25 U of *Taq* DNA polymerase (Biotools); 1 ng of *femA* DNA template. The reagents were first incubated at 94°C for 5 min and then cycled 40 times in a

DNA PE 9600 thermocycler (Perkin–Elmer) using the following temperatures and cycle times: 94°C for 30 s, 49°C for 45 s, 72°C for 30 s. A final extension step of 10 min at 72°C was performed.

Array Hybridization

Glass slides carrying aldehyde groups on their surface (Diaglass, AAT, Namur, Belgium) have been spotted with various aminated capture probes according to the manufacturer. The spots had diameter of 400 μm, the distance between two spots (center to center) being 600 μm.

Hybridization of CMV Target Amplicons

Five microliters of PCR product was added to 60 μl of hybridization solution and this solution was loaded on the array framed by an hybridization chamber (MJ Research Inc., Watertown, MA).

The hybridization solution was made of 2× SSC, 5× Denhardt, pH 7, and contained 100 μg/ml DNA from salmon sperm. After heating at 98°C, the hybridization was performed during 2 h at 65°C.

Hybridization of femA Gene Amplicons

Five microliters of PCR product was denatured with 5 μl of 0.1 N NaOH for 5 min at room temperature then 60 μl of hybridization solution (AAT, Namur, Belgium) was added. This hybridization mix was loaded on the array framed by an hybridization chamber.

We added 10 nM CMV[2] biotinylated DNA as positive control for hybridization. The hybridization chambers were sealed with a plastic coverslip and slides were incubated during 2 h at 53°C.

Detection of Hybridized DNA

For fluorescent detection, slides were washed four times (1 min per wash) with a 10 mM maleate buffer containing 15 mM NaCl and 0.1% Tween, pH 7.5. The slides were incubated for 45 min with streptavidin–Cyanin 3 conjugate diluted 500× (Amersham, Buckinghamshire, UK). The slides were then washed five times in the same washing buffer. Then slides were dried for 5 h and scanned with a fluorescent confocal scanner GMS 418 (Genetic Microsystem, Woburn, MA).

The colorimetric Silver Blue detection kit was purchased from AAT and used according to the manufacturer's instructions. A streptavidin–gold conjugate replaced the streptavidin–cyanin 3. After 45 min of streptavidin–gold incubation, glass slides were washed five times in the washing buffer and then incubated at room temperature for 15 min in 800 μl of the Silver Blue solution. This Silver Blue solution is the combination of 1/1 vol of two solutions, the first one

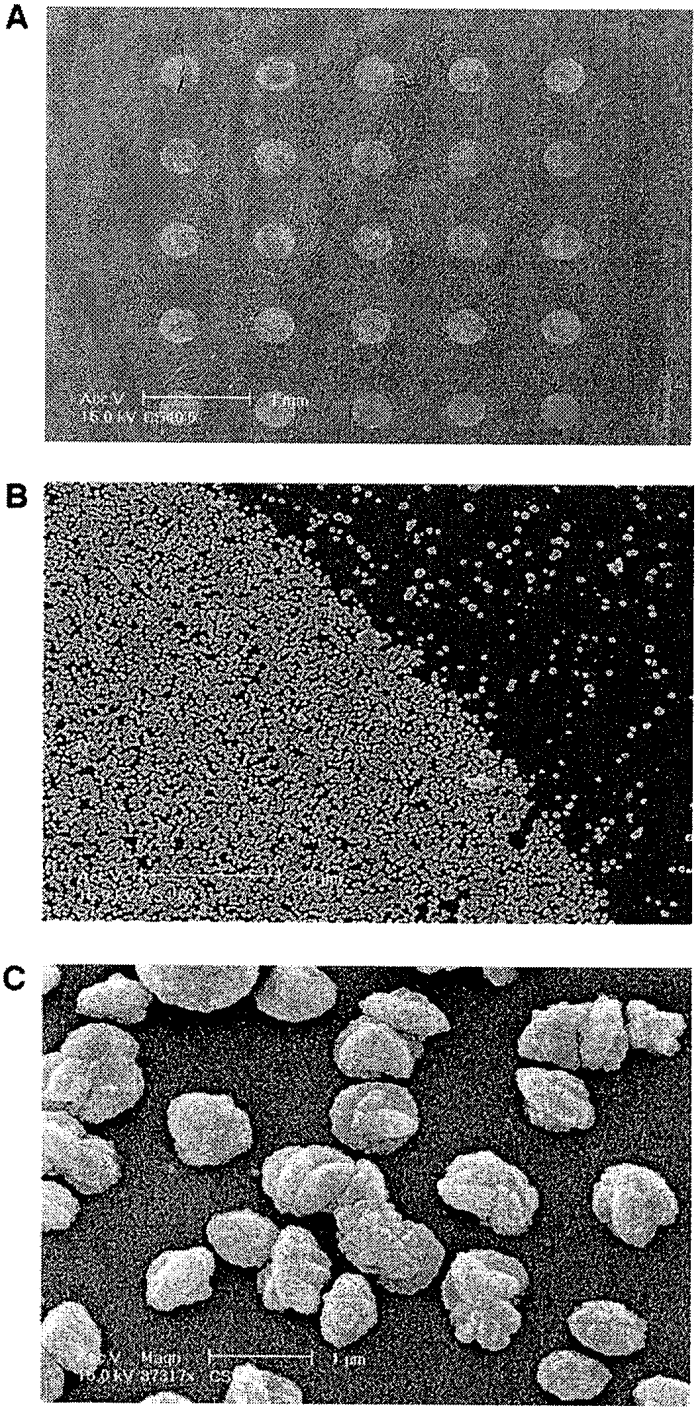

FIG. 2. Electron scanning microscope visualizations at different magnifications of a silver deposit after a 15-min incubation of Silver Blue solution on 10-nm gold particles on glass surface. (A) Visualization of 25 spots on the array. (B) Spatial limit between specific signal and background. (C) Visualization of individual silver precipitates.

[2] Abbreviation used: CMV, cytomegalovirus.

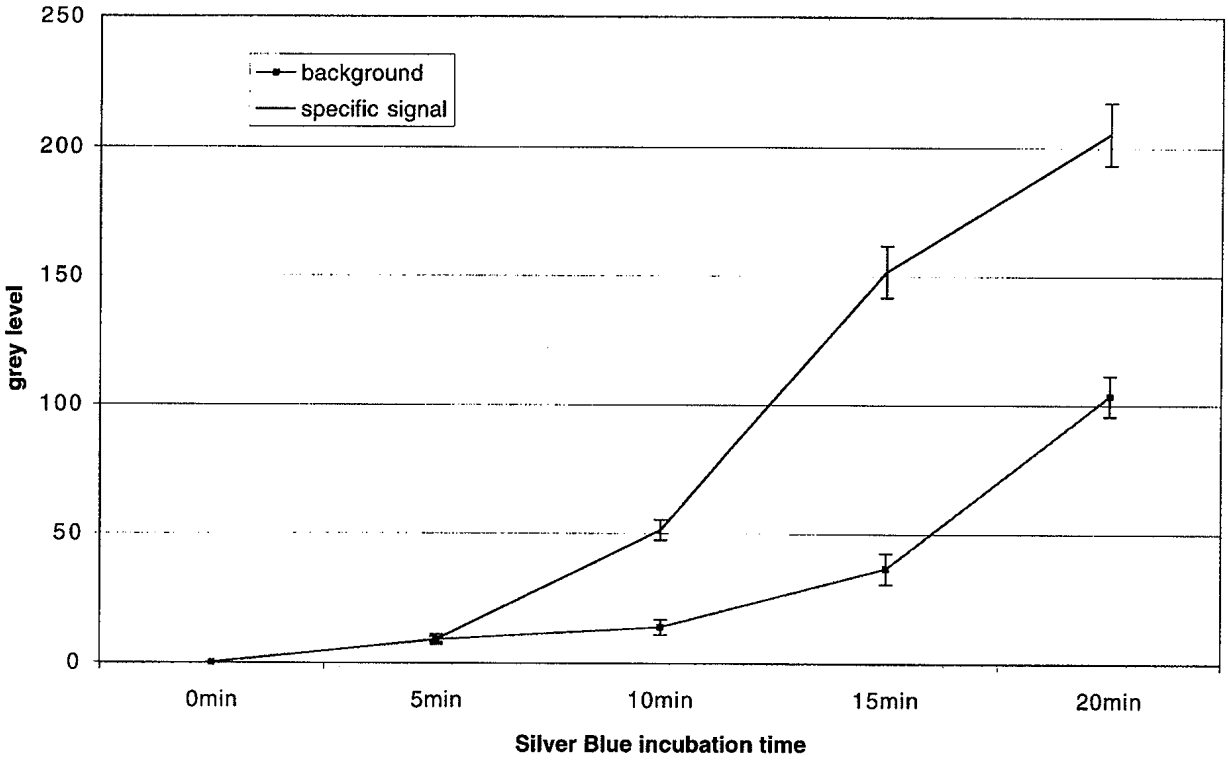

FIG. 3. Kinetics of silver deposition by self-nucleation (background) or on gold particles (specific signal). The biotinylated DNA was spotted at a concentration of 30 nM before reacting with streptavidin–gold conjugate. Results were expressed as the mean of gray level of the pixels inside a spot minus the background calculated as the mean of gray level of pixels around the spot. Results were the mean of four replicates ±2 s.

containing the silver salt ($AgNO_3$) and the second one containing the hydroquinone. Slides were rinsed in water, air-dried 5 h at 37°C, and read with an array colorimetric workstation (AAT). The workstation is a computer tower containing a CCD camera with the appropriate illumination and software for image analysis, quantification of the spots, and statistical treatment of the data.

RESULTS

The principle of the colorimetric method for detecting hybridized DNA on microarray is illustrated in Fig. 1. First, the target DNA is labeled with biotin by the incorporation of biotin–dUTP during amplification. After target hybridization on the array, streptavidin–nanogold particles are added for binding to biotin. Silver labeling relies on the catalytic activity of gold resulting in the reduction of silver ions into metallic silver and a deposition on gold particles. The silver shell around gold particle, in turn, autocatalyzes further silver depositions. At the end of the reaction, silver deposit onto gold particles leads to an increase of particle size going from 10 to about 1000 nm. Silver Blue solution was optimized for applications on microarray. A picture of the silver particles on the array is presented in Fig. 2. The high sensitivity of the method results from an increase of the particles volume of around 1 million times compared to their initial volume. This enhancement allows a direct visual detection of the microarray labeled spots and a straightforward analysis using a colorimetric detector.

Optimization of the Silver Reduction

Silver solutions are sensitive to UV or sunlight and spontaneous conversion of silver solution into metallic grains can occur, leading to nonspecific silver deposition. To limit this drawback, at least two requirements have to be met: first the microarray handling has to be as clean as possible and the silver precipitation reaction must be controlled. Several parameters influence the rate of the reaction including temperature, pH, the silver salt type and concentration, and reducing agent concentration. The composition of the Silver Blue solution has been optimized in order to obtain within one incubation the largest silver precipitation on the gold particles with the minimum of nonspecific deposit. However, the background increases with incubation time as illustrated in Fig. 3. The highest signal to noise ratio was obtained after 15 min of incubation. These conditions were used in further experiments.

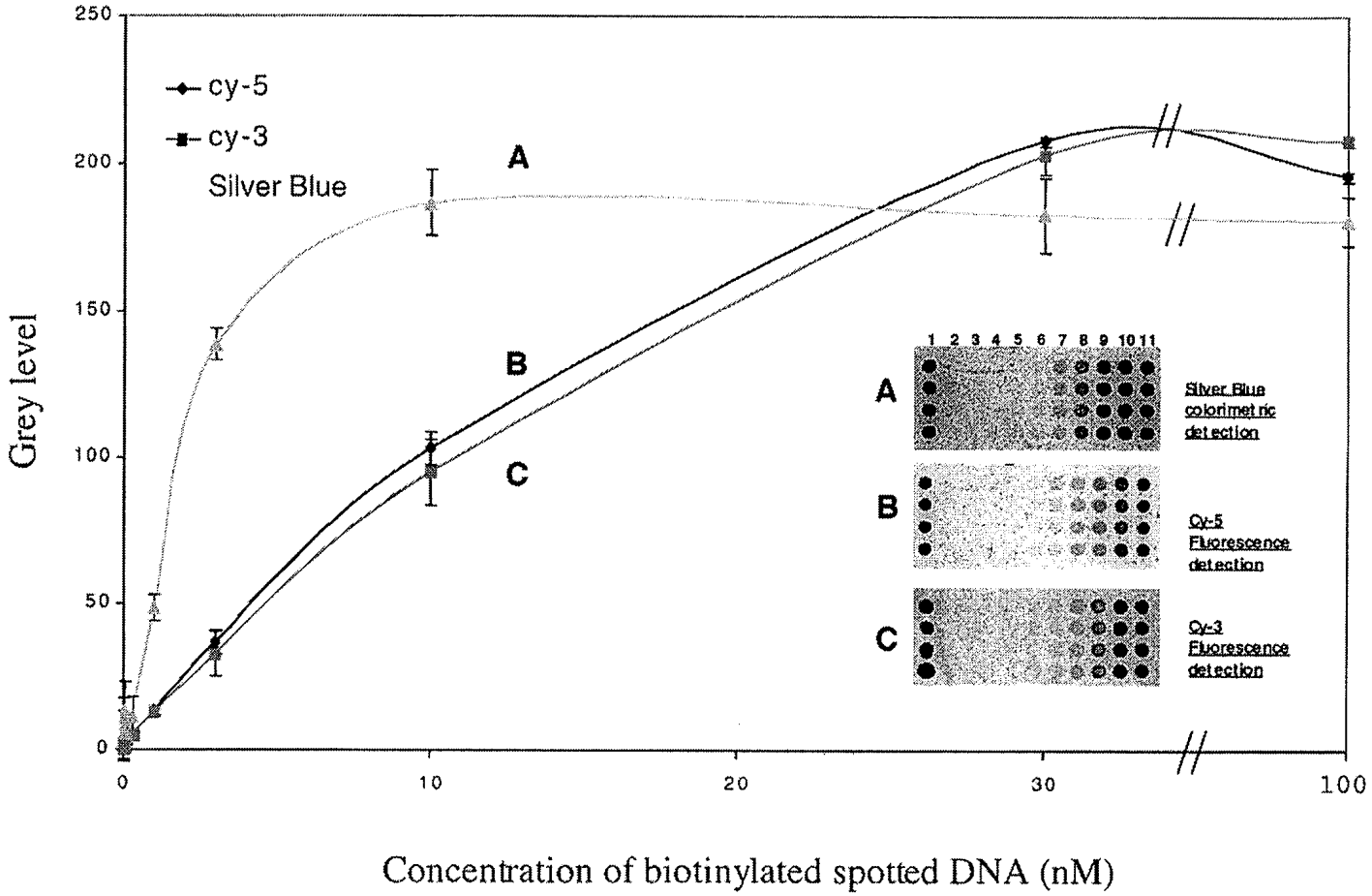

FIG. 4. Comparison of Silver Blue detection (A), fluorescent Cy-5 detection (B), and fluorescent Cy-3 detection (C) of microarray spotted with increasing concentrations of 257-bp CMV DNA 5′ aminated and multibiotinylated. The four rows of the arrays were replicates. The following DNA concentrations were spotted: 100 nM on line 1, 0.01 nM on line 2, 0.03 nM on line 3, 0.1 nM on line 4, 0.3 nM on line 5, 1 nM on line 6, 3 nM on line 7, 10 nM on line 8, 30 nM on line 10, and 100 nM on line 11. (Inset) Quantification of raw data presented in main figure. Results are expressed as the mean of gray level of the pixels inside a spot minus the background calculated as the mean of gray level of pixels around the spot. Results are the mean of four replicates ±2 s.

Revelation Results

A comparison of sensitivity between fluorescence and Silver Blue detection was performed on arrays spotted with various concentrations of CMV-biotinylated DNA. The fixed biotinylated DNA concentrations ranged from 0.01 to 100 nM. Each was made in quadruplicate (Fig. 4). This array was detected with both detection methods.

Results show that in fluorescence as well as in silver detection, gray levels of the spots were well proportional to the concentration of spotted capture probes. The sensitivity of both detection systems was identical with a minimum detection when spotting 1 nM biotinylated DNA (Fig. 4, lane 6). The results obtained with 0.3 nM biotinylated DNA detection were not significatively different from background.

Since the volume of capture probe dispended per spot was estimated to be 1 nl, and assuming that 100% of capture probes were fixed on the array, we calculated that silver detection and Cy-3 and Cy-5 fluorescence allow the detection of 1 amol of multibiotinylated DNA per spot.

Hybridization Results

We then determined the sensitivity of target DNA detection after hybridization on microarray using both detection systems. Unlabeled CMV capture probes were first spotted at a concentration of 150 nM on the array. Various controls were included on the array. Biotinylated DNA capture probes were used as positive control of fixation to indicate the spotting reliability. The negative hybridization controls were capture probes not complementary to target DNA. Different concentrations of biotinylated CMV target DNA ranging from 0.1 to 100 fm in 65 μl were incubated on separate arrays. Silver Blue detection was again com-

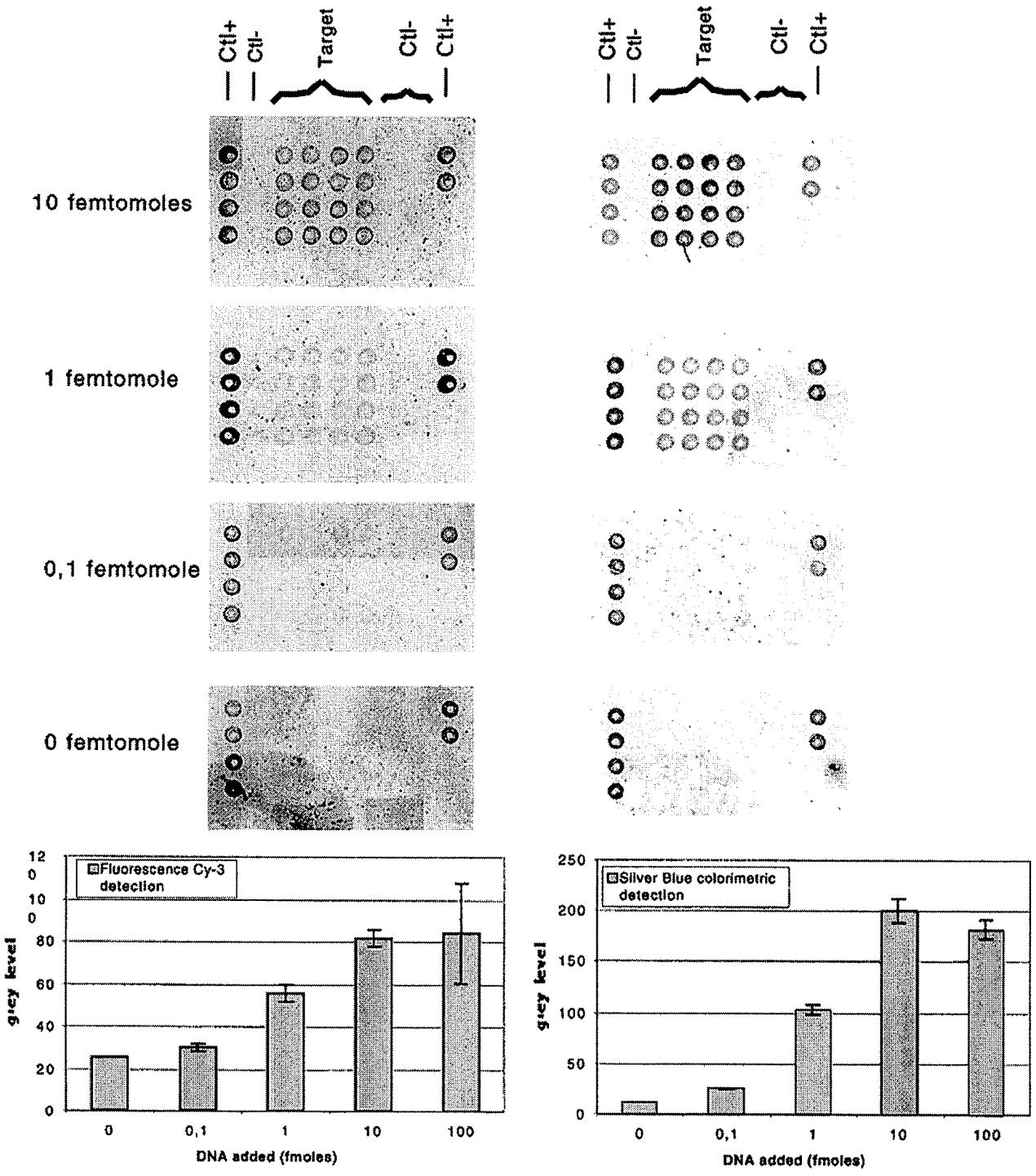

FIG. 5. (Top) Visualization of hybridizations of different concentrations of multibiotinylated HCMV target DNA on the microarrays. Comparison between fluorescent Cy-3 detection (left) and Silver Blue detection (right) methods. The four rows of the array were replicates. The microarray contained the following capture probes: columns 1 and 9, spotted with fixation control; columns 2, 7, and 8, spotted with negative control of hybridization; columns 3–6, spotted with HCMV-specific capture probe. (Bottom) Quantification of raw data presented in top. Comparison between fluorescent Cy-3 detection and Silver Blue detection method. Results are expressed as described in the legend to Fig. 4, inset. Results are the means of 16 replicates ±2 s.

pared to Cy-3 fluorescence detection. The results presented in Fig. 5 show that as few as 0.1 fmol of target DNA amplicons could be detected on the arrays with both detection methods. The detection signal increased steadily between 0.1 and 10 fmol of target DNA and then reached a plateau.

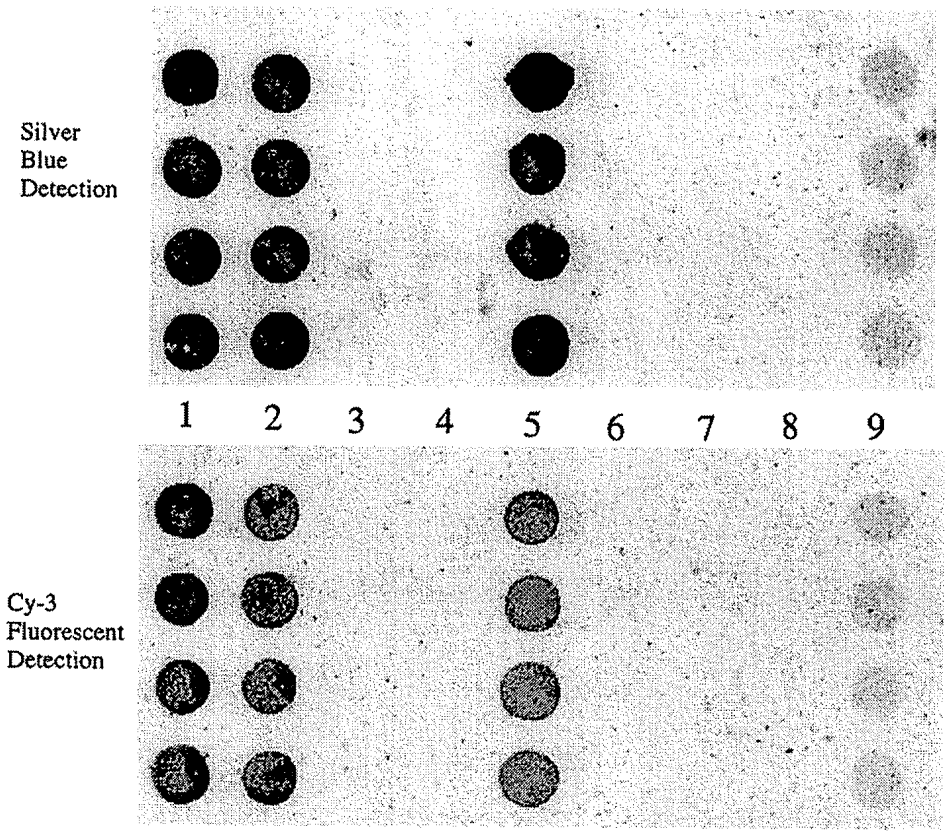

FIG. 6. Detection of the *Staphylococcus epidermidis femA* amplicons on a commercial microarray. Comparison between Silver Blue colorimetric method and fluorescent Cy-3 detection. The four rows of the array were replicates. The microarray contained the following capture probes: columns 1 and 9, fixation controls; column 2, negative control of hybridization; column 3, HCMV-specific capture probe used as positive hybridization control; and columns 4 to 8, five specific capture probes for five *Staphylococcus* species, *S. aureus* (line 4), *S. epidermidis* (line 5), *S. haemolyticus* (line 6), *S. hominis* (line 7), and *S. saprophyticus* (line 8).

Application

The colorimetric Silver Blue detection system was then tested on a DNA microarray developed for the determination of *Staphylococci* species (Staphychips, AAT). The microarray contains five capture probes specific for the *femA* gene of five *Staphylococcus* species: *S. aureus, S. epidermidis, S. haemolyticus, S. hominis,* and *S. saprophyticus* (16). The *femA* gene from *S. epidermidis* was amplified by PCR and the biotinylated amplicons were incubated on the microarray. Hybridization on the array was revealed in fluorescence as well as in colorimetry (Fig. 6). The results were identical with both methods and gave correct identification of the species *S. epidermidis.*

DISCUSSION

Colorimetric detection using silver precipitation has been shown here to be well adapted for detection and analysis of hybridization on microarray. Its sensitivity is comparable to detection in fluorescence using a confocal scanner. This high sensitivity is the result of an amplification step that brings small nanoparticles to grow up 1 million times in volume. With a controlled background, this new technology allows a very good detection sensitivity of hybridized DNA onto glass microarrays which is equivalent to fluorescence. Like in fluorescence, the detection limit is 0.1 fmol of biotinylated target DNA hybridized on the array. The metallic silver deposition specifically occurs on hybridized target DNA, a feature compatible with miniaturization required by the arrays technology (Fig. 2). Since the combination of this gold label and silver enhancement is electron dense, deposits can be read by a simple device such as the colorimetric array workstation.

Another advantage of the method is that silver deposit is stable and the array can be stored for a very long period of time. The Silver Blue colorimetric detection method can be used in similar way on protein arrays using antibodies labeled with nanogold particles. In parallel to this method, Taton *et al.* (13) proposed to use nanogold particles coated with DNA probes to detect DNA hybridized on the array. In this case, the labeling of the target DNA with nanogold particles alters the melting temperature profile of tar-

gets on the array and thus allows the discrimination of targets with single nucleotides mismatches. The limitation of the method is that for each application, nanogold particles must be prepared with the specific probes while in the present paper, standard reagents such as streptavidin–gold and Silver Blue solutions can be prepared and made in a reproducible form.

This colorimetric detection method is also well suited for supports others than glass such as plastic supports, for instance, acrylic layer or polycarbonate. These new supports for microarrays will be interesting for automation since it will be possible to use array on plastic supports which we can mold to create sealed chambers inside and which are adaptable to automate handling. Fluorescent detection is not applicable on plastic arrays because of the strong autofluorescence of these polymers.

The current results indicate that this new silver colorimetric detection method compares favorably with conventional fluorescence detection and could be a cheap, versatile, and as sensitive alternative.

ACKNOWLEDGMENT

The authors thank the "Walloon Region" for the financial support (Convention No. 9914016).

REFERENCES

1. Schena, M. (1996) Genome analysis with gene expression microarrays. *BioEssays* **18,** 427–431.
2. Brown, P. O., and Botsein, D. (1999) Exploring the new world of the genome with DNA microarrays. *Nature Genet.* **21,** 33–37.
3. Chenchik, A., Chen, S., Makhanov, M., and Siebert, P. (1998) Profiling gene expression in a human glioblastoma cell line using ATLAS human cDNA expression array I. *Clontechnique* **13,** 16–17.
4. Heller Renu, A., Schena, M., Chai, A., Shalone, D., Bedilion, T., Gilmore, J., Woolley, D., and Davis, R. W. (1997) Discovery and analysis of inflammatory disease-related genes using cDNA microarrays. *Proc. Natl. Acad. Sci. USA* **94,** 2150–2155.
5. Hacia, J. G., Edgemon, K., Sun, B., Stern, D., Fodor, S. P., and Collins, F. S. (1998) Two color hybridization analysis using high density oligonucleotide arrays and energy transfer dyes. *Nucleic Acids Res.* **26,** 3865–3866.
6. Rajeevan Mangalathu, S., Dimulescu, I. M., Unger, E. R., and Vernon, S. D. (1999) Chemiluminescent analysis of gene expression on high density filter arrays. *J. Histochem. Cytochem.* **47,** 337–342.
7. Chen, J. W., Wu, R., Yang, P. C., Huang, J. Y., Sher, Y. P., Han, M. H., Kao, W. C., Lee, P. J., Chiu, T. R., Chang, F., Chu, Y. W., Wu, C. W., and Peck, K. (1998) Profiling expression patterns and isolating differentially expressed genes by cDNA microarray system with colorimetry detection. *Genomics* **51,** 313–324.
8. Mayer, G., and Bendayan, M. (1999) Immunogold signal amplification: Application of the CARD approach to electron microscopy. *J. Histochem. Cytochem.* **47,** 421–429.
9. Bendayan, M. (1995) Colloidal gold post-embedding immunocytochemistry. *Prog. Histochem. Cytochem.* **29,** 1–631.
10. Hacker, G. W. (1998) High performance nanogold-silver in situ hybridization. *Eur. J. Histochem.* **42,** 111–120.
11. Zehbe, I., Hacker, G. W., Su, H., Hauser-Kronberger, C., Hainfield, J. F., and Tubbs, R. (1997) Sensitive in situ hybridization with catalysed reporter deposition, streptavidin-nanogold and silver acetate autometallography: Detection of single-copy human papillomavirus. *Am. J. Pathol.* **150,** 1553–1561.
12. Lah, J., Hayes, D. M., and Burry, R. W. (1990) A neutral pH silver development method for the visualization of 1 nanometer gold particles in pre-embedding electron microscopic immunocytochemistry. *J. Histochem. Cytochem.* **38,** 503–508.
13. Taton, A., Mirkin, C. A., and Letsinger, R. L. (2000) Scanometric DNA array detection with nanoparticle probes. *Science* **289,** 1757–1760.
14. Zammatteo, N., Alexandre, I., Ernest, I., Le, L., Brancart, F., and Remacle, J. (1997) Comparison between microwell and bead supports for the detection of human cytomegalovirus amplicons by sandwich hybridization. *Anal. Biochem.* **253,** 180–189.
15. Vannuffel, P., Heusterpreute, M., Bouyer, M., Vandercam, B., Philippe, M., and Gala, J. L. (1999) Molecular characterization of femA from *Staphylococcus hominis* and *Staphylococcus saprophyticus,* and femA-based discrimination of staphylococcal species. *Res. Microbiol.* **150,** 129–141.
16. Hamels, S., Gala, J. L., Dufour, S., Vannuffel, P., Zammatteo, N., Leclerc, G., and Remacle, J. DNA microarray for simultaneous diagnosis of *Staphylococcus* genus, species and their methicillin-resistance. Submitted for publication.
17. Patolsky, F., Ranjit, K. T., Lichtenstein, A., and Willner, I. (2000) Dendritic amplification of DNA analysis by oligonucleotide-functionalized Au-nanoparticles. *Chem. Commun.* **2000,** 1025–1026.